EVALUATING DEPOSITIONAL COMPLEXITY AND COMPARTMENTALIZATION OF THE
ROSE RUN SANDSTONE (UPPER CAMBRIAN) IN EASTERN OHIO

Mihir P. Shah

A Thesis

Submitted to the Graduate College of Bowling Green
State University in partial fulfillment of
the requirements for the degree of

Master of Science

December 2013

Committee:

James Evans, Advisor

Charles Onasch

Jeff Snyder

ABSTRACT

The Upper Cambrian Rose Run Sandstone in eastern Ohio includes mixed siliciclastic and carbonate lithofacies, deposited in a shallow marine, tidally- influenced, environment. A study of 17 wells including 4 cores with total thickness of 21 m, from Holmes County (well# 2892), Coshocton County (wells# 2989 and # 3385), and Morgan County (well# 2923) reveals 14 siliciclastic and 5 carbonate lithofacies. Intertidal deposits include heterolithic wavy bedded sandstone and mudstone (lithofacies SMw), heterolithic lenticular bedded sandstone and mudstone (lithofacies SMk), heterolithic flaser bedded sandstone and mudstone (lithofacies SMf), interbedded planar laminated sandstone and mudstone (lithofacies SMl), interpreted as tidalites, massive mottled sandstone (lithofacies Smm), and massive mudstone (lithofacies Mm). Subtidal clastic deposits include medium-scale planar tabular cross-bedded sandstone (lithofacies Sp), herringbone cross-bedded sandstone (lithofacies Sx), massive sandstone (lithofacies Sm), glauconite-rich massive sandstones (lithofacies Smg), hummocky stratified sandstone (lithofacies Sh), and laminated mudstone (lithofacies Ml). Interbedded carbonates include dolo-mudstones (lithofacies Cm), bioturbated and mottled dolo-mudstones (lithofacies Cmm), dolo-packstones with rip-up clasts ("flat-pebble conglomerate") (lithofacies Cpmr), dolo-packstones with mud drapes ("cryptalgal lamination") (lithofacies Cpl), and convoluted bedded dolo-mudstone (lithofacies Cmmc). The Rose Run Sandstone in this region is interpreted to be deposited in a shallow marine environment of normal salinity with extensive tidal flats, mixed siliciclastic-carbonate deposition, strong tidal influence, and reworking of carbonate materials.

This study reveals compartmentalization of Rose Run Sandstone at different scales. The reservoir quality is mainly controlled by amount of dolomite cement, quartz and feldspar overgrowths, and clay content, which influences porosity and possibly permeability. Interlaminated clay/mud baffles are common small-scale features. Textural and mineralogical

variability caused by different grain size may influence reservoir quality. Interbedded dolostone vary in thickness from 20 cm to around 1.5 m, act as baffles to fluid flow in all directions, and create fluid flow compartments preventing effective pore fluid interconnectivity between sandstone units. Core and geophysical log analysis from 17 wells suggests depositional complexity as one of major reasons for compartmentalization of Rose Run Sandstone in the study area. The unit is better developed in eastern part of study area from where its thickness reduces in all other directions. Also, there is better connectivity among sand bodies in north-south direction, which is interpreted to be approximately parallel or sub-parallel to the paleo-shoreline. Together, structure contour and sand-isolith maps reveals up-dip stratigraphic traps in the study area and in areas with better well control, the structure contour map shows local structural complexity in the form of isolated anticlinal features which at places are interpreted as pre-depositional highs.

ACKNOWLEDGEMENTS

TABLE OF CONTENTS

LIST OF FIGURES

LIST OF TABLES

INTRODUCTION

Reservoir Compartmentalization

General Concepts

Reservoir compartmentalization refers to case where the petroleum accumulation in the reservoir unit is segregated into a number of individual, or disconnected, compartments. In other words, reservoir compartmentalization occurs when flow between compartments is prevented due to sealed boundaries in the reservoir. There are two basic types of boundaries in such situations: "static seals" that are completely sealed and capable of withholding or trapping petroleum columns over geological time; and "dynamic seals" where baffles with low to very low permeability can reduce petroleum migration to very low rates (Jolley et al., 2010).

Compartmentalization can happen on different scales. At the macro-scale levels compartmentalization might be related to the distribution of sandstone, such as if it pinches out against non permeable bodies creating stratigraphic barriers. Faulting may juxtapose reservoir rocks with non-reservoir rocks. A fault itself can act as barrier or pathway depending on whether fault zone is well cemented or not. At the meso-scale levels, compartmentalization could be due to change in lithofacies, gradation of reservoir to non-reservoir rock, change in cement type or cement quantity. At the micro-scale levels, compartmentalization might be related to diagenetic effects or due to variability in microstructures, textures, and diagenetic modification. For example, diagenesis can compartmentalize a reservoir when authigenic mineral growth associated with specific lithofacies reduces permeability. All of these directly affect the oil and gas producing potential of the reservoir. Regardless of the cause, reservoir compartmentalization impacts the volume of moveable oil or gas that might be connected to any given well drilled in a

field. Thus, it might affect the volume of reserves that can be booked for that field, the field's ultimate recovery, and thus can also seriously impact the profitability of a field (Jolley et al., 2010).

Tidal Depositional System

The Knox Group (Cambrian to Ordovician) is subdivided into the Copper Ridge Dolomite, Rose Run Sandstone, and Beekmantown Dolomite. This study is focused on the Rose Run Sandstone, which is a mixed siliciclastic-carbonate sequence in eastern Ohio. Numerous authors have suggested that deposition of the Knox Group was in a tidal-flat to shallow- marine environment along a broad continental shelf (Riley et al., 1993). Sedimentary dynamics are often more complex, where land meets the ocean, mainly because of diversity of the processes at work (e.g., rivers, tides, waves). This complexity becomes more pronounced in a mixed siliciclastic-carbonate environment where fluvial sediments are brought to areas with organisms producing a significant amount of sediments, where the former can potentially impact the latter with changes in environmental conditions (Ryan-Mishkin et al., 2009).

Tide-dominated settings display a wide variety of sediment types, textures, and sedimentary structures because of the relative interplay of tidal currents and tidal range with river systems and wave action. The daily reversals of tidal currents in oceanic settings influence a range of environments from the shoreline to deep-water, for example environments subjected to tidal action include beaches, tidal inlets, tidal deltas, lagoons, spits, barrier islands, and tidal flats (Klein, 1977). Tidal environments can be classified according to their tidal range, as macro-, meso-, and micro-tidal wherein the tidal range of a macro-tidal coast is $\geq$ 4m, a meso-tidal coast is between 2m and 4m, and a micro-tidal coast is $\leq$ 2m (Boggs, 2006). The relation between main types of tidal depositional system and tidal range is shown in Figure 1.
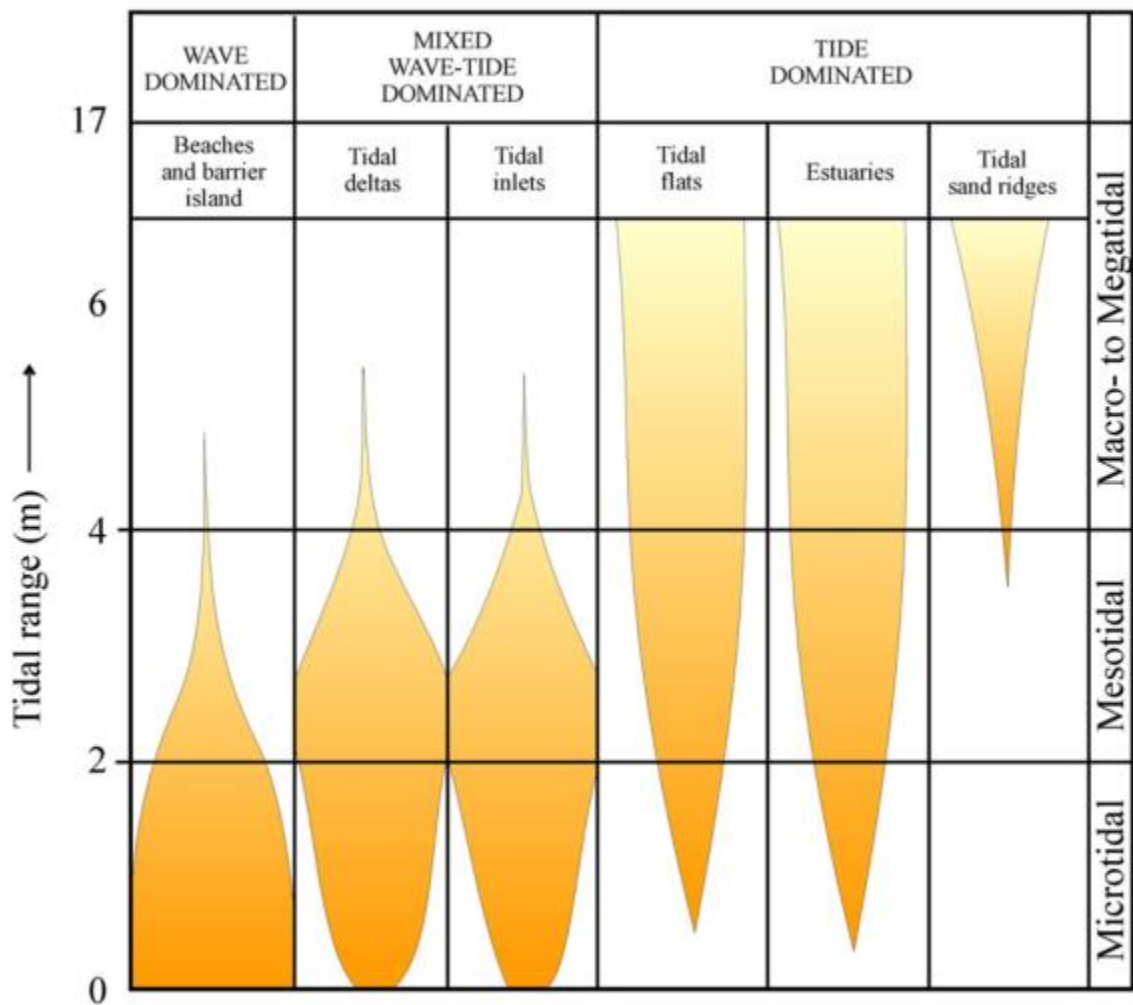
Figure 1. Main types of tidal depositional systems and their tidal range (adapted from Hayes, 1979)

Tidal flats

Tidal flats are widespread along shorelines that have a large tidal range. The tidal flats can be subdivided into upper tidal flat (supratidal zone), mid tidal flat (intertidal zone), and low tidal flat (subtidal zone). The supratidal zone occupies that part of coastal area that is above the mean high-tide level. This zone corresponds with the uppermost parts of beach ridges (backshore and aeolian dunes) and is inundated by the sea only during highest tides and storms. Various sub-environments of supratidal zone include salt marshes, mangrove swamps, and washover fans. The intertidal zone lies between mean low tide and mean high tide levels, and includes environments such as proximal tidal channels and intertidal flats of estuaries and deltas, as well as the foreshore of open coasts. The subtidal zone occurs below the mean low-tide level, where tidal currents and wave currents dominate. Different sub-environments of the subtidal zone include distal tidal channels of estuaries and deltas, wave-and tide- influenced delta fronts, and tide-influenced shorefaces (Longhitano et al., 2012).

Carbonate tidal flats (peritidal setting)

According to James and Dalrymple (2010), carbonate tidal flats are low-energy repositories of generally fine-grained sediment consisting mostly of allochthonous calcareous particles born in the subtidal carbonate factory, and these settings are dynamic and sensitive to storms, hurricanes, sea-level changes, and developments in adjacent areas. Depending on the facies, peritidal settings can be further subdivided into subtidal, intertidal, and supratidal zones like in clastic tidal flats. The subtidal zone consists of the carbonate factory, and the sediments in this zone are highly bioturbated, include pelleted lime mud, and are variably rich in shelly and skeletal material from benthic invertebrates and calcareous algae. Landward of this zone, the benthic community loses its members and the sediment is mainly allochthonous. Sediments in intertidal zone are also highly bioturbated and could be difficult to distinguish from shallow

subtidal deposits. However, grain size could be a key indicator due to allochthonous nature of sediments in this zone. Supratidal zones deposits are characterized by microbial mats and biofilms giving rise to microbially laminated mudstone. This zone receives sandy and muddy sediment only in event of storms or hurricanes (James and Dalrymple, 2010).

Purpose of Study

The Rose Run Sandstone is upper Cambrian in age and is mainly composed of siliciclastics (sandstone and shale) and carbonates (now mostly dolostone). In Ohio, the Rose Run Sandstone occurs entirely in the subsurface and is restricted in the eastern part of Ohio. The overlying Knox unconformity is the most important regional feature that affects the heterogeneity and reservoir performance of the Rose Run Sandstone (Riley and Baranoski, 1991). The subcrop of Rose Run Sandstone (where the unit truncates against the Knox unconformity) is shown in Figure 2.

Previous workers recognized that the Rose Run Sandstone is a highly compartmentalized reservoir which makes it a complex hydrocarbon play. It has been speculated that compartmentalization of the Rose Run Sandstone occurs at various scales, from regional to microscopic scales. On a regional scale, the heterogeneities of the Rose Run Sandstone could be due to stratigraphic, structural, and depositional variations whereas on smaller scale heterogeneities are mainly associated with mixture of carbonate and siliciclastic rocks and diagenetic modifications (Riley and Baranoski, 1991).

Chuks (2008) mainly used analysis of core and thin sections of the Rose Run Sandstone to interpret lateral pinch out and variation in lithology (Figure 3). However, Chuks's study was focused on interpretation of depositional environment, whereas this project involves evaluating compartmentalization of Rose Run Sandstone at various scales. The goal of this

Figure 2. Subcrop of the Rose Run Sandstone (shaded area) in Ohio (Adapted from Riley, 1994).

Subcrop marks the area where Rose Run Sandstone truncates against the Knox unconformity.
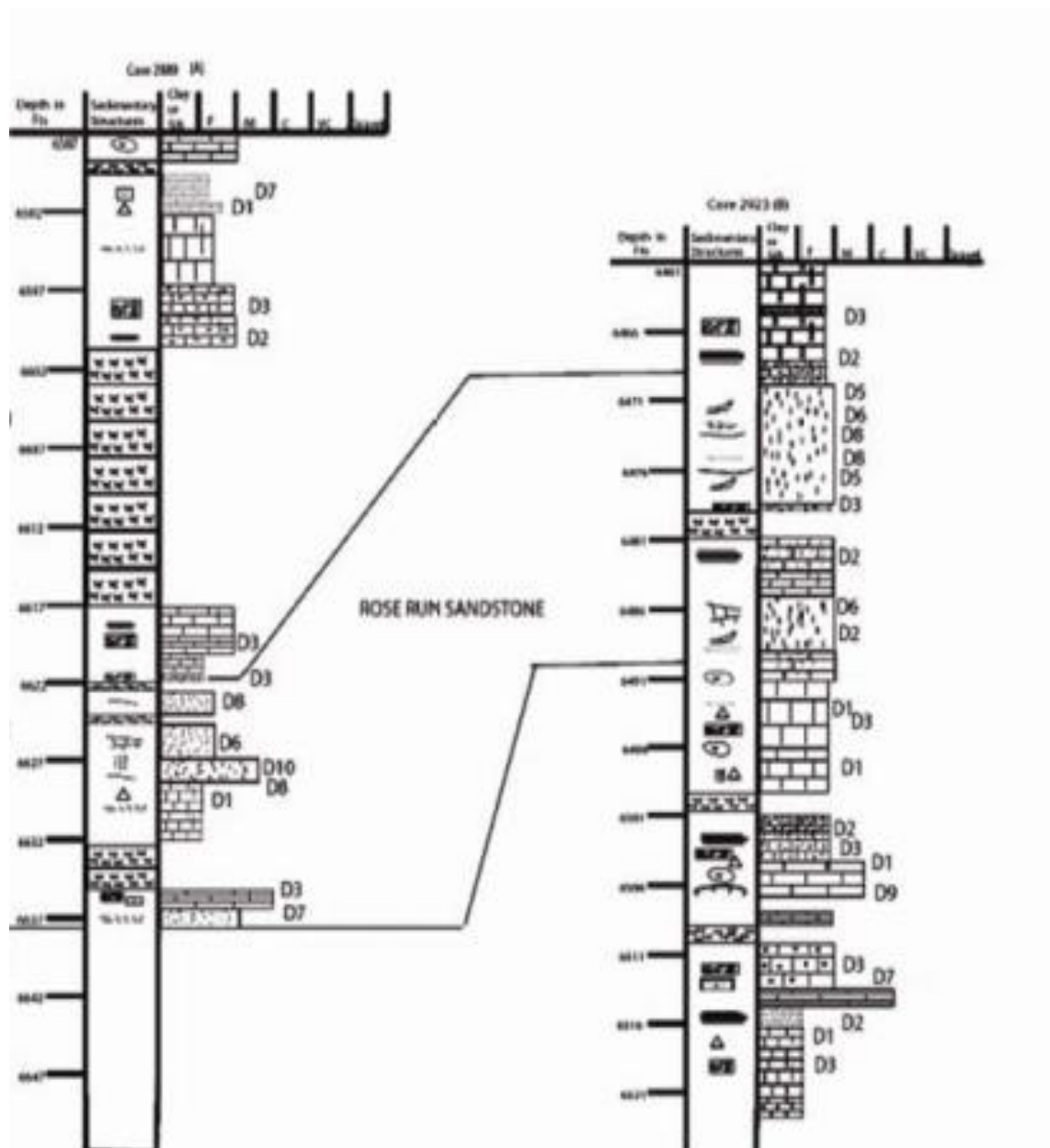
Figure 3. Core logs showing lateral and vertical variation in Rose Run Sandstone from core # 2989 and core # 2923. Details of lithofacies (D1, D2, etc) are shown in Table 4 (From Chuks, 2008).

project is to understand heterogeneities which leads to reservoir compartmentalization in the Rose Run Sandstone at macro-, meso-, and micro-scales.

To understand compartmentalization at macro- scale, a geophysical log model was created using isopach, sand isolith, and structure contour maps from 17 wells in eastern Ohio. The well data are based primarily on gamma- ray and density logs. This study constructs isopach, sand isolith, and structure contour maps to help illustrate hydrocarbon trapping mechanisms such as up-dip or lateral pinch outs of sandstone units, and also to help in understanding the depositional trend, distribution, and geometry of the Rose Run Sandstone in the study area.

Meso-scale compartmentalization was evaluated by studying hand specimens from 4 wells (# 2923, # 2989, # 2892, and # 3385). A total length of about 21 m of core samples was studied. These samples reveal heterogeneity through different lithofacies associated with the Rose Run Sandstone. An interpretation of different lithofacies was key to understanding the depositional process of the Rose Run Sandstone.

Micro-scale compartmentalization was evaluated by carrying out microfacies analysis from 10 thin sections. The primary goal of microfacies analysis is to understand the heterogeneity of the Rose Run Sandstone by investigating small scale variations in texture, mineralogy, and diagenesis. Microfacies analysis was used to estimate and determine mineral composition using the point counting method. A total of around 300 grains per thin section were counted and the percentage composition of the various components was calculated for each thin section.

Together, all of this information generated an understanding of the size, spatial distribution, and architecture of an ancient shallow marine environment. This represents a case

study which can be used to improve reservoir modeling for similar compartmentalized

reservoirs.

GEOLOGIC BACKGROUND

Tectonic setting and history

What is today both Ohio and Pennsylvania were part of Laurentia during the late Precambrian to early Cambrian. Towards the end of Precambrian and continuing into the Cambrian, the Laurentian continental plate began to separate from an eastern continental mass (Baltic plate), which resulted in formation of the Iapetus Ocean. According to Hansen (1998), Ohio was then on the stable, passive margin of the Laurentian continent, which had the ancient Canadian Shield as its nucleus (Figure 4). Physiographically, Laurentia was composed of a continental slope, continental rise, and continental shelf in the vicinity of Ohio and Pennsylvania (Riley et al., 1993). The Precambrian rocks in what is now Ohio and western Pennsylvania were uplifted and eroded during the early and middle Cambrian. With the rise in sea level in middle Cambrian, deposition of basal sands initiated on the Precambrian unconformity in Ohio and western Pennsylvania, and the southern margin of Laurentia subsided in response to increasing amount of sediments and lithospheric cooling.

By middle Cambrian, the Rome trough had begun to form along the southern margin of this exposed landmass (Riley, 1994). According to Harris (1978), the Rome trough is the failed arm of a triple junction, extending from the Mississippi embayment through Kentucky to Pennsylvania, and finally into New York. The aulacogen is believed to be originated on Precambrian crustal-block faults derived from stresses during opening of the Iapetus Ocean (Riley et al., 1993).

According to Riley (1994), the erosion of the uplifted continental land mass served as a source for the sands deposited throughout much of the late Cambrian. By then, they were mixed
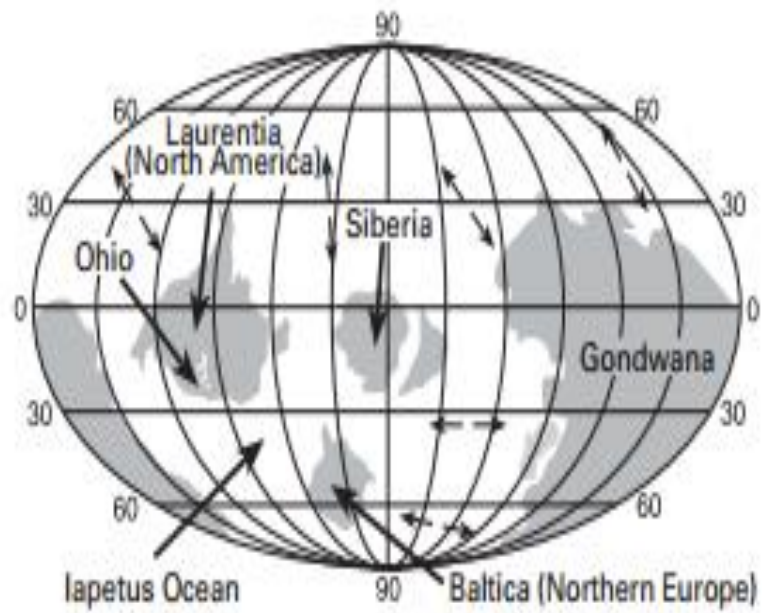
Figure 4. Continental configuration in Late Cambrian (from Hansen, 1998).

with the shelf carbonates of the Knox Group that eventually dominated sedimentation on the shelf. Towards the end of Cambrian, deposition of siliciclastics ceased, but deposition of carbonates continued.

According to Riley (1994), during Early to Middle Ordovician, change in stresses caused the collision of continental shelf of Laurentia with the Gondwana plate, which resulted in narrowing of Iapetus Ocean. This collision created a subduction zone, wherein the continental shelf of Laurentia buckled during the initial period of plate collision. It was faulted, folded, and uplifted, initiating a period of regional erosion of older rocks from north to south (present day east to west). This regional erosional surface is known as Knox unconformity.

In middle Ordovician during a high stand in sea level, the Knox unconformity was submerged and the post-Knox group sediments such as the shales of Wells Creek Formation were deposited on top of it.

Regional Stratigraphy

The distribution, stratigraphy and thicknesses of the different groups and formations in Ohio, specially the Knox Group and its correlative equivalent, are given in Figure 5. In this region, the Precambrian is represented by Grenville Province meta-igneous or igneous (extrusive and/or intrusive) rocks and meta-sedimentary rocks. The Precambrian basement is overlain by the basal Cambrian rock unit, the Mt. Simon Sandstone. The Mt. Simon Sandstone is a friable, fine- to coarse- grained sandstone. In Ohio, the unit ranges from 0 to nearly 121 m in thickness (Saeed, 2002). The middle to upper Cambrian Rome Formation and Conasauga Formation formed as offshore, shallow shelf and prodelta deposits derived from a northwest source area (Ryder et al., 1997). The Rome Formation, which is primarily dolomite, is more than 213 m thick in eastern Ohio, and thins to the west, becoming sandy in central Ohio. The overlying Conasauga Formation consists of red and green shales with interbedded glauconitic siltstone,
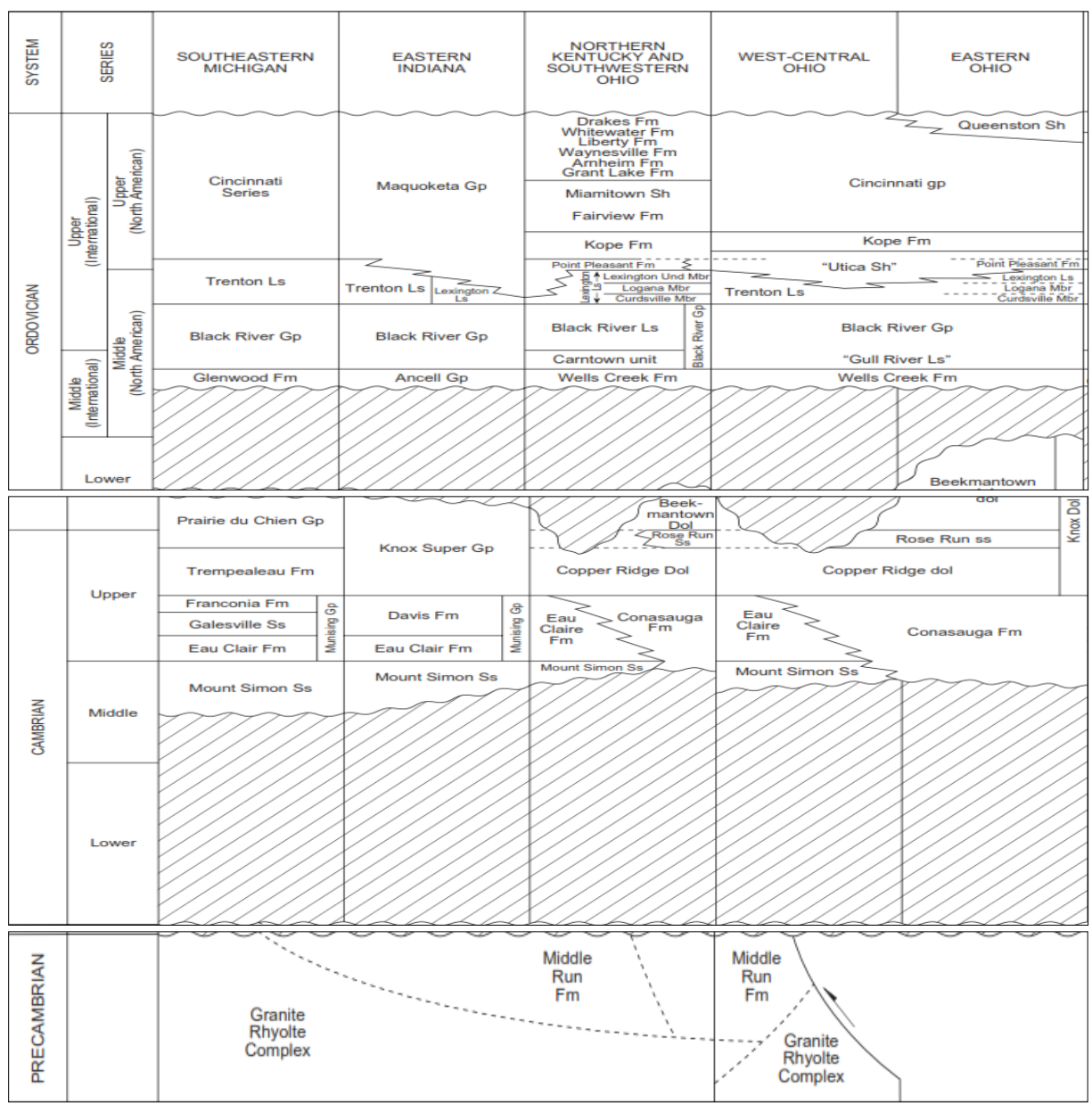
Figure 5. Showing regional stratigraphy of the Rose Run Sandstone (from Patchen et al., 2006)

limestone, dolomite, and very fine-grained sandstone, with thickness ranging from 12 to 137 m (Janssens, 1973). The Conasauga Formation grade westward into the Eau Claire Formation which is composed of sandstone, siltstone, shale, and dolomite. These are offshore deposits related in part to the overlying unit, the Kerbel Formation, a coarsening-upward sandstone that is interpreted to be a wedge of deltaic sediments (Banjade, 2011). According to Ryder et al. (1997), the Knox Group is the unit of deposition between the Conasauga Group and the Knox unconformity. The Knox Group is made up mostly of dolostone with minor sandstone and chert. The unit is subdivided into the Copper Ridge Dolomite, the Rose Run Sandstone (a thin unit of sandstone), and the Beekmantown Dolomite (Figure 5). The Copper Ridge Dolomite is the equivalent of the Ore Hill Member of the Gatesburg Formation of Pennsylvania, while the Beekmantown Dolomite is the correlative equivalent of the lower part of the Beekmantown Group of Pennsylvania (Riley et al., 1993).

Rose Run Sandstone

Natural gas was first produced from the Rose Run Sandstone in 1965 in Holmes County, Ohio. Since then the Rose Run Sandstone has been the focus of exploration activity in eastern part of Ohio and recently it is being considered as a potential reservoir for CO_2 sequestration. However, there is still a belief among petroleum geologists (personal communication with geologists) that potential hydrocarbon production from the Rose Run Sandstone is limited by compartmentalization of the reservoir.

Lithology

The lithology of the Rose Run Sandstone is comprised of interbedded sandstone, shale, and dolostone. Sandstones consist of quartz arenite, sub-feldspathic arenite and feldspathic arenite (Enterline, 1991 ; Atha, 1981). Based on core analysis, subsurface mapping, and petrophysical analysis, the Rose Run Sandstone consists of cross- bedded and flaser-bedded,

argillaceous sandstone, interbedded glauconitic sandstone and dolostone, bioturbated dolostone, and laminated dolostone (Riley et al., 1993 ; Chuks, 2008).

Stratigraphy and Age

The Knox Dolomite (Cambrian to Ordovician) is formally divided into Copper Ridge Dolomite, Rose Run Sandstone, and Beekmantown Dolomite. The Rose Run Sandstone was first described by Freeman (1949) from the Judy and Young #1 Rose Run Iron Co. well in Bath county, northeastern Kentucky (Riley et al., 1993).   The Rose Run Sandstone is Upper Cambrian to Early Ordovician in age and the fossil assemblages in the Knox Group during Late Cambrian are as shown in Table 1. The unit can be found in Ohio, West Virginia, and Kentucky. The Rose Run Sandstone comprises interbedded sandstone and dolomite in the northeastern part of Kentucky (Atha, 1981). According to McGuire and Howell (1963) and Patton and Dawson (1969), the Rose Run Sandstone grades into dolomite in the western and southern Kentucky, whereas in the northwestern part of the state, it is truncated by the Knox unconformity. In Ohio, the Rose Run Sandstone is restricted to the eastern part of Ohio. This unit forms in the western part of the Appalachian basin but is erosively truncated at the Knox unconformity by Middle Ordovician. According to Riley et al., (1993), the Knox unconformity inclines gently about 9.5 m/km to the southeast from Ohio into the southwest Virginia and Pennsylvania. To the east, the Rose Run Sandstone pinches out into a dolomitic unit (Atha, 1981). Riley et al. (1993) state that the Rose Run Sandstone is approximately equivalent to other clastic intervals. In the Michigan basin, the Jordan Sandstone was correlated by Janssens (1973) and McGuire and Howell (1963) to the Rose Run Sandstone. The Jordan Sandstone is 182 m thick in Michigan, and thins to the southeast into Ohio, where it is truncated by the Knox unconformity, and eroded over the Findlay-Algonquin arch.

Table1. Fossil assemblage found in Knox Group in Late Cambrian (From Chuks, 2008).

Major Groups	Taxa	References
Trilobites	*Saukia sp* *Ptychaspis-prosaukia sp* *Conaspis sp* *Elivinia sp*	Riley et al., 1993
	Dunderbergia sp *Aphelaspis sp* *Crepicephalus sp* *Cedaria sp* *undetermined polymeroids*	Babcock, 1994
Echinoderms	*undertermined ossicles*	
Graptolite	*undertermined dendroid*	
Scyphozoan	*Medusa or jelly fish*	Hagadorn et al., 2002

Depositional Environment

Riley et al. (1993) used subsurface mapping, petrophysical and core analysis to divide Rose Run Sandstone into four lithofacies, namely 1) cross-bedded and flaser-bedded, argillaceous sandstone, 2) interbedded glauconitic sandstone and dolostone, 3) bioturbated dolostone and 4) laminated dolostone. Based on sedimentary structures as given in (Table 2) from the three principal facies, Riley et al. (1993) interpreted the Rose Run Sandstone to represent peritidal to shallow marine environments (Table 2).

Enterline (1991) used three cores (the Beckwith well and the Parabek well from Ashtabula County in Ohio, and the Hammermil well from Erie County in Pennsylvania) to interpret the depositional environment of the Rose Run Sandstone. On the basis of sedimentary structures, Enterline (1991) interpreted it as a tidal flat environment with migrating tidal channels (Table 3). During the course of his study four facies types were delineated: the sandstone facies overlain by oncolite facies, overlain by bioturbated facies, which is finally overlain by the algal laminated/stromatolite facies at the top (Enterline, 1991).

Atha (1981) used 6 cores [the Geib # 1 well in Holmes County (permit no. 1288), Barth # 1 and Vickers # 1 in Coshocton County (permit no. 2653 and 2268), Denny #1 in Columbiana County (626), Trepanier # 1 in Jackson County (102), and U.S. Steel # 1 in Scioto County (212)] to examine the Rose Run Sandstone. Atha (1981) observed stacked hemispheroid stromatolites, wavy and lenticular bedding, herringbone cross stratification, reactivation surfaces, flat-pebble conglomerate, massive bedding and large rounded limestone intraclasts from the cores. Consequently, he interpreted that the depositional unit formed in peritidal environment.

Chuks (2008) used 4 cores from wells located in Scioto County (core # 3409), Jackson County (core # 2898), Coshocton County (core # 2989), and Morgan County (core # 2923) to

Table 2. Lithofacies and interpreted depositional environment of the Rose Run Sandstone based on following sedimentary structures (Riley et al., 1993).

Lithofacies	Lithology	Sedimentary structure	Interpretation
1	Heterolithic sandstone and shale	Wavy bedded, flaser bedded and cross laminated	Shallow subtidal
2	Limestone	Massive (ooids and peloids)	Carbonate sand shoals
3	Dolostone	Massive, bioturbated	Carbonate tidal flats
4	Dolostone	Scours, intraclasts	Carbonate tidal flats
5	Limestone	Algal lamination, stromatolites	Carbonate tidal flats
6	Sandstone	Herringbone cross bedding	Shallow subtidal

Table 3. Lithofacies and interpreted depositional environment of the Rose Run Sandstone. (From Enterline, 1991).

Lithofacies	Lithology	Sedimentary structure	Interpretation
1	Very fine to coarse grained, rounded to well rounded sandstone	Low to high angle cross bedding, rip up clast, current ripples, herringbone cross bedding	Tidal channel (clastics)
2	Dolomite	Oncolites, rip-up clasts	Tidal channel (carbonate)
3	Dolomite	Massive with bioturbation	Intertidal environment
4	Dolomite	Algal laminated or stromatolites, mud cracks	Lower supratidal to upper intertidal

interpret the depositional environment of the Rose Run Sandstone. On basis of sedimentary structures, he interpreted the depositional environment as tidally influenced, subtidal environments with associated tidal flat deposits and related subtidal channels with migrating sandbars (Table 4). Chuks (2008) created a tidally –influenced shallow marine depositional model for the Rose Run Sandstone (Figure 6).

The differences in interpretation of depositional environment among various workers could be mainly related to different locations of the cores studied. Some of these cores are separated by distances >10's of km, hence it is understandable that they are influenced by the same depositional processes, but variation in relative importance of environmental parameters such as water depth, relative importance of waves versus tides, and sediment supply leads to development of variety of sedimentary structures. This results in differences in interpretations of depositional environment.

Table 4. Lithofacies and interpreted depositional environment of the Rose Run Sandstone.
(Chuks, 2008).

| Lithofacies	Lithology	Sedimentary structure	Interpretation
D1	Packstone	Mottling, Massive	Bioturbated carbonate
D2	Heterolithic sandstone	Laminated	Tidal rhythmites
D3	Arenaceeous Packstones	Intraclasts	Reworked arenaceous dolostone (desiccation cracks)
D4	Sandstone	Intraclasts	Reworked mud chips (desiccation cracks)
D5	Heterolithic sandstone and mudstone	Flaser, wavy, and lenticular bedding	Ripple marks with mud drapes (tidal)
D6	Sandstone	Planar tabular cross bedding	Sand bars/dunes
D7	Oolitic grainstone	Ooids	High energy beach and shoal
D8	Sandstone	Current ripple lamination	Ripple marks with mud drapes (tidal)
D9	Carbonate mudstone	Algal lamination	Stromatolites
D10	Sandstone	Massive, burrows	Bioturbated sandstone
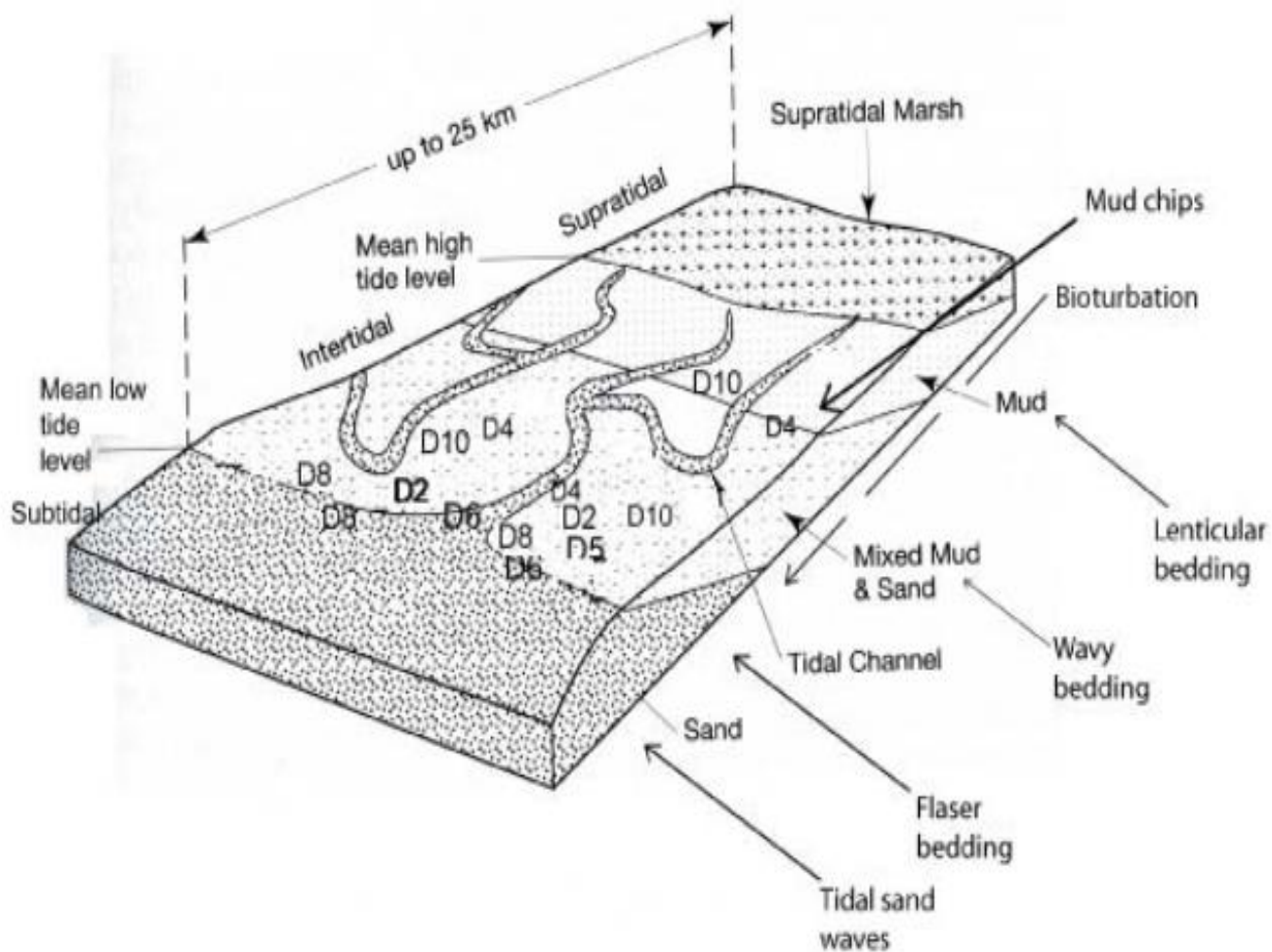
Figure 6. Depositional model of the Rose Run Sandstone based on sedimentary structures observed (Chuks, 2008).

METHODS

Study Area

The study area was selected based on availability of good core sections and geophysical logs from different wells. Using the GIS based interactive maps on Ohio Division of Geological Survey website, information about cores and geophysical logs was obtained and ultimately the area of study was determined. The study area covers an area of about 10,000 km^2 (125 km N-S × 80 km E-W) as shown in Figure 7.

Petrofacies Analysis

A total of 10 sandstone samples were chosen for thin section analysis. Core sections were then cut into chips and sent to Applied Petrographic Services, Inc. for preparation of thin sections. Thin section analysis was carried out using a petrographic microscope and involved studying textural and mineralogical heterogeneity in the Rose Run Sandstone. Point counting involved identification of ≥300 grains per thin section, following the Gazzi-Dickinson method (Dickinson and Suczek, 1979). Porosity was estimated as percent void space.

Core Analysis

The cores are held at Horace Collins Core Laboratory in Columbus, Ohio. The cores were laid out in boxes of 1 to 2 m length. A total of 4 cores were examined, with a total thickness of about 21 m. Each core was observed at cm-scale to analyze textural and mineralogical variations and sedimentary structures in the Rose Run Sandstone. Interesting zones in the cores were sampled and photographed using a digital camera. A total of 15 samples were collected from 4 cores and 10 samples were selected to carry out detailed micro-facies analysis. On several occasions, small intervals of the Rose Run Sandstone were found missing which could be due to
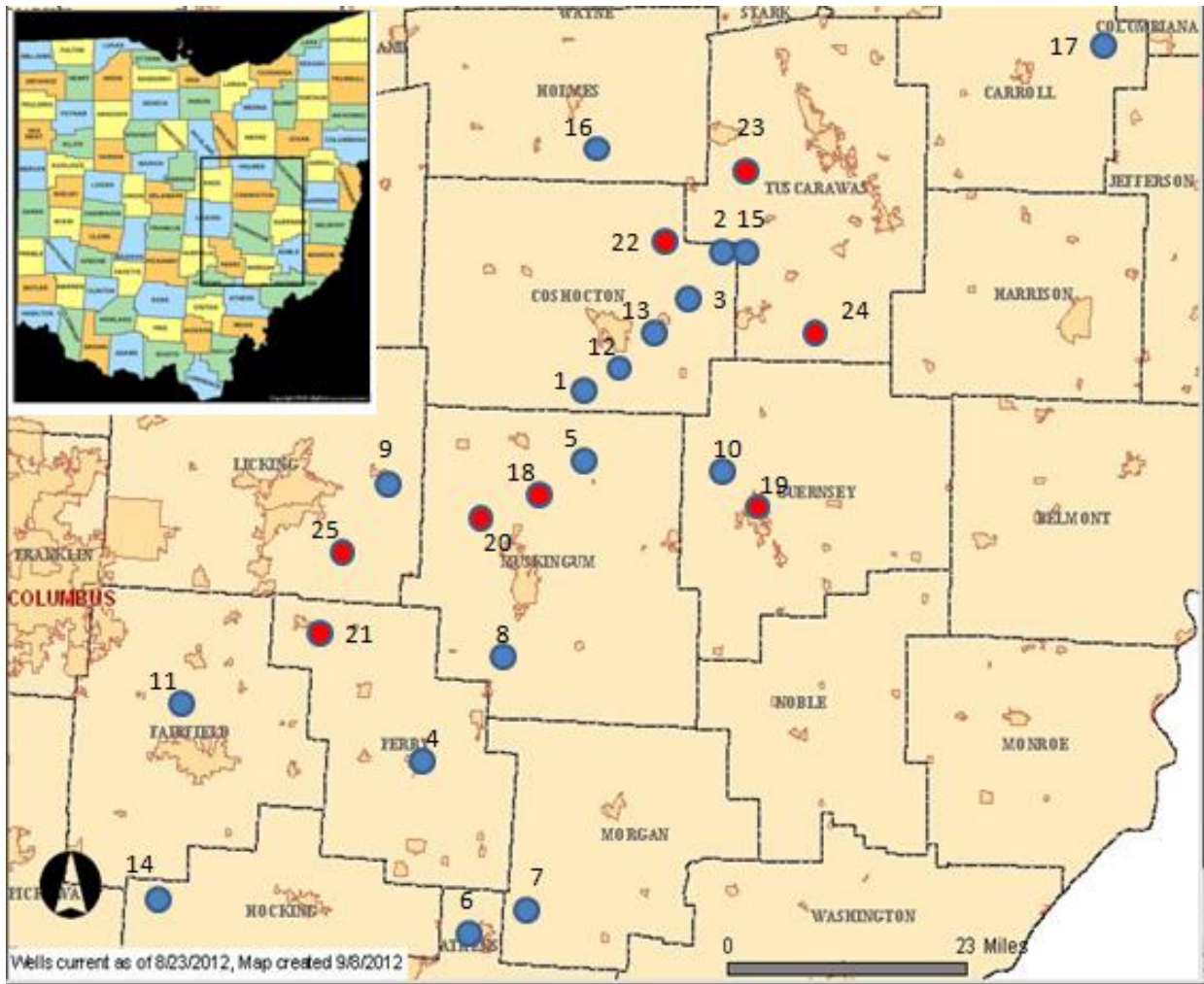
Figure 7. Map showing distribution of wells and core (Table 5) used for the study. Blue circles indicate the location of well logs that were used, and red circles indicate the location of well logs that were not used due to poor quality. The inset map shows the location of the study area in Ohio.

poor recovery of core or it had been previously sampled which was evident from markers kept in core boxes.

Geophysical Log Analysis

Geophysical log analysis involved interpreting data from 17 well logs. This study used gamma- ray logs and density logs for analysis. The well logs were ordered from Ed Kuehnle and Midak Fadge at ODNR-Division of Geological Survey, and were obtained as scanned images of paper logs. Out of 25 sets of logs originally requested (Table 5), only 17 wells were used because some of them are of poor quality and difficult to read. All the digitized geophysical logs were imported into Adobe Illustrator and were photo enhanced to improve the visual quality of the geophysical logs. Table 6 shows the details of the well log used.

Gamma-ray log

The gamma-ray (GR) log measures the natural radioactivity of strata in a well and hence GR log response is related to the presence of radioactive minerals as ^{238}U, ^{40}K, and ^{232}Th. Because shales are rich in clay which often contains radioactive minerals, shale typically shows higher readings in the GR log. Also, the cation exchange capacity of clay causes adsorption of radioactive minerals such as uranium or thorium. In general, sandstone or carbonates will show lower gamma ray reading unless they have been associated with radioactive minerals (Miall, 1984). The GR log was used to distinguish between shale and sandstone or dolostone in Rose Run Sandstone.

Density log

The density log measures the electron density of rocks by bombarding them with gamma-rays and measuring the resulting backscatter of radiation. The amount of backscattering is roughly proportional to the bulk density of the formation and it provides a good estimate of the

Table 5. Details of well logs ordered from ODNR.

This study assigned well numbers	API Well Number	Longitude	Latitude	OGS Core no.	Logging Total Depth	
					Feet	Meters
1	34031221830000	-81.906551	40.174255	3384	6108(DTD)	1862
2	34031240920000	-81.650407	40.358834	2713	6985	2130
3	34031226530000	-81.773847	40.318718	3006	6660(DTD)	2030
4	34127273750000	-82.263862	39.740896	none	5256	1602
5	34119283180000	-81.896663	40.075895	none	6419	1957
6	34009230620000	-82.075643	39.428049	none	6502	1982
7	34115212490000	-82.019424	39.492655	2923	6521(DTD)	1988
8	34119282210000	-82.061556	39.837447	none	5898	1798
9	34089256390000	-82.228258	40.167166	none	5068	1545
10	34059239450000	-81.705564	40.025888	none	7370	2247
11	34045212620000	-82.674197	39.835653	none	3696	1127
12	34031269120000	-81.868122	40.20141	none	6294	1919
13	34031260430000	-81.802739	40.264876	none	6630	2021
14	34073233590000	-82.712561	39.525245	none	3815	1163
15	34031259620000	-81.638502	40.337347	2989	6902	2104
16	34075212790000	-81.765885	40.539246	2892	6701	2043
17	34133241310000	-81.170109	41.060848	none	7539	2298
18	34119278970000	-82.145716	40.08316	none	5425	1654
19	34059239830000	-81.694296	39.992231	none	7140	2177
20	34119284240000	-81.920711	40.077561	none	6060	1848
21	34127271710000	-82.423247	39.850253	none	3053	931
22	34031235480000	-81.669012	40.357338	none	7032(DTD)	2144
23	34157241010000	-81.690348	40.40133	none	6870(DTD)	2095
24	34157209520000	-81.437863	40.31123	2964	7708	2350
25	34089255850000	-82.351729	40.017781	none	3891	1186

Note: Drilling total depth (DTD) is used where logging total depth (LTD) is not available.

Table 6. Additional details of available well logs.

This study assigned well numbers	Logging Company	Date of completion	Geophysical logs	Well terminates in	Hydrocarbon Production from RRS	Data use
1	Schlumberger	7/4/1973	Gamma and Density	RRS	No	used
2	Schlumberger	12/22/1980	Gamma and Density	RRS	Yes	used
3	Schlumberger, Gearhart-owen	11/4/1978	Gamma and Density	RRS	No	used
4	Appalachian Well Surveys	6/2/2008	Gamma and Density	RRS	No	used
5	Timco, Inc., Superior Well Services	1/26/2001	Gamma and Density	RRS	No	used
6	Schlumberger	7/17/1984	Gamma and Density	RRS	No	used
7	Schumberger	1/26/1972	Gamma and Density	TPL	No	used
8	Eastern	6/21/1999	Gamma and Density	RRS	No	used
9	Eastern	3/20/1998	Gamma and Density	RRS	Yes	used
10	Appalachian Well Surveys	12/7/2002	Gamma and Density	RRS	No	used
11	Superior Well Services	7/9/2000	Gamma and Density	RRS	Yes	used
12	Superior Well Services	11/18/2003	Gamma and Density	RRS	No	used
13	Perfection services Inc, Schlumberger	2/14/1988	Gamma and Density	RRS	No	used
14	Eastern	11/5/1992	Gamma and Density	RRS	Yes	used
15	Gearhart-Owen	3/23/1987	Gamma and Density	RRS	No	used
16	Birdwell	12/1/1963	Gamma	TPL	No	used

Table 6. Cont.

This study assigned well number	Logging Company	Date of completion	Geophysical logs	Well terminates in	Hydrocarbon Production from RRS	Data use
17	Eastern	12/12/1997	Gamma and Density	RRS	Yes	used
18	Allegheny	9/3/2005	none	RRS	No	not used due to poor quality
19	Allegheny	5/18/2003	none	RRS	No	not used due to poor quality
20	Eastern	8/25/1996	none	RRS	Yes	log is not deep enough
21	Schlumberger	6/25/1979	none	RRS	No	not used due to poor quality
22	Enervest Operating	12/19/1986	none	RRS	Yes	not used due to poor quality
23	Schlumberger	9/8/1965	none	RRS	No	not used due to poor quality
24	Schlumberger	8/31/1996	none	RRS	No	not used due to poor quality
25	Perfection Services Inc	8/28/1994	none	RRS	Yes	not used due to poor quality

Note: Abbreviations – RRS for Rose Run Sandstone, CL for Clinton Group, TPL for Trempaleau Formation, and BR for Black River Formation.

porosity in the unit. The density log was used to differentiate between sandstone and dolostone and a value of ≤2.70 g/cm^3 is used to recognize sandstone. Core-log correlation from different wells shows some sandstone beds having a density value of about 2.70 g/cm^3 and hence it was used as cut off value to differentiate between sandstone and dolostone.

Formation top and bottom were picked by observing the distinctive log patterns and also by consulting well reports. The geophysical logs from 17 wells were used to make a structure contour map, an isopach map, a sand-isolith map, and two electro-log correlation profiles of the Rose Run Sandstone. The subsurface maps were created using the Surfer (version 8) program. Surfer requires inputting X, Y, Z values to make maps. Longitude and latitude were used for X and Y values and Z value were either the depth to the top of the Rose Run Sandstone, or the total thickness of the Rose Run Sandstone, or the sand thickness of the Rose Run Sandstone. With the surfer program, krigging was the gridding method used for the construction of subsurface maps. Krigging estimates the value at unknown points by averaging the known values of its neighbors. This method is generally considered as the default grid method for contouring. Surfer was also used in generating profile along a section of structure contour map. For subsurface maps, all the elevation or thickness values used have been converted from feet to meters.

Lithocorrelation profiles

Correlation of stratigraphic units is necessary to conduct regional facies analysis. Two correlations profiles (north-south and east-west) have been generated to understand the geometry of the unit. These correlation profiles were constructed using pattern matching technique involving recognition and matching of distinctive density log. By matching density log shapes, correlations can be made between wells separated by 10's of km. Density logs were used for correlation because it served to distinguish between sandstone and dolostone.

Structure Contour map

A structure contour map was generated from the elevation of the top of Rose Run Sandstone with respect to mean sea level. The elevation of the top of the Rose Run Sandstone was calculated by subtracting ground level elevation from core depth (after correcting for the elevation of well head). The values are all shown as elevation below mean sea level (MSL). Information about the ground level elevation and the well head elevation were obtained from well completion reports, which are available at the Ohio Geological Survey web site (www.dnr.state.oh.us/geosurvey). The details of the data set used to create the structure contour map of the Rose Run Sandstone are given in Table 7 and the map itself is shown in Figure 38, 39, and 41.

Isopach map

An isopach map represents the total thickness of a stratigraphic interval by subtracting the elevation of the top stratigraphic contact from the elevation of the bottom stratigraphic contact. For the Rose Run Sandstone, the contacts were identified using both the gamma ray and density log (Table 8). In total, 16 wells were used for the construction of isopach map. Data from well # 17 was not used because it is located too far away from other wells and hence it increased the uncertainty in the interpretation of the data set. The same well was used to construct structure contour map because there is not as much difference in the trend of the structure. The isopach map of the Rose Run Sandstone is shown in Figure 43.

Sand-Isolith map

A sand-isolith map of the Rose Run Sandstone was created by taking into account only sandstone thickness (calculated by subtracting the thickness of dolomite and shale intervals from the total thickness). In total, 16 wells were used to construct the sand-isolith map (Table 9). Both the gamma-ray log and density log were used to determine sand interval thickness needed to

construct the sand-isolith map. The sand-isolith map of the Rose Run Sandstone is shown in

Figure 45.

Table 7. Data used to create structure contour map.

This study well number	API well number	Core depth to upper contact of RRS		Elevation of ground level + well head ht.		Elevation of upper contact of RRS	
		Feet	Meters	Feet	Meters	Feet	Meters
1	34031221830000	-5986	-1825	800	244	-5186	-1581
2	34031240920000	-6914	-2107	1030	314	-5884	-1793
3	34031226530000	-6618	-2017	1128	344	-5490	-1673
4	34127273750000	-5154	-1571	916	279	-4238	-1292
5	34119283180000	-6276	-1913	966	295	-5310	-1618
6	34009230620000	-6394	-1949	895	273	-5499	-1676
7	34115212490000	-6460	-1969	862	263	-5598	-1706
8	34119282210000	-5654	-1723	754	230	-4900	-1494
9	34089256390000	-5003	-1525	966	295	-4037	-1230
10	34059239450000	-6994	-2132	853	260	-6141	-1872
11	34045212620000	-3554	-1083	866	264	-2688	-819
12	34031269120000	-6148	-1874	841	256	-5307	-1618
13	34031260430000	-6454	-1967	1060	323	-5394	-1644
14	34073233590000	-3730	-1137	1015	309	-2715	-828
15	34031259620000	-6616	-2017	860	262	-5756	-1754
16	34075212790000	-6402	-1951	1088	332	-5314	-1620
17	34133241310000	-7370	-2246	1189	363	-6181	-1884

Notes: Negative elevation values mean depth below mean sea level (MSL). The abbreviation RRS means Rose Run Sandstone.

Table 8. Data used to create Isopach map.

This study well number	API well number	Elevation of the top of RRS		Elevation of bottom of RRS		Total RRS thickness	
		Feet	Meter	Feet	Meter	Feet	Meter
1	34031221830000	-5986	-1825	-6056	-1846	70	21
2	34031240920000	-6914	-2107	-6974	-2126	60	18
3	34031226530000	-6618	-2017	-6660	-2030	42	13
4	34127273750000	-5154	-1571	-5200	-1585	46	14
5	34119283180000	-6276	-1913	-6406	-1953	130	40
6	34009230620000	-6394	-1949	-6418	-1956	24	7
7	34115212490000	-6460	-1969	-6510	-1984	50	15
8	34119282210000	-5654	-1723	-5742	-1750	88	27
9	34089256390000	-5003	-1525	-5043	-1537	40	12
10	34059239450000	-6994	-2132	-7066	-2154	72	22
11	34045212620000	-3554	-1083	-3600	-1097	46	14
12	34031269120000	-6148	-1874	-6224	-1897	76	23
13	34031260430000	-6454	-1967	-6542	-1994	88	27
14	34073233590000	-3730	-1137	-3786	-1154	56	17
15	34031259620000	-6616	-2017	-6626	-2020	10	3
16	34075212790000	-6402	-1951	-6407	-1953	5	2

Notes: Negative elevation values mean depth below mean sea level (MSL). The abbreviation RRS means Rose Run Sandstone.

Table 9. Data used to create sand-isolith map.

This study well number	API well number	Elevation of top of RRS		Elevation of bottom of RRS		Total RRS thickness		Total sandstone thickness	
		Feet	Meter	Feet	Meter	Feet	Meter	Feet	Meter
1	34031221830000	-5986	-1825	-6056	-1846	70	21	30	9
2	34031240920000	-6914	-2107	-6974	-2126	60	18	40	12
3	34031226530000	-6618	-2017	-6660	-2030	42	13	25	8
4	34127273750000	-5154	-1571	-5200	-1585	46	14	22	7
5	34119283180000	-6276	-1913	-6406	-1953	130	40	52	16
6	34009230620000	-6394	-1949	-6418	-1956	24	7	18	5
7	34115212490000	-6460	-1969	-6510	-1984	50	15	24	7
8	34119282210000	-5654	-1723	-5742	-1750	88	27	46	14
9	34089256390000	-5003	-1525	-5043	-1537	40	12	13	4
10	34059239450000	-6994	-2132	-7066	-2154	72	22	48	15
11	34045212620000	-3554	-1083	-3600	-1097	46	14	20	6
12	34031269120000	-6148	-1874	-6224	-1897	76	23	35	11
13	34031260430000	-6454	-1967	-6542	-1994	88	27	42	13
14	34073233590000	-3730	-1137	-3786	-1154	56	17	46	14
15	34031259620000	-6616	-2017	-6626	-2020	10	3	8	2
16	34075212790000	-6402	-1951	-6407	-1953	5	2	5	2

Notes: Negative elevation values mean depth below mean sea level (MSL). The abbreviation RRS means Rose Run Sandstone.

RESULTS

Core Descriptions

The core sections from 4 wells were studied, with emphasis on distribution of texture, mineralogy, sedimentary structures and lithofacies. In total, 14 siliciclastic and 5 carbonate lithofacies were identified in the unit.

Core 2892

In this core, the thickness of sandstone is 2 meters, as shown in figure A-II (Appendix II), and this sandstone interval is overlain and underlain by compact dolostone. Previous workers have sampled most of this sandstone interval, but around 40 cm of core was available for analysis. In this core, lithofacies which have been identified are massive sandstone and massive glauconite-rich sandstone. Figure 8 shows gamma-ray log and caliper log for the same well. The top and bottom contacts of Rose Run Sandstone are marked based on core observations for the same well at same depth. Although the interval below Rose Run Sandstone has a similar GR log signature, investigation of core found all of it to be dolostone.

Core 2923

The total thickness of the sandstone in this well is about 15 m (Figure 9) with core recovery of about 14 m (Figure A-II). The core boxes laid out for this well contained only the Rose Run Sandstone, including sandstone, shale and dolostone. In total, 13 lithofacies were identified in this core, 8 siliciclastic and 5 carbonate lithofacies. The core shows gradational contacts between sandstone and dolostone but abrupt (erosive) contact can be seen between sandstone and shale. The core is very heterogeneous and displays a wide variety of sedimentary structures. Other interesting features in this core included vugs filled with chert, mottling, open (unhealed) fractures in sandstone and dolostone, and stylolites. A total of 7 thin sections were

made from this core. Figure AII shows logged section of the core and Figure 9 shows the well logs for this well. The top and bottom contacts of the Rose Run Sandstone are marked based on lower density value (indicating sandstone). Examination of the core study confirmed the Rose Run Sandstone at the same depth as seen in geophysical logs.

Core 2989

The total thickness of sandstone in this well is around 3 m, as shown in figure A-II. A total of 9 lithofacies, (7 siliciclastic and 2 carbonate), have been identified from this core. This core also shows all the three lithologies, sandstone, shale, and dolostone. A small part of the core is found missing in its lower section, as shown in figure A-II. Figure 10 shows the gamma-ray log and density log for the same well. The elevation of the top and bottom of the Rose Run Sandstone in this well are marked by matching the depth of the core. The density log for the Rose Run Sandstone interval in this core is about $2.7 g/cm^3$, which is higher than typical sandstone, probably due to cementation. Core analysis also found the hand samples to be well cemented. No thin sections were made from this core.

Core 3385

The cored interval of Rose Run Sandstone in this well is about 2.5 m. The total thickness of Rose Run Sandstone in this well could not be ascertained because geophysical logs for the well are not available. A total of 9 lithofacies, (7 siliclastic and 2 carbonate), were identified in this core. All the three lithologies can be found in this core. A total of 3 thin sections were made from different interval in core, as shown in figure A-II.
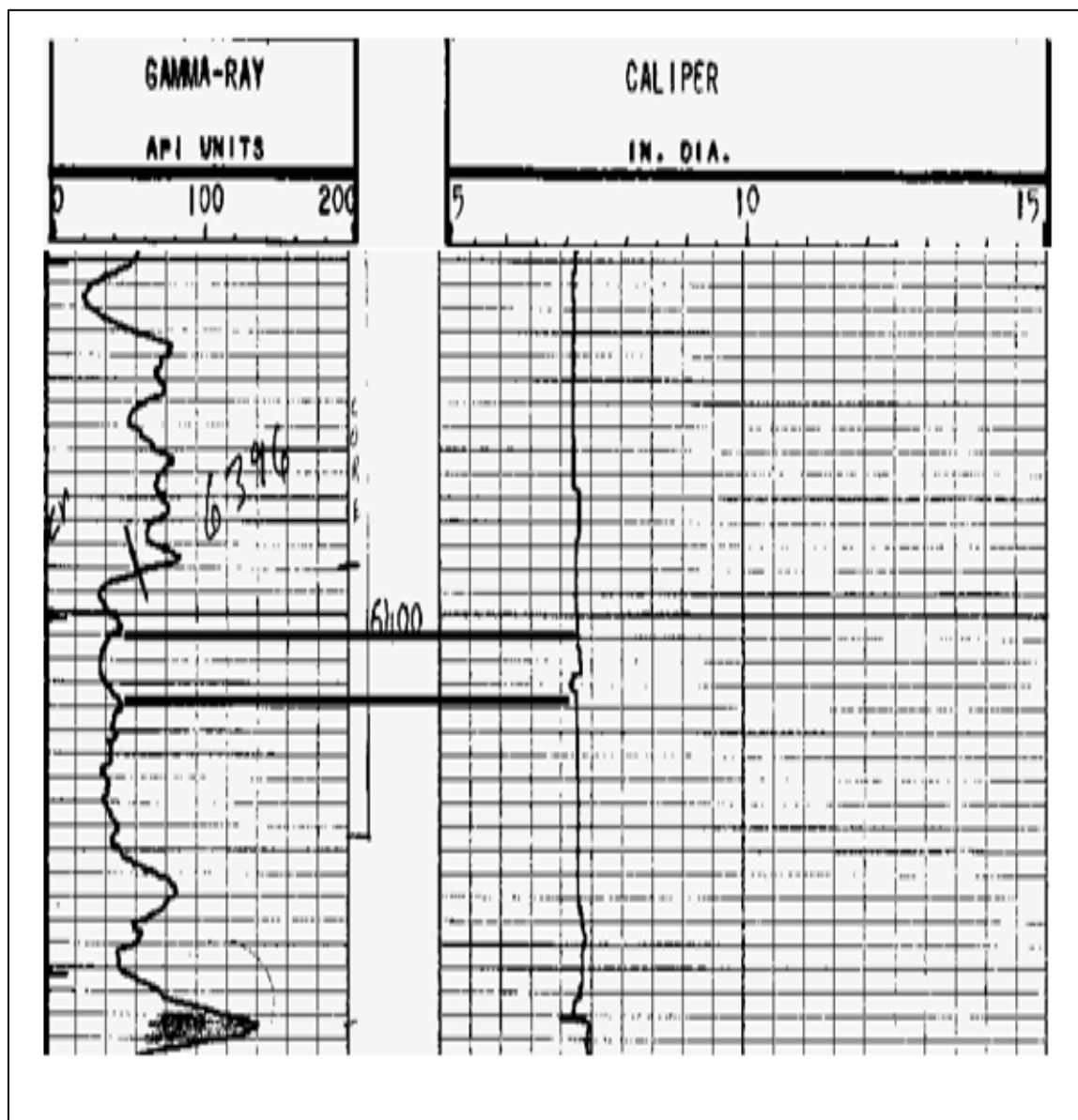
Figure 8. Gamma-ray and caliper log for the well # 16.
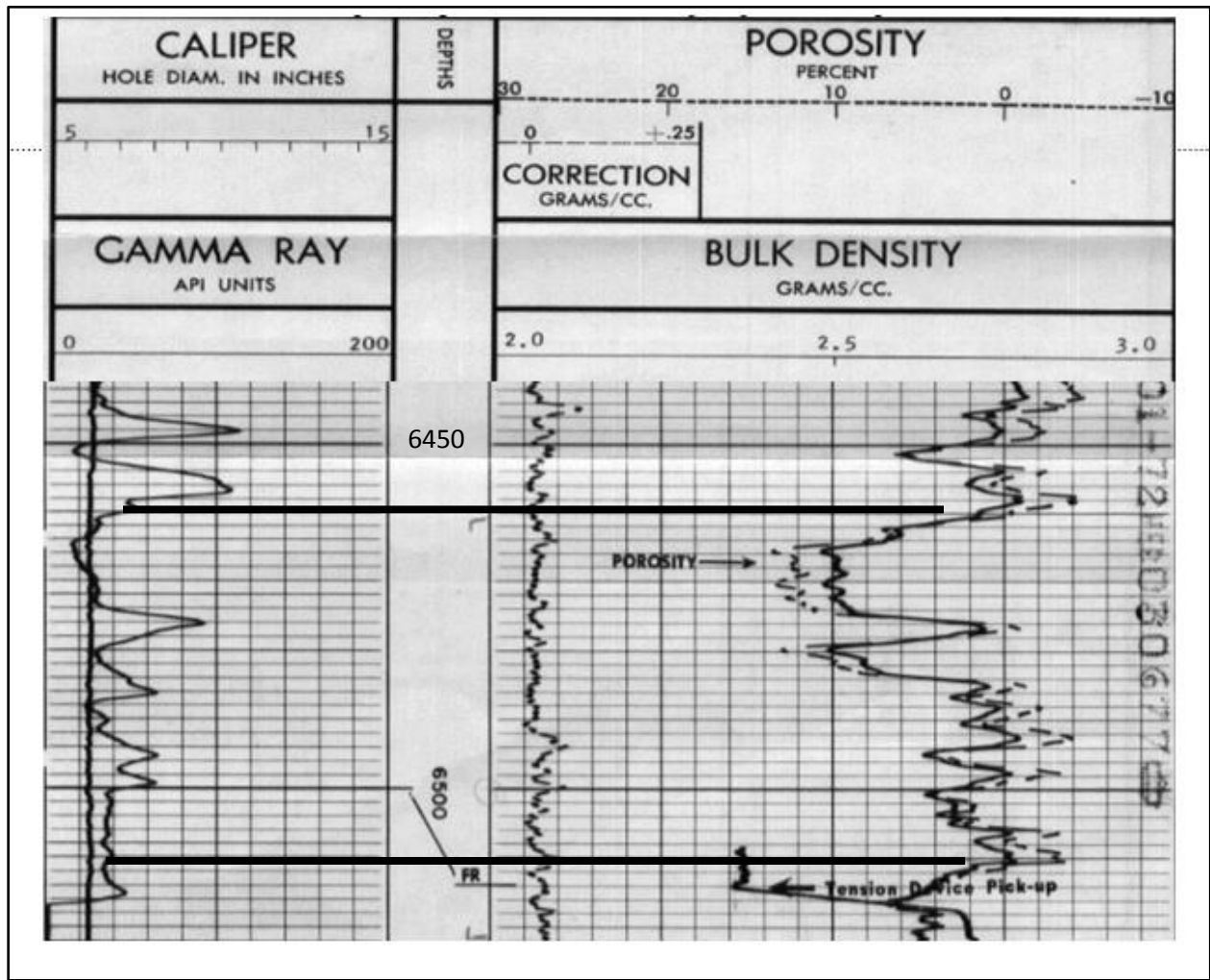
Figure 9. Gamma-ray and density log for the well# 7.
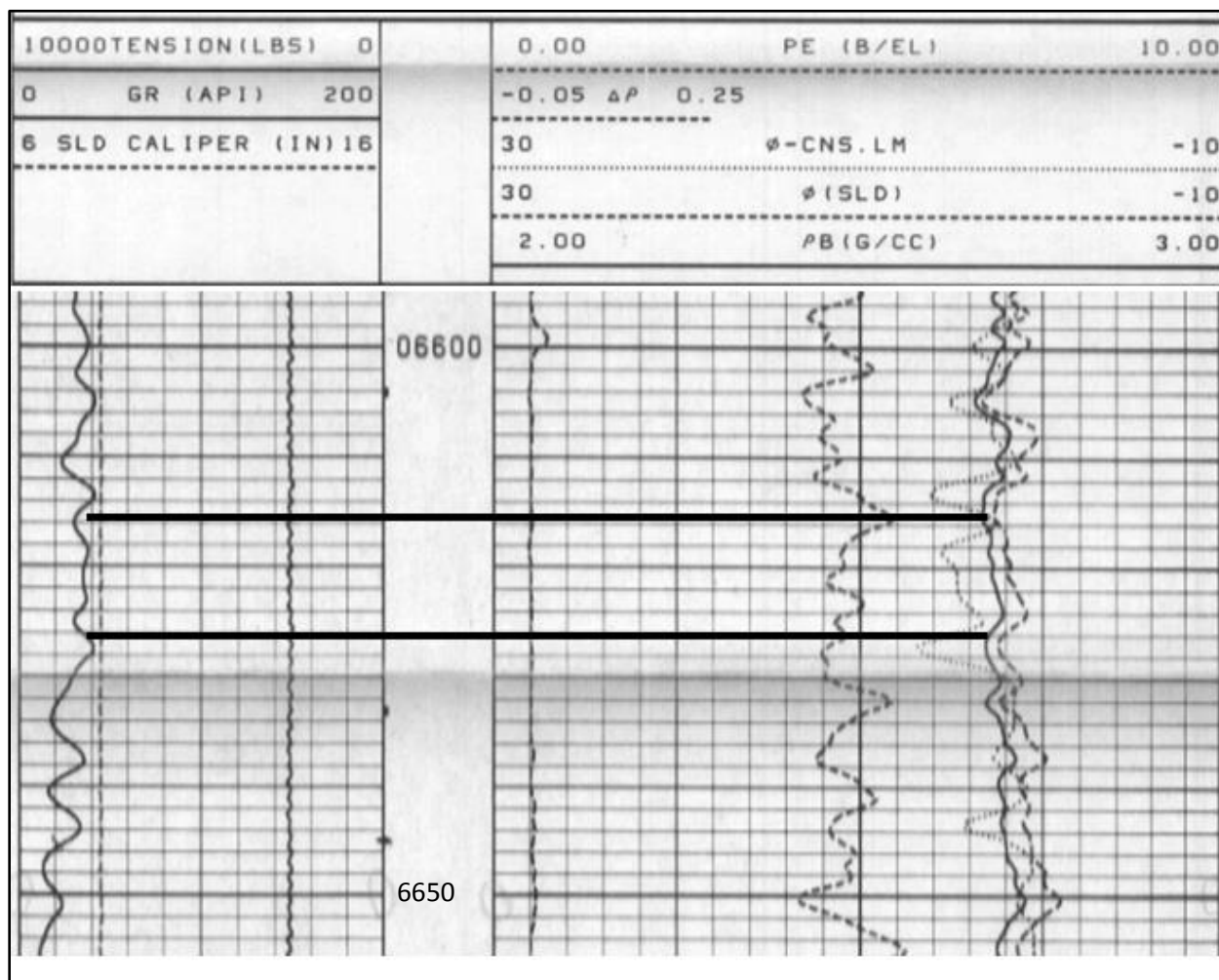
Figure 10. Gamma-ray and density log for the well #15.

Lithology and Thin Section Analysis

The main lithologies found in the Rose Run Sandstone are sandstone, dolostone, and mudstone.

Sandstone

The primary lithology in the Rose Run Sandstone is a fine- to coarse- grained, poorly to well sorted, sub angular to rounded, dolomitic quartz arenite. The most common and distinctive sedimentary structures observed in the Rose Run Sandstone are: massive bedding, planar-tabular cross bedding, herring-bone cross stratification, mottling, planar lamination, wavy and flaser bedding. Interbedded mud laminae or shale baffles are a common phenomenon in the unit (Figure 19). Core # 2923 shows the lower part of the unit is well cemented whereas upper part of the unit is more porous and may be more permeable. Glauconitic sandstones are the most porous lithologies in the sandstone.

Based on point count data of 4 samples, the most common framework constituents are monocrystalline quartz (23% ± 4%), polycrystalline quartz (22% ± 3%), and plagioclase feldspar (8% ± 3 %). Chert grains typically show mean value of 6% with 2% standard deviation. Very minor amount of sedimentary (<1%) and volcanic rock fragments (<1%) are also observed from the unit. Accessory minerals (6% ± 1%) in the Rose Run Sandstone mainly include glauconite and pyrite. All the samples show significant amount of dolomite cement (14% ± 2%), which is the primary cementing agent in the unit. The other cementing agents found in the unit are quartz overgrowths (5% ± 2%), feldspar overgrowths (<1%) and clay coatings (1%). Sandstone samples show about 6% ± 2% of matrix. The porosity of the unit is about 5% ± 1%. Porosity is mainly of intergranular nature. Photomicrograph of dolomitic sandstone and its framework constituents is shown in figure 11 and 12.
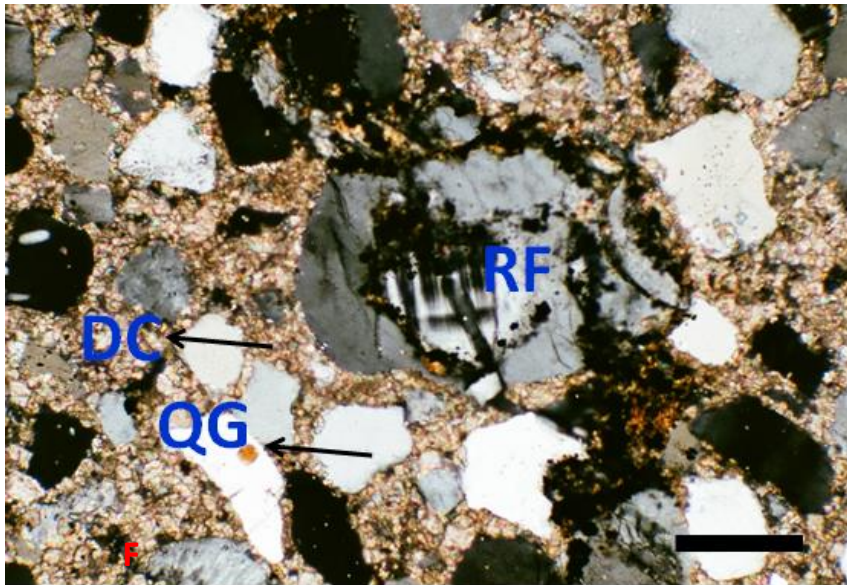
Figure 11. Photomicrograph of dolomitic sandstone with rock fragment. Key: RF = rock fragment, DC = dolomite cement, and QG = quartz grain. Scale bar = 1 mm.
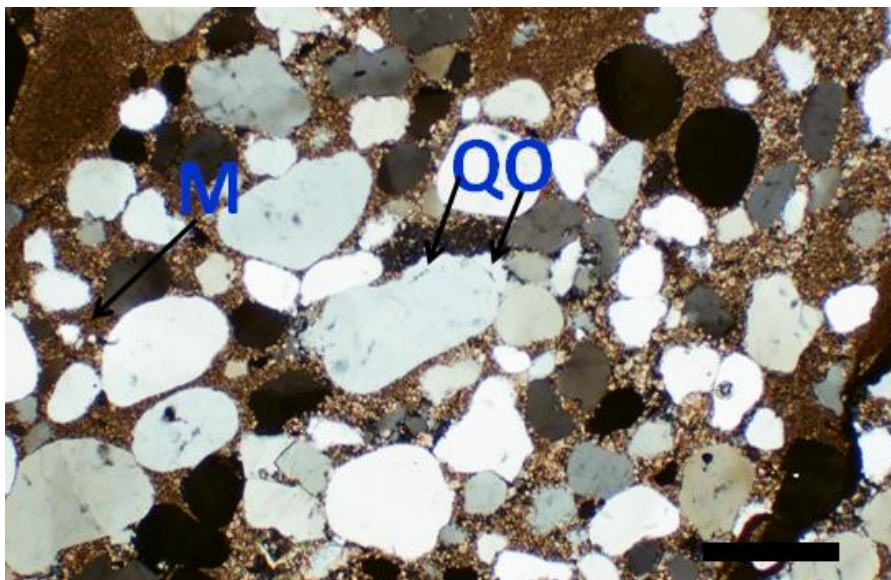
Figure 12. Photomicrograph showing quartz overgrowth and matrix in the Rose Run Sandstone. Key: M = matrix and QO = quartz overgrowth. Scale bar = 1 mm.

Dolostone

Dolostone is the second most common lithology in the Rose Run Sandstone and it is mainly interbedded with sandstone. The original carbonate has been completely destroyed by dolomitization which mainly occurs in the form of tightly packed subhedral crystals. Some of the replacements preserve the original texture as a "ghost" fabric. In this study, only a few ghost structure can be seen but could not be identified, however Riley et al. (1993) found the presence of ooid and peloid ghosts in thin sections. Dolostone occasionally shows floating quartz grains in cores and thin section (Figure 14). Some dolostone contain calcite in fractures, probably due to "de-dolomitization". Finally, small amount of mica, glauconite, and pyrite can be seen in thin sections. Thin section analysis suggests very little porosity (<1%) in dolostone samples, however, fractures present in the dolostone can locally increase porosity and permeability locally. Photomicrographs of dolostone are as shown in Figure 13, 14, 15, and 16.

Mudstone

The mudstone accounts for about 10% of the Rose Run Sandstone. The mudstone shows both massive and laminated bedding. Laminated mudstone is interpreted as shale. Mud laminae or drapes are commonly interbedded with both dolostone and sandstone. Photomicrograph of mudstone is shown in Figure 15.

Lithofacies Analysis

In total, 14 siliciclastic (Table 10) and 5 carbonate lithofacies (Table 11) were identified based on composition, texture, and sedimentary structure present in the unit. Description of each lithofacies was followed by the interpretation of process responsible for each lithofacies. Individual lithofacies are then grouped into assemblages, which serve to uniquely identify the environment that produced that facies. Lithofacies assemblages are groups of genetically related
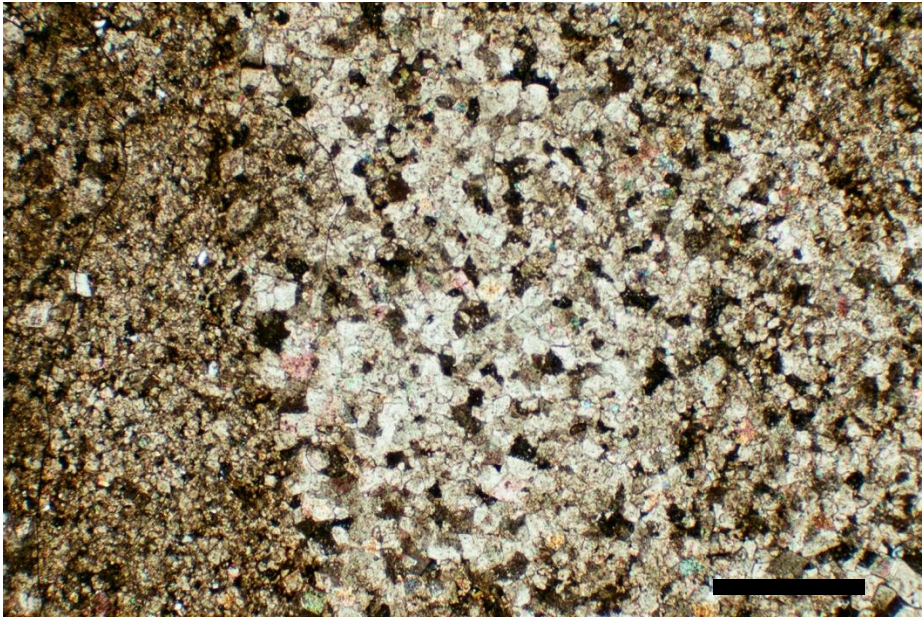
Figure 13. Photomicrograph of dolostone in the Rose Run Sandstone. Scale bar = 1 mm.
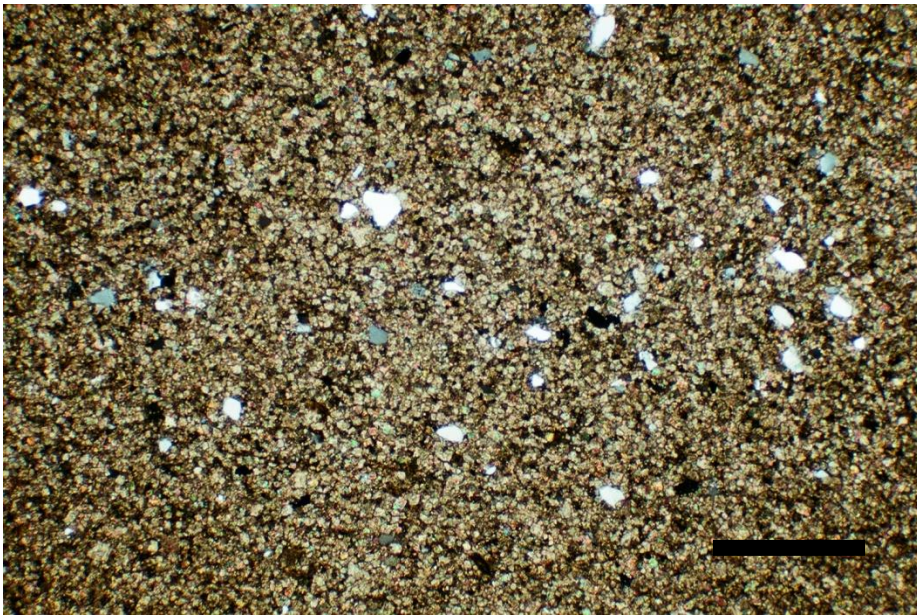
Figure 14. Photomicrograph showing floating quartz grain in the Rose Run Sandstone. Scale bar = 1 mm.
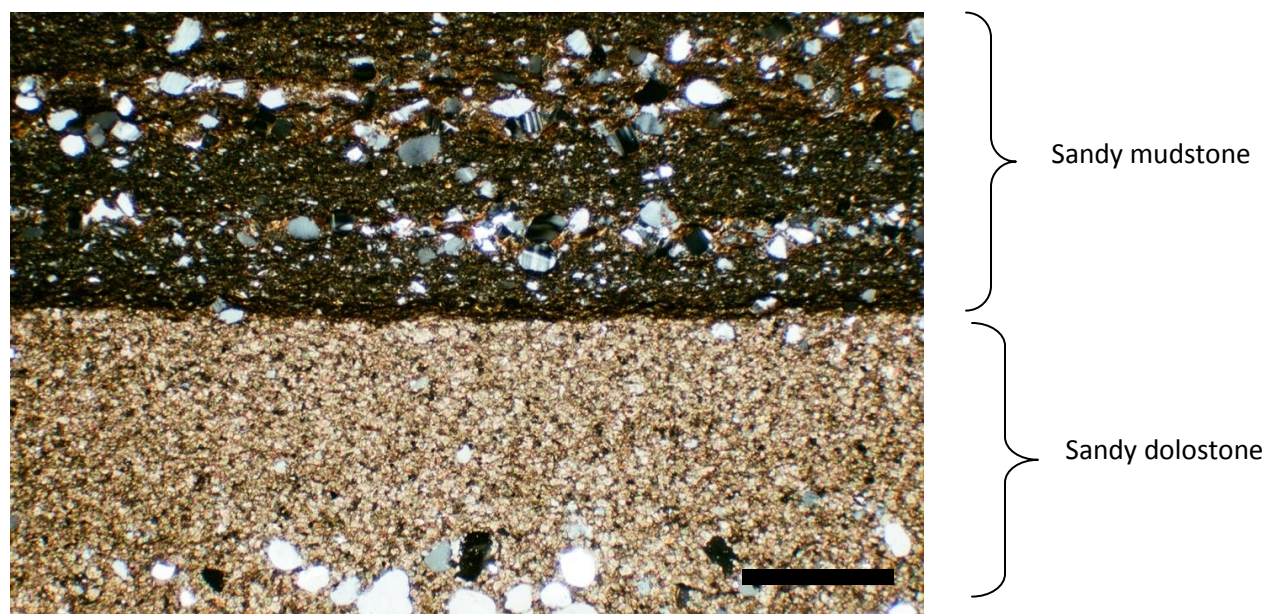
Figure 15. Photomicrograph of sandy dolostone and sandy mudstone in the Rose Run Sandstone.
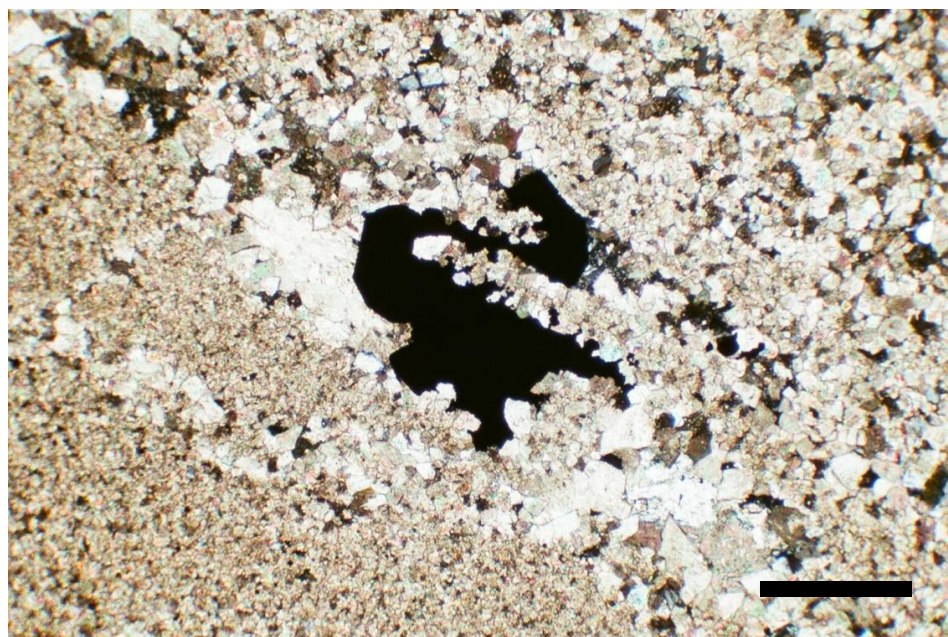
Scale bar = 1 mm.

Figure 16. Photomicrograph of pyrite mineral in dolostone. Scale bar = 1 mm.

facies. Finally, after describing individual lithofacies and interpreting their process of deposition, and after identifying lithofacies assemblages, it was possible to interpret the depositional environment. Lithofacies classification scheme used involved the upper case letter representing the lithology and lower case letter representing the sedimentary structure present. The Dunham classification (Dunham, 1962) has been adopted to characterize carbonate lithologies.

Heterolithic lenticular bedded sandstone and mudstone (Lithofacies SMk)

Lithofacies SMk consists of ripple laminated or lenticular bedded fine grained, rounded, sorted quartz arenite and interbedded mudstone. The mudstones are in the form of mud drapes having an average thickness < 1 cm. The ripples are isolated in mud matrix. Lithofacies SMk mainly alternates with lithofacies SMl. The average thickness of the lithofacies SMk is about 10 cm.

Lenticular bedding is a sedimentary structure consisting of sand ripples alternating with mud drapes with relatively larger quantities of mud to sand. According to Reineck and Wunderlich (1968), lenticular bedding consists of sand lenses of irregular form embedded in mud layers. The sand lenses are isolated small-scale ripples, which have travelled over the mud bed and are subsequently covered by mud. These sand lenses may be connected or isolated. Lithofacies SMk is interpreted as a deposit formed in an environment where a fluctuating tidal current flow produces sandy ripples, but the environment is dominated by mud. In the Rose Run Sandstone lithofacies SMk is interpreted to be deposited in mud flat part of intertidal zone.

Heterolithic wavy bedded sandstone and mudstone (Lithofacies SMw)

Lithofacies SMw consists of ripple laminated or wavy bedded fine- to medium- grained, rounded and sorted quartz arenite and interbedded mudstone. The average thickness of the mud layer in lithofacies SMw is generally <1 cm (Figure 17). Commonly, lithofacies SMw is overlain

Table 10. Summary of siliciclastic lithofacies in the Rose Run Sandstone.

Lithofacies	Lithology	Sedimentary structure	Interpretation
SMw	Heterolithic sandstone and mudstone	Wavy bedding	Tidal rhythmites with ripple marks
SMk	Heterolithic sandstone and mudstone	Lenticular bedding	Tidal rhythmites with ripple marks
SMf	Heterolithic sandstone and mudstone	Flaser bedding	Tidal rhythmites with ripple marks
SMl	Heterolithic sandstone and mudstone	Planar lamination	Tidal rhythmites
Sl	Sandstone	Planar lamination	Upper plane bed
Sp	Sandstone	Planar tabular cross bedding	Migration of dunes
Sx	Sandstone	Herring bone cross bedding	Dune cross bedding with tidal reversals
Sm	Sandstone	Massive	Rapid deposition or destratification
Smm	Sandstone	Massive Mottled	Bioturbation
Smg	Glauconite rich sandstone	Massive	Deposition of pellets
Smi	Sandstone	Massive with mudstone intraclasts	Higher energy conditions
Sh	Sandstone	Hummocky stratification	Storm events
Ml	Mudstone	Laminated	Lower energy conditions
Mm	Mudstone	Massive	Lower energy conditions, destratified shale

Table 11. Summary of carbonate lithofacies in the Rose Run Sandstone.

Lithofacies	Lithology	Sedimentary Structure	Interpretation
Cm	Dolo-mudstone	Massive	Probable carbonate tidal deposition
Cmm	Dolo-mudstone	Mottled	Probable bioturbation
Cmmc	Dolo-mudstone	Convoluted bedding	Dewatering in tidal environment
Cpmr	Dolo-packstone	Mud rip up clasts	Flat pebble conglomerate (beach stratification)
Cpl	Dolo-packstone and mudstone	Wavy lamination	Probable cryptalgal lamination

by lithofacies Sm and underlain by lithofacies SMf. The average thickness of lithofacies SMw is about 4.5 cm, and its color varies between dark grey and white.

Wavy bedding is found as a heterolithic deposit consisting of alternating rippled sand and mud drapes (Reineck and Wunderlich, 1968). Bedload processes are responsible for transporting sand-sized sediment, and suspension deposition is responsible for depositing clay-sized sediment (Klein, 1977). The variation from lenticular to wavy bedding represents a decrease in the deposition and preservation of mud. Areas with high content of suspended mud (intertidal or supratidal environment) are more likely to have wavy or lenticular bedding (James and Dalryrmple, 2010). In a mixed flat region, the combinations of high energy conditions that exist during flood and ebb tides deposits the sand, while during slack water conditions finer sediments settle into bedform troughs. Thus, lithofacies SMw is likely to be a mixed flat deposit. According to Klein (1977), the mixed lithologies of sand and mud arranged alternatively is a characteristic of mixed tidal flat environment where such deposition is related to changes in bottom current velocity during a tidal cycle. In the Rose Run Sandstone, lithofacies SMw is interpreted to be deposited in mixed flat region.

Heterolithic flaser bedded sandstone and mudstone (Lithofacies SMf)

Lithofacies SMf consists of flaser bedded fine- grained, sorted, rounded, quartz arenite and mud (Figure 17). The average thickness of lithofacies SMf is about 3 cm and is usually overlain by lithofacies SMw and underlain by lithofacies Sm.

Flaser bedding is a sedimentary structure characterized by alternating ripple laminated and discontinuous mud layers created by the deposition of mud in the troughs of previous sand ripples (Martin, 2000). It is formed during alternating intervals of relatively fast moving flow depositing sand with ripples, and slack water intervals where mud is deposited (Martin, 2000). As shown in Figure 17, flaser bedding consists of small amount of mud compared to sand, or in
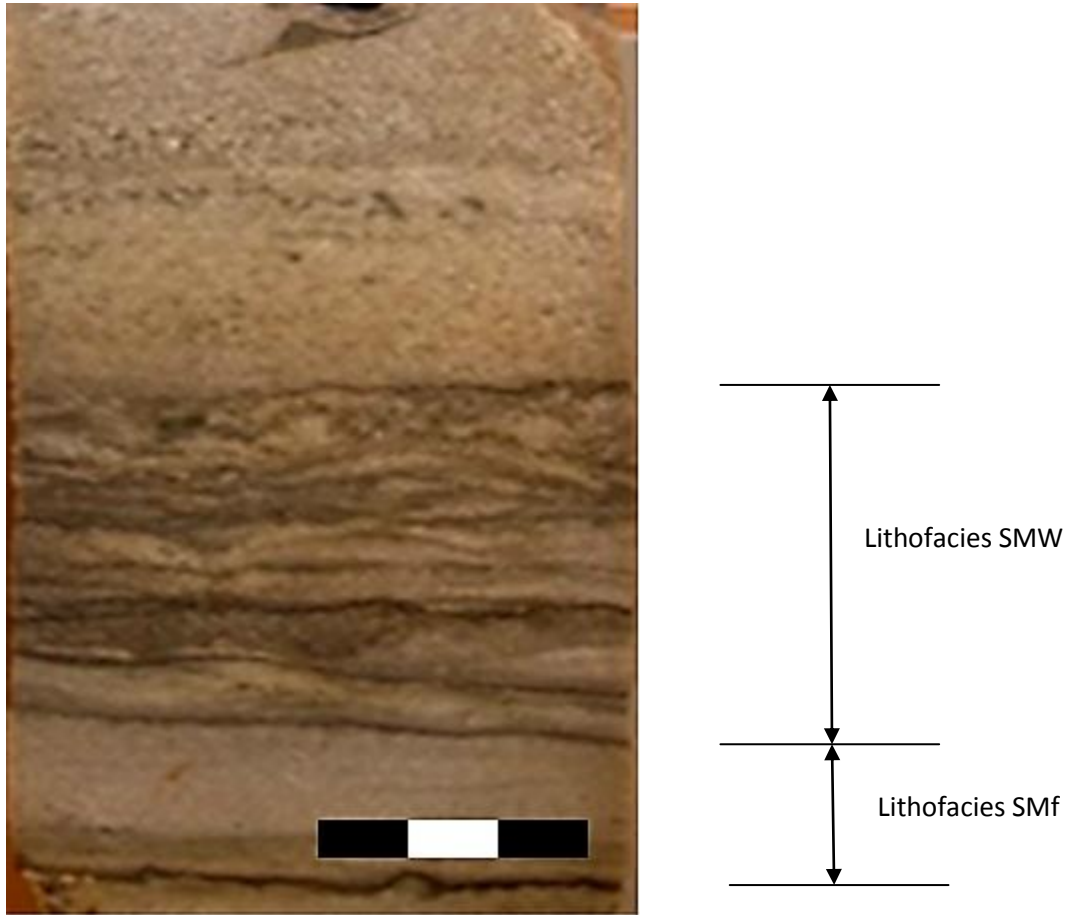
Figure 17. Wavy and flaser bedding in core # 3385.Scale bar = 3 cm.

other words, with an increase in mud content, flaser bedding changes gradually to wavy bedding and lenticular bedding (James and Dalryrmple, 2010). In the deposit, the amount of mud is a direct reflection of the amount of mud in suspension, hence the change from flaser bedding to lenticular bedding indicates an environmental shift from sand flats to mud flats (Figure 18). In the Rose Run Sandstone, lithofacies SMf is interpreted to be deposited in sand flat environment.

Interbedded planar laminated sandstone and mudstone (Lithofacies SMl)

Lithofacies SMl consists of planar laminated, fine-grained, sorted, rounded to subrounded, quartz arenite interbedded with mud. The thickness of mud layer is usually < 1 cm. Lithofacies SMl is usually overlain by lithofacies Sm or lithofacies Sp and is underlain by lithofacies Sh or lithofacies Sm. Lithofacies SMl as shown in Figure 19 is a common lithofacies found in the cores of Rose Run Sandstone.

Lithofacies SMl is interpreted as the deposits of tidal rhythmites in intertidal zone. Tidal rhythmites are packages of laterally and/or vertically accreted, laminated to thinly bedded fine- to medium-grained sandstone, siltstone, and mudstone of tidal origin showing rhythmic change in laminae thickness and grain size (Mazumder and Arima, 2004). Alternate layers of sand and mud in tidal rhythmites are deposited due to change in current speed during deposition, as controlled by the tides. Mud is deposited during slack water conditions (at high tide or low tide) whereas the coarse layers are deposited during maximum energy conditions, approaching low tide or high tide (James and Dalryrmple 2010). In the Rose Run Sandstone, lithofacies SMl is interpreted to be deposited in intertidal environment.

Planar laminated sandstone (Lithofacies Sl)

Lithofacies Sl consists of planar laminated medium-grained, sorted, subrounded to rounded, quartz arenite. The average thickness of lithofacies Sl is about 2 cm and lithofacies Sl is
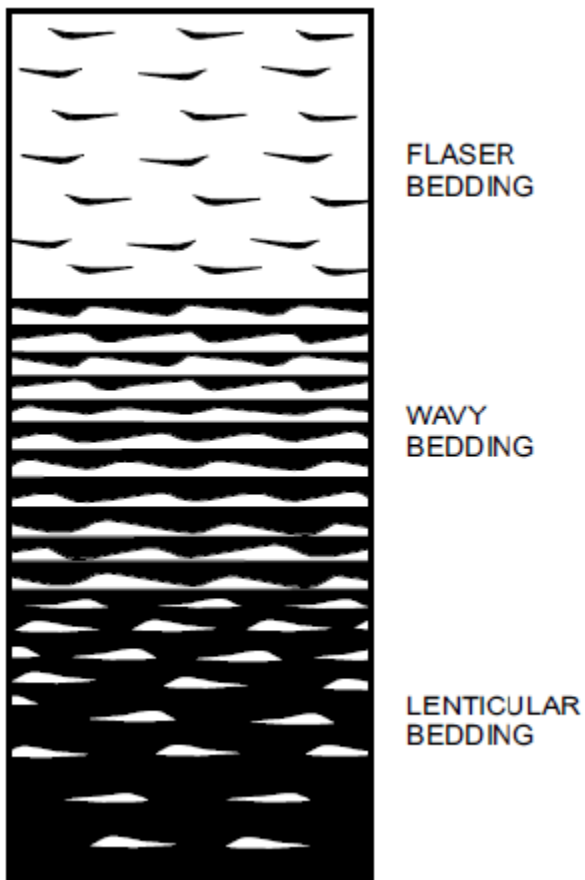
Figure 18. Diagram showing (A) flaser bedding, (B) wavy bedding, (C) and lenticular bedding.

The transition from flaser to lenticular bedding indicates increase in deposition and preservation

of mud (modified from Reineck and Wunderlich, 1968).

associated with hummocky stratified sandstone (lithofacies Sh) and massive sandstone (lithofacies Sm).

Planar laminated sandstones can be formed in variety of environments, and its presence is not diagnostic environmental indicator. According to Boggs (2006), planar lamination can be formed in variety of ways. It can be formed either by settling of sediments from suspension (lower plane bed) or by traction transport of sand under high flow conditions (upper plane bed). Planar laminated sandstone is often part of sequences such as tempestite, turbidites, and tidalites.

Planar-tabular cross bedded sandstone (Lithofacies Sp)

Lithofacies Sp consists of planar-tabular cross bedded, fine- to medium- grained, sorted, subrounded, quartz arenite. The average thickness of lithofacies Sp is about 7 cm and lithofacies Sp is commonly overlain by lithofacies Smi or lithofacies Sx. It is mainly underlain by lithofacies Sm. Lithofacies Sp, as shown in Figure 20, is a common lithofacies in the Rose Run Sandstone.

According to Boggs (2006), the sand deposits dominate in the shallow subtidal zone as well as in the lower intertidal zone and in the tidal inlet channels. Within the tidal inlet channels, tidal currents can achieve enough velocity to cause transport of sandy sediment and produce 2-D dune bed forms. Migration of these 2-D dunes produces planar-tabular cross bedding (James and Dalryrmple, 2010). Lithofacies Sp is interpreted to be deposited within the tidal channels in sand flat to subtidal environments.

Hummocky stratified sandstone (Lithofacies Sh)

Lithofacies Sh consists of hummocky stratified fine- grained, sorted and rounded quartz arenite. The color of lithofacies Sh varies from white to dark gray. It shows a sharp lower bounding surface and gradational upper contact. Lithofacies Sh is overlain by lithofacies Sm and is underlain by lithofacies Cm (Figure 21).
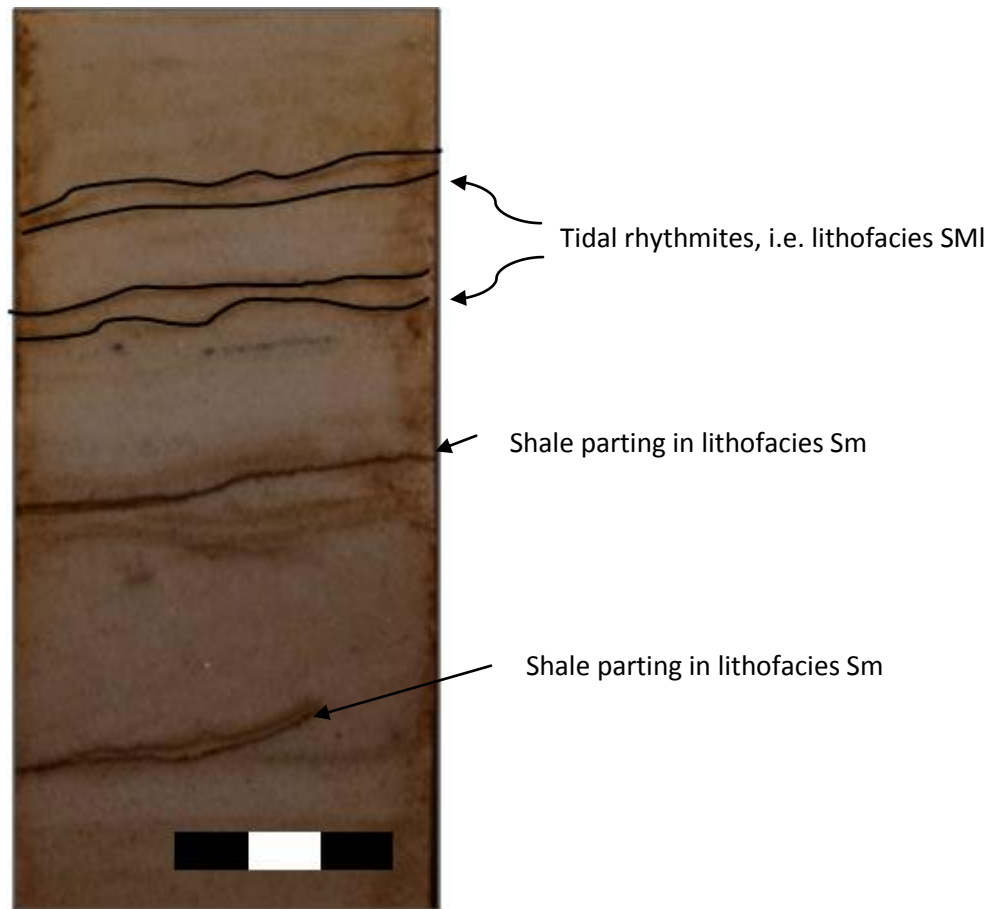
Figure 19. Lithofacies SMl (highlighted lines) and lithofacies Sm in core # 2923. The photo also shows shale partings in the core. Scale bar = 3cm.

According to Harms et al. (1975), hummocky stratification is formed by strong current surges of varied direction that are generated by relatively large storm waves. The strong storm wave first erodes the seabed into low hummocks and swales, which are then infilled by fallout from suspension resulting in laminae of material. Hummocky stratification is commonly found in shallow marine environments, but it has been reported in some lacustrine environment (Boggs, 2006). According to James and Dalryrmple (2010), the hummocky stratification is most likely to form above the storm wave base under combined flows with strong oscillatory component but a weak unidirectional component, and where the aggradation rates are enough to preserve the hummocky bedforms. In the Rose Run Sandstone, lithofacies Sh is interpreted to be deposited in shallow subtidal environments.

Massive Sandstone (Lithofacies Sm)

Lithofacies Sm consists of massive fine- to medium- grained, rounded to subrounded, well to moderately sorted, quartz arenite. Its average thickness is about half a meter. Lithofacies Sm is the most common lithofacies found in the Rose Run Sandstone.

The term massive is used here to describe sandstones which are internally structureless. The massive or structureless appearance of sandstone could also be due to post-depositional processes such as pedogenesis, bioturbation, and diagenesis (Martin and Turner, 1998). Also, liquefaction of sediment owing to sudden shock has been suggested as a means of destroying original stratification to produce massive bedding. However, no other evidence of fluid escape structures were seen in this unit. So destratification is either due to very rapid deposition from suspension (Boggs, 2006) or bioturbation (Martin and Turner, 1998) as discussed below.

Planar- tabular cross bedding (lithofacies Sp)
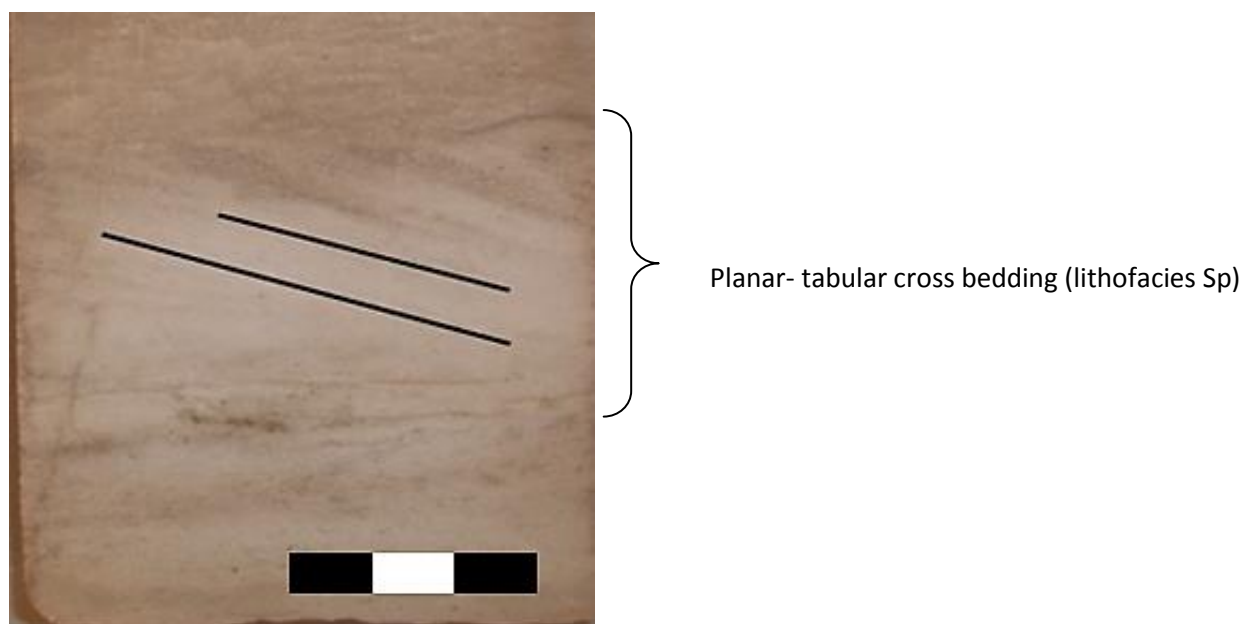
Figure 20. Planar- tabular cross bedding in core # 2923 (lithofacies Sp). Scale bar = 3 cm.

Lithofacies Sl

Lithofacies Sh

Lithofacies Sh

Erosional scour

Tempestite

Tempestite
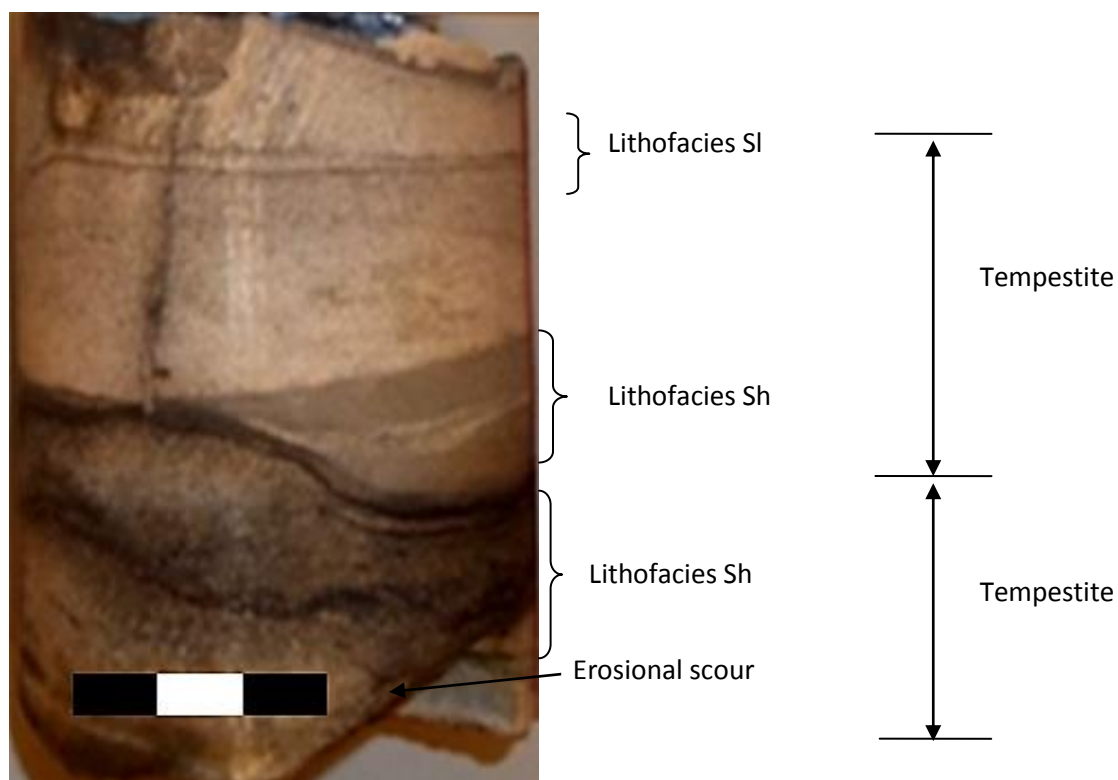
Figure 21. Hummocky stratification (lithofacies Sh) in core # 2923. Scale bar = 3 cm.

Massive Mottled Sandstone (Lithofacies Smm)

In some cases, massive sandstone (lithofacies Sm) displays a mottled appearance (Figure 22). Lithofacies Smm consists of massive, mottled, fine-grained, sorted, rounded, quartz arenite. Its average thickness is about 12 cm. As shown in Figure 22, the mottling is represented by lighter colored in distinct areas in otherwise darker massive sandstone.

The term mottling or mottled bedding is generally referred when the bioturbation activity is intense in the rock. Mottling in the Rose Run Sandstone is more pronounced in what are interpreted to be middle or upper tidal flats, which is consistent with its origin resulting from bioturbation. In the Rose Run Sandstone, lithofacies Smm is interpreted to be deposited in an intertidal environment.

Glauconite- rich sandstone (Lithofacies Smg)

Lithofacies Smg consists of massive, glauconite-rich, fine- to medium- grained, sorted, and rounded quartz arenite. The average thickness is about 15 cm. The color of lithofacies Smg varies from off-white to greenish white depending on the amount of glauconite present. In some cases, lithofacies Smg is very poorly cemented. In general, lithofacies Smg (Figure 23) is more porous than most lithofacies in Rose Run Sandstone.

The glauconite in the unit is interpreted to form from diagenesis of organic matter and primary clays. One mode of origin is authigenesis of primary fecal pellets, which were transported by waves or tidal currents. Burst (1958) suggested that one of the requirements for "glauconitization" (authigenesis of glauconite) is an environment with a suitable redox potential. This is usually attained in a locally reducing environment associated with decaying organic matter, in an otherwise oxidizing environment. The suitable conditions for a locally reducing environment can be found inside fecal pellets or foraminiferal tests, or other organic-rich components.

Mottled sandstone (lithofacies Smm)

Figure 22. Massive mottled sandstone (lithofacies Smm) from core # 2989. Scale bar = 3 cm.
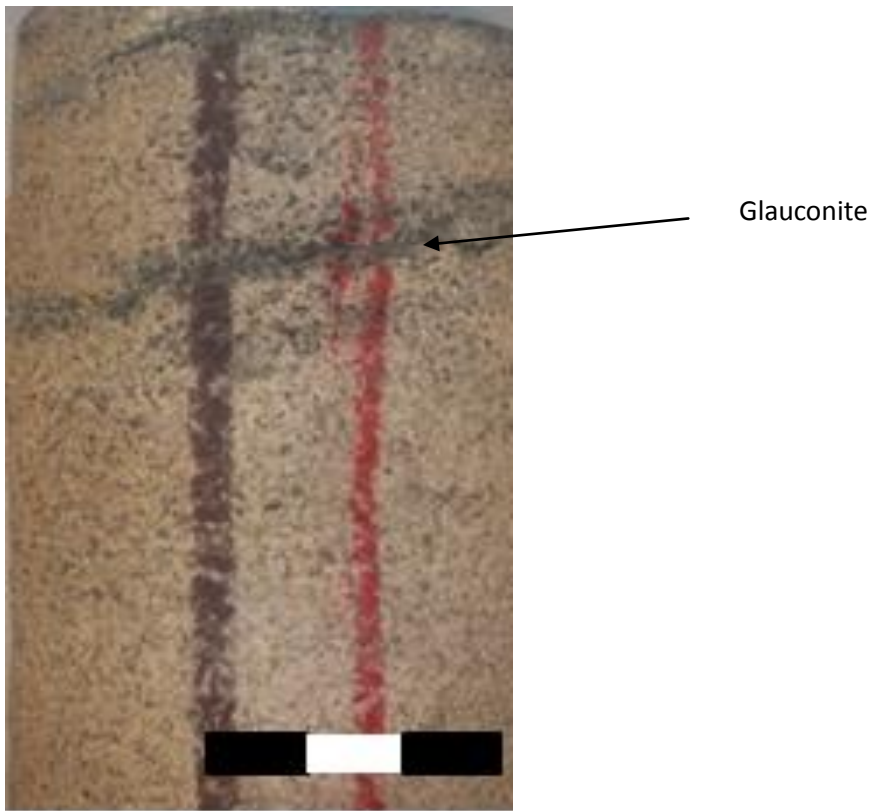
Figure 23. Massive glauconitic sandstone (lithofacies Smg) from core # 3385. Scale bar = 3 cm.

Intraclasts in massive sandstone (Lithofacies Smi)

Lithofacies Smi consists of massive, intraclast-rich, medium-grained, sorted, and subrounded quartz arenite. The color ranges from white to gray. The size of individual mudstone intraclasts is generally < 1 cm (Figure 24).

Intraclasts are formed by fragmentation or erosion of pre-existing cohesive sediments in a high-energy environment such as a tidal zone, or as a result of events such as a storm. The intraclasts typically accumulate close to their place of origin, after being transported to the site of deposition by currents. Given the relationship to other lithofacies, the intraclasts in lithofacies Smi are likely to be formed due to bank erosion of tidal channels, which are then transported and deposited along with sands in the middle or lower tidal flats.

Herringbone cross stratified sandstone (Lithofacies Sx)

Lithofacies Sx consists of herringbone cross-bedded, medium- grained, sorted, rounded quartz arenite (Figure 25). The thickness of lithofacies Sx is about 5 cm. It is typically overlain by massive sandstone (lithofacies Sm) and underlain by planar-tabular cross bedded sandstone (lithofacies Sp).

Herringbone cross-stratification, refers to adjacent crossbeds with opposing dip direction, and it is often used as an indication of tidal deposition (Klein, 1977). Herring-bone cross-stratification is formed due to reversals of tidal currents of equal energy. Each cross-strata set represents dune or sand wave migration during a single part of a tidal cycle. Herringbone cross-stratification is not common, because it requires the current energy to be equal in both directions, which happens rarely in nature. In the Rose Run Sandstone, lithofacies Sx is interpreted to be deposited in shallow subtidal environment.

Massive mudstone (Lithofacies Mm)

Lithofacies Mm consists of massive mudstone. Its average thickness is about 2 cm. It is interbedded with both sandstone and dolostone.

Individual beds of lithofacies Mm are interpreted to be deposited in calm or slack water conditions. Slack water conditions occur for a period at the end of each flood or ebb during the pause before current reversal. The thin nature of lithofacies Mm is more suggestive of its deposition in intertidal and subtidal zone rather than supratidal region where it's mostly mud deposits. In the Rose Run Sandstone, lithofacies Mm is interpreted to be deposited in intertidal environment as massive nature of lithofacies is most likely due to bioturbation which is more pronounced in intertidal zone.

Laminated mudstone (Lithofacies Ml)

Lithofacies Ml consists of laminated well sorted, mudstone. The average thickness of the lithofacies Ml is about 3cm. The lithofacies is typically light to dark grey color (Figure 26). Lithofacies Ml usually alternates with lithofacies Sm or lithofacies Cm. Figure 26 shows erosional contact between lithofacies Ml and lithofacies Sm

The very fine grained nature of Ml suggests deposition of mud in calm water conditions. In the Rose Run Sandstone, lithofacies Ml, being devoid of bioturbation, is interpreted to be deposited in subtidal environments.

<div align="center">Carbonate lithofacies</div>

The original carbonate fabric of the Rose Run Sandstone was completely destroyed by dolomitization in the unit**.** In total, 5 carbonate lithofacies have been observed in the Rose Run Sandstone. Dolostone can be highly mottled, which is interpreted to be due to bioturbation. Riley et al. (1993) and Chuks (2008) also reported oolitic grainstones in the Rose Run Sandstone. Cementation in carbonate lithofacies is mainly micritic in nature, which also reduces primary

Figure 24. Massive sandstone with intraclasts (lithofacies Smi) and planar-tabular cross bedded

(lithofacies Sp) from core # 2923. Scale bar = 3 cm. I = Intraclast

Herringbone cross-stratified sandstone
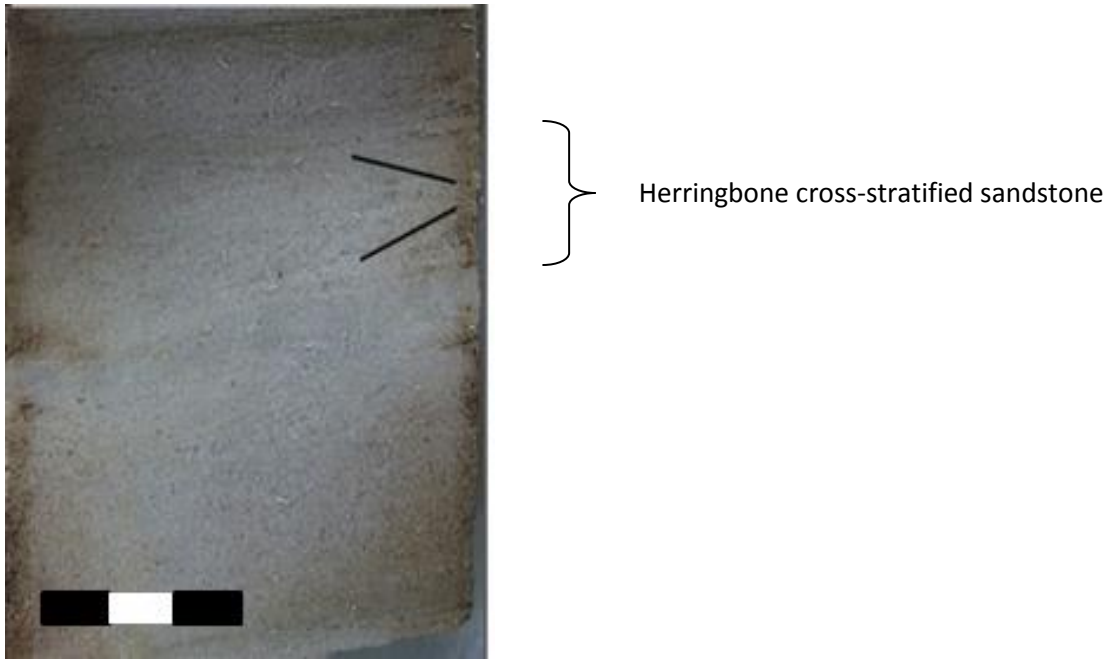
Figure 25. Herringbone cross-stratification (lithofacies Sx) from core # 2923. The black lines are drawn to highlight the herring bone structure. Scale bar = 3 cm.
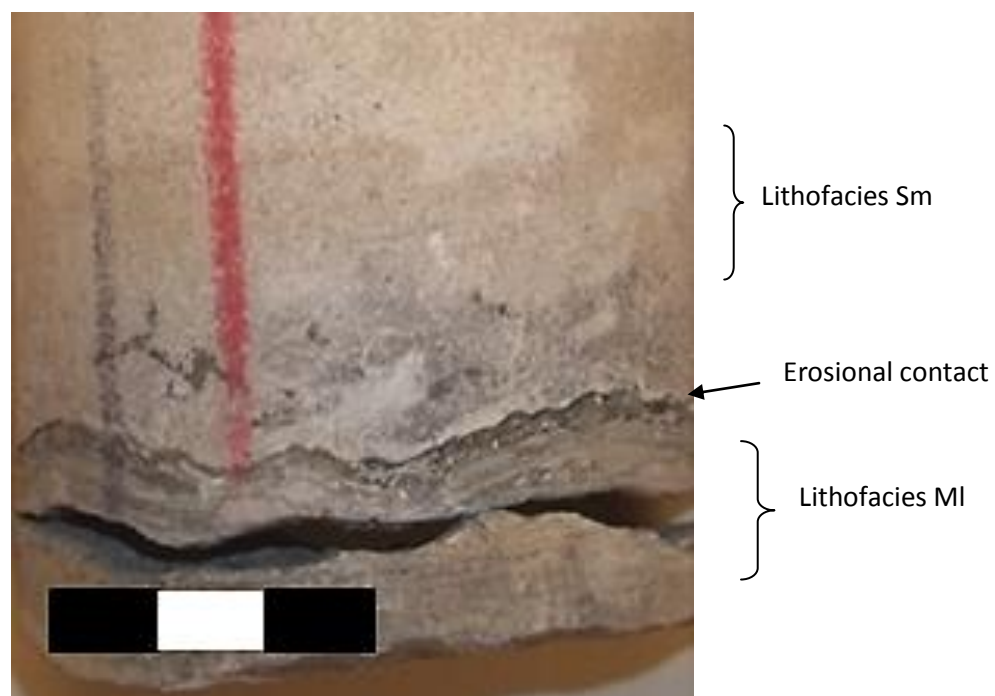
Figure 26. Erosional contact between lithofacies Sm and lithofacies Ml. Scale bar = 3 cm.

porosity. However, small-scale unhealed and healed fractures are common phenomenon in the unit giving rise to secondary fracture porosity, which may aid permeability in the unit. Carbonate lithofacies found in the Rose Run Sandstone include massive dolo-mudstone (lithofacies Cm), dolo-packstone with mud drapes (lithofacies Cpl), dolo-packstone with mud rip up clasts (Cpmr) massive mottled dolo-mudstone (lithofacies Cmm), and convoluted bedded mudstone in dolo-mudstone (lithofacies Cmmc). Carbonate lithofacies in Rose Run Sandstone are interpreted to be deposited in peritidal environments.

Massive dolo-mudstone (Lithofacies Cm)

Lithofacies Cm consists of massive, fine-grained dolomitic mudstone or micrite that is highly compact and cemented, with very little porosity. The average thickness of lithofacies Cm is about 20 cm. Quartz and silt grains can be found in the dolo-mudstone at various intervals in cores (Figure 14). At places, the unit shows unhealed fracture, which can supplement the permeability assuming the fracture is not formed while coring. After lithofacies Sm, lithofacies Cm is the most common lithofacies found in the Rose Run Sandstone.

Lithofacies Cm does not show any "ghost" features indicating its massive nature is mainly because of massive nature of original limestone. By definition, carbonate mudstone (Dunham, 1962) is a rock made up of more than 90% mud (micrite) and the original components are not bound together during deposition (Folk, 1974). Micrite is "lime mud", dense, dull-looking sediment made of clay sized crystals of $CaCO_3$. Most micrite today forms from the breakdown of calcareous algae skeletons (Prothero and Schwab, 1996). In Rose Run Sandstone, lithofacies Cm is interpreted to be deposited in subtidal lagoonal environments.

Dolo-packstone with mud drapes (Lithofacies Cpl)

Lithofacies Cpl consists of heterolithic fine grained, dolo-packstone. The mud drapes in

dolo-packstone are <1cm in thickness and are grayish in color. Mud drapes are generally planar

to slightly undulating and show little variation in thickness. Figure 27 shows lithofacies Cpl in

core # 2923.

The heterolithic nature of lithofacies Cpl is interpreted as cryptalgal lamination.

Cryptalgal lamination forms when cyanobacteria trap and bind sediments. The biofilms or

"mats" formed by cyanobacteria tends to cover intertidal, supratidal, and some shallow subtidal

surfaces (Logan et al., 1994). Kerans (1990) interpreted similar lithofacies to be deposited in

upper tidal flats. According to James and Dalrymple (2010), supratidal zones are characterized

by the presence of cryptalgal laminations. In the Rose Run Sandstone, lithofacies Cpl is

interpreted to be deposited in supratidal environments which is consistent with observations of

other authors listed above.

Massive mottled Dolo-mudstone (Lithofacies Cmm)

Llithofacies Cmm consists of grey to brown, fine to medium crystalline, mottled

dolostone. The mottling in the dolo-mudstone consists of patches of grey color, which are

usually less than 1 cm in diameter, in an otherwise dark dolo-mudstone. The average thickness of

lithofacies Cmm is about 10 cm. At places, lithofacies Cmm includes dolomite rip-up clasts.

Lithofacies Cmm is a common lithofacies in the Rose Run Sandstone (Figure 28).

The mottling in dolo-mudstone is believed to be due to burrowing activities of the

organisms. According to James (1984), the bioturbation is more intense in lower intertidal and

subtidal zone, because this area is frequently covered by water and hence, the salinity in the

region is normal to slightly above normal. In contrast, the upper intertidal or supratidal zones the

salinity would be relatively high to be tolerated by burrowing organisms (Bathurst, 1975;

Friedman and Sanders, 1978). In the Rose Run Sandstone, lithofacies Cmm is interpreted to be deposited in subtidal lagoonal environments.

Dolo-packstone with rip-up clasts (Lithofacies Cpmr)

Lithofacies Cpmr consists of brown, fine grained dolo-packstone. The intraclasts are angular to sub angular and are about 1 cm in diameter. Individual clasts are composed of dolo-mudstones and are irregularly distributed in the dolo-packstone. The thickness of lithofacies Cpmr extends up to 10 cm. Some quartz grains can also be observed in the unit (Figure 29).

Angular intraclasts can be interpreted as flat pebble conglomerates. The Flat-pebble conglomerates are important component of carbonate deposits that have been described from modern supratidal to beach environments. More recently, some researchers have found that flat-pebble conglomerates beds may represent subtidal environments below fair-weather wave base (Kazmierczak and Goldring, 1978). In the Rose Run Sandstone, lithofacies Cpmr is interpreted to be deposited in subtidal environment under high energy conditions. Presence of quartz grains indicates proximity to siliciclastic supply.

Convoluted bedded mudstone in Dolo-mudstone (Lithofacies Cmmc)

Lithofacies Cmmc consists of convoluted bedded, sorted, rounded, dolomitic mudstone (Figure 30). The thickness of lithofacies Cmmc is about 3 cm. The convolute bedding consists of soft-sediment folds and disrupted laminae.

Convoluted bedding is a type of soft sediment deformation structure which develops during deposition, or shortly after deposition, when the sediments are in liquid-like or unconsolidated form. Convoluted bedding is reported from many sedimentary environments and is a well known feature of many turbidites. Einsele (1963) cited examples of convolute lamination in recent environments that are under the influence of tides, as well as some fossil ones within units of probably shallow-marine origin. Convolute bedding is also known to be

Figure 27. Dolo-packstone with algal mats (lithofacies Cpl) from core # 2923 Scale bar = 3 cm.

Figure 28. Massive mottled dolo-mudstone (lithofacies Cmm) in core # 2923. Scale bar = 3 cm.

Figure 29. Dolo-packstone with rip up clasts (shown by arrow) in core # 2923. Scale bar = 3 cm.
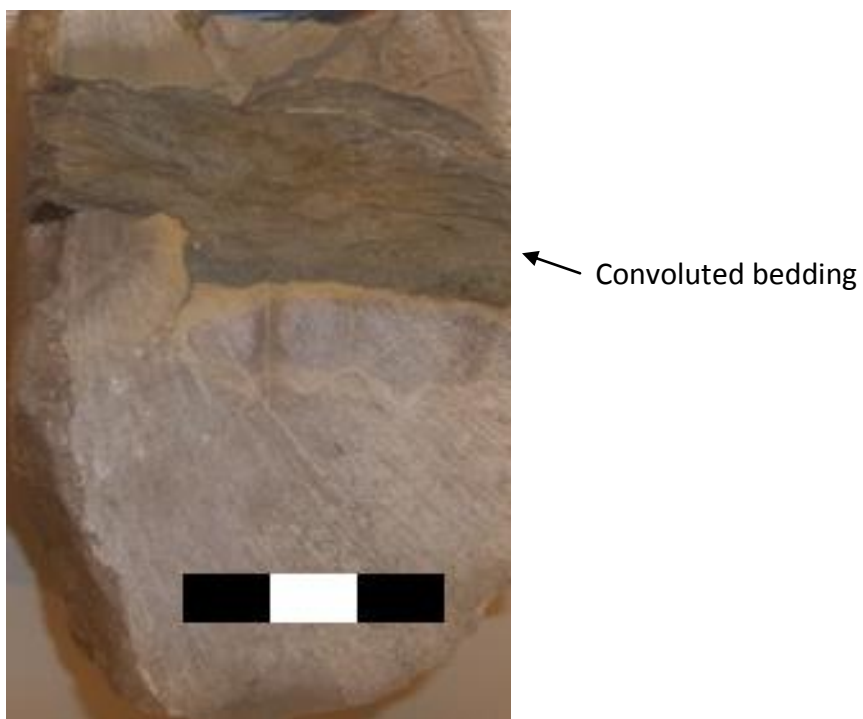
Figure 30. Convoluted bedding in dolo-mudstone (lithofacies Cmmc) from core # 3385. Scale

bar = 3 cm.

formed in carbonate tidal flats on account of drying and wetting of deposits causing its shrinkage and expansion during tidal cycles. In the Rose Run Sandstone, lithofacies Cmmc is interpreted to be deposited in intertidal environments.

Lithofacies Associations

Facies Associations can be described as groups of facies genetically related to one another and which have some environmental significance (James and Dalryrmple, 2010). Facies associations are key in interpretation of depositional environment because individual lithofacies are not unique in terms of depositional processes, and in some cases the same lithofacies can be produced by several processes. Grouping individual lithofacies into associations serves as a measure for the interpretation of depositional environments.

Tidalites

The tidalite facies assemblage includes heterolithic flaser bedded sandstone and mudstone (lithofacies SMf), heterolithic wavy bedded sandstone and mudstone (lithofacies SMw), heterolithic lenticular bedded sandstone and mudstone (lithofacies SMk), and heterolithic planar laminated sandstone and mudstone (lithofacies SMl or tidal rhythmites). Tidalites can be found in core # 2923, # 2989, and # 3385. Figure 49 shows tidalite assemblage in core # 2989.

Tidalites encompass all of the deposits of tidal currents. The alteration of flood and ebb tidal currents and the intervening slack water intervals cause alternating deposition of sand and mud. The intertidal zone can be divided into mud flats, mixed flats, and sand flats based on the relative abundance of mud and sand (Klein, 1977). The variation from flaser to wavy to lenticular bedding has been interpreted to represent an increase in the deposition and preservation of the mud during slack water periods, and hence migration of environment from high- energy sand flats to mixed flats to low- energy mud flats (James and Dalrymple, 2010). Because this environment is inundated for half of the total duration of tidal cycle and experiences

both bedload and suspension deposition, it results in mixed lithologies and the associated

features described above. The subtidal zone encompasses the part of the tidal flat that normally

lies below mean low tide level. Tidal influence in this part of environment is particularly

important within tidal channels, where bedload transport and deposition are predominant,

although this zone is influence by waves to some extent (Boggs, 2006)

Tidal Inlet Channel Assemblage

Tidal inlet channels are places where sandy deposits are found in flood-tide and ebb-tide

deltas. This facies assemblage includes planar- tabular cross bedded sandstone (lithofacies sp),

massive sandstone (lithofacies Sm), herringbone cross stratified sandstone (lithofacies Sx) and

sandstone with intraclasts (lithofacies Si). Individual lithofacies in this assemblage ranges from

10 cm to 50 meter thick. The total thickness of this assemblage is typically about 1 m thick.

Lithofacies Sm is the most common lithofacies in this assemblage and is usually associated with

lithofacies Sx and lithofacies Sp. Medium- angle, planar-tabular cross bedded sandstone is also a

common component in this assemblage, being either unidirectional (lithofacies Sp) or

bidirectional (lithofacies Sx). Figure 32 shows tidal inlet channel assemblages in core 2923.

Tempestite Assemblage

A tempestite is a storm deposit, which shows evidence of erosion of pre-existing

sediments, resuspension, and redeposition by fallout from suspension (Ager, 1974). Storm wave

erosion happens above storm weather wave base. From base to top, an idealized sequence of a

tempestite consists of, a scoured base overlain by hummocky stratified sandstone, overlain by

planar-laminated sandstone, overlain by ripple laminated sandstone, and finally overlain by

mudstone at the top. Hummocky stratified sandstone is the most distinguish feature of tempestite

sequence. Based on experimental studies, it is observed that hummocky stratification is formed

above the storm wave base under combined flows (having a strong oscillatory component but a

weak unidirectional component), and where the sediment aggradation rates are sufficient to preserve the hummocky bedforms (James and Dalrymple, 2010)

In the present study, several incomplete tempestite sequences are observed in different parts of cores (Figure 21 and A-II). The sequence consists of a scoured erosional base, overlain by hummocky stratified sandstone, overlain by parallel laminated sandstone. The entire assemblage is on an average 6 cm thick (Figure 21). The hummocky stratified sandstone is identified in the core based on its curved surface and difference in thickness of sequential infill material.

Peritidal Carbonate Facies Assemblage

Carbonate deposits are found throughout the Rose Run Sandstone and are observed in cores #2923, #2989, and #3385. In some wells, geophysical log analysis (next section) indicates carbonate deposits make up to almost 50% or more of the Rose Run Sandstone. The thickness of carbonate interval averages about 60 cm and carbonate is interbedded with sandstone and mudstone. In total, 5 carbonate lithofacies have been observed from the core study (Table 11). The combination of lithofacies is interpreted as a peritidal facies association (James and Dalrymple, 2010).

In the Rose Run Sandstone, observed sedimentary features typical of peritidal carbonate environments include carbonate mud, intraclasts, soft sediment deformation (convolute bedding), stromatolites, cryptalgal lamination, flat pebble conglomerate, storm deposits, and desiccation cracks (e.g. James and Dalrymple, 2010). For carbonate deposition, it is necessary that the area of deposition has minimal siliciclastic sediment supply. The interbedded siliciclastic suggests carbonate tidal flats adjacent to siliciclastic tidal flats (A- II) but somehow sufficiently

Legend
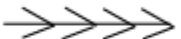
☐	Sandstone
▬	Mudstone
⊓	Dolostone
↖	Fining upward sequence
↗	Coarsening upward sequence
⟩⟩⟩⟩	Herringbone cross stratification
	Planar tabular cross bedding
− − −	Shale parting or mud cracks
═══	Tidal rhythmites
● ●	Mottling
▭ ▭	Intraclasts
⌐ ⌐ ⌐	lenticular bedding
∿∿∿	Wavy bedding
⋯⋯	Flaser bedding
⟍	Fracture
⌒⌒	Hummocky stratification
⌣⌒	Erosional contact
⬭	Vug
⋀⋁⋀	Stylolite
◖ ◖	Rip up clast
⊠	Missing interval

Figure 31. Symbols used in the study to represent sedimentary structures in core sections.
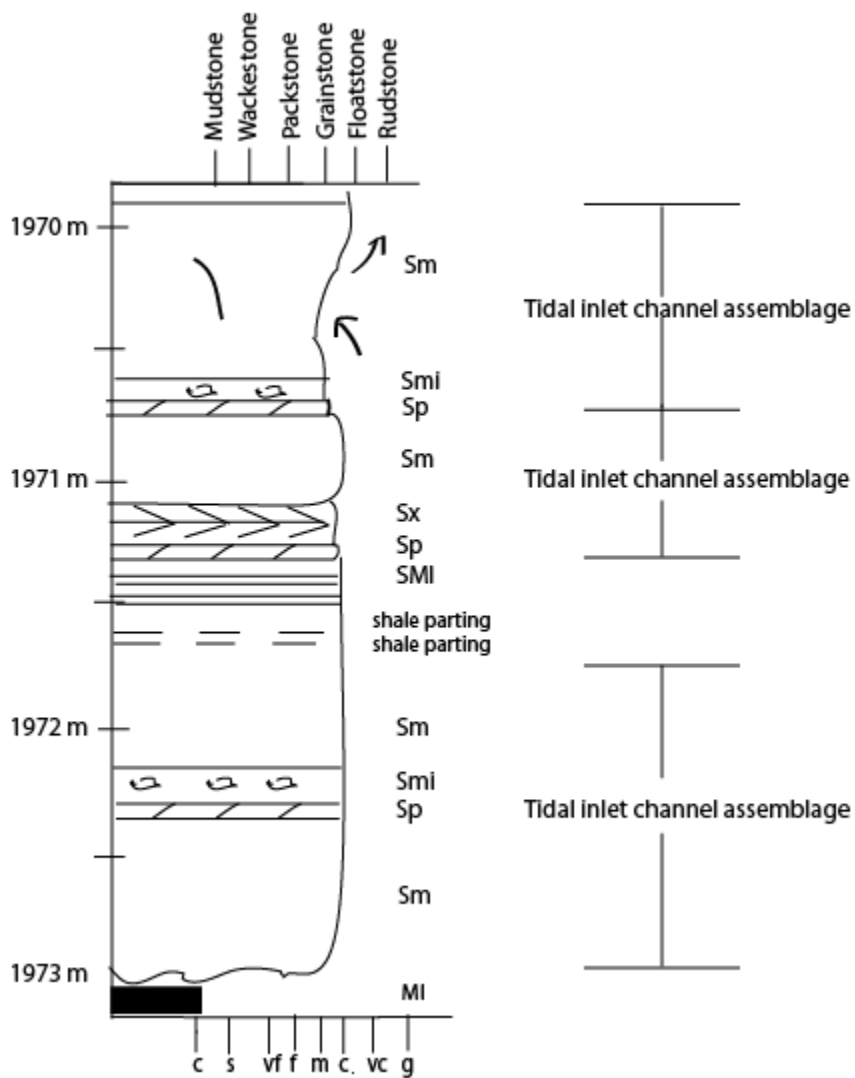
Figure 32. Tidal inlet channel assemblage in core # 2923.

isolated such that siliciclastic sediment supply did not "shut down" the subtidal carbonate factory.

Basin Mapping Results

Geophysical logs from a total of 17 wells were analyzed to understand the structure, distribution, and architecture of the Rose Run Sandstone in the study area. Gamma-ray logs and density logs were the primary data sources consulted in the study. Geophysical logs were used to create litho- correlation profiles, a structure contour map, an isopach map, and a sand isolith map.

Litho-correlation Profiles

Each lithology has distinct geophysical log signature, which makes the log a useful tool to identity and correlate distinct lithologies. Two litho-correlation profiles (Figure 33) are generated using the density log as it served to identify sand bodies in Rose Run Sandstone. Because shale interval accounts for <10%, based on geophysical logs, it has been neglected in the log correlations. The quality of well logs not being sufficiently good, for each well used in this profile, a core diagram was generated showing sandstone and dolostone from the density log, as shown in Figure 34. Correlation was done by peak pattern matching. To better understand the extent and geometry of sand bodies, one reference well is used in common for both profiles (Figure 33). The north-south profile is interpreted (see later section) to be approximately parallel to subparallel the paleo-shoreline whereas the east-west profile is interpreted as approximately perpendicular to the paleo-shoreline.

North-South profile

The north-south profile was constructed from 4 wells (Figure 35). The profile can be interpreted to show multiple (2-5) sand bodies per well. Based on the signature of density logs,

none of the individual sand bodies are continuous across the profile. However, it seems there is better continuity of sand bodies between three of the northern wells (# 3, # 12, # 5) in maps. The most continuous sand body extends about 50 km between well # 12 to well # 8, though there is some thickness variation between wells (Figure 35). In general, the log correlation profiles can be interpreted to show an elongate sheet- like to lenticular shape sand bodies. The Rose Run Sandstone shows higher thickness in middle of profile (# 12, # 5, # 8) with an average thickness of 30 m, whereas the unit thins out in the north and south end of the profile (# 3 and # 6 respectively), showing an average thickness of 10 m.

East-West profile

East-west profile was constructed using 4 wells (Figure 36). The profile can be interpreted to show multiple sand bodies (2 to 4) per well. Variations in the signature of density logs between wells seem to suggest discontinuous sand bodies along the profile. Pinching out of sand is more pronounced in east-west direction than in north-south. The thickness of Rose Run Sandstone reduces towards the western side of the profile (# 9 and # 11). This reduced thickness could be post-depositional as both the wells lies within the area of the subcrop (where Rose Run Sandstone truncates against Knox unconformity) of Rose Run Sandstone (Figure 2).

Structure contour map

The structure contour map is generated at the top of Rose Run Sandstone using elevation with respect to mean sea level. The structure contour map shows the orientation of the surface at the top of Rose Run Sandstone in the study area (Figure 38, 39, and 41). The deepest well is in the northeastern corner of study area, where the top of Rose Run Sandstone is at a depth of - 1884 m, whereas the shallowest well is in the western part of the study area, at a depth -819 m. All depths are depths below mean sea level. The structure contour map shows a planar upper contact of the Rose Run Sandstone, which shallows from east- to- west, in the study area

indicating dipping of the Knox unconformity towards east. There is a change in depth of almost 1000 m from the western edge to the eastern edge of the study area and in area with better well control the local relief variation is about 200 m. There is also a deepening of the top of unit from north to south, but not as significantly (the upper contact is about 200-300 m deeper in the south).

The structure contour map (Figure 38) does not show any structural complexity of the top of the Rose Run Sandstone using a 50- m contour interval. However, using a contour interval of 10 m (Figure 39), the structure contour map shows the presence of local anticlinal structure which is interpreted as pre-depositional high as the isopach value is anomalously low in that area (Figure 40). The fold is not a dome (contour lines do not close), so better resolution would be necessary to use such features as petroleum targets.

Isopach map

The isopach map was constructed using gamma- ray and density logs. The isopach map values (Figure 42 and 43) show large thickness variation within the Rose Run Sandstone. Among the study area well field, the average thickness of Rose Run Sandstone is around 18 m. However, the range was between 2 m and 40 m.

Compartmentalization of the Rose Run Sandstone can be seen in the distribution of the unit through the study area. In general, there is a linear trend of thicker sandstone in the northeast to thinner sandstone in the southwest. The lesser thickness of the Rose Run Sandstone in the western part of study area could be due to erosion, as some wells lies within the area of subcrop of the unit. Hence, the distribution pattern of the Rose Run Sandstone in the study area is result of primary deposition and post-depositional erosion. There seem to be a major depositional center or basin low in the eastern part of the study area from where the thickness of sandstone decreases in all directions. However, there is also quite a lot of local variation in the

thickness. The local variation could be due to minor fault offsets and erosion in the study area. The map conveys the general trend of the unit in the study area, although the scale of map and lack of well control in some areas increases the uncertainty of the results.

Sand-Isolith map

The sand-isolith map of the Rose Run Sandstone was created by subtracting the thickness of dolomite and shale intervals from the total thickness of the unit, using both the gamma-ray and density logs. Each well shows a high variation of sand content and its value ranges from 16 m to 2 m. The average sand content in each well is about 60 % (with 2.70 g/cm^3 as the cut off value), the rest being dolostone and mudstone. The sand-isolith map of the Rose Run Sandstone is shown in Figure 45.

In general, the map shows higher sand thickness (10-16 m) on the eastern side, and the sand thickness reduces in all other directions. Towards the western side of the area, sand truncates against the Knox unconformity. This might be evidence for stratigraphic traps where sand bodies truncate against the Knox unconformity in the up-dip direction. This can be confirmed from the production data of well logs used in the study. Well # 9, # 11, and # 14 on the west side of the map are producing, and all the 3 wells fall on the subcrop of Rose Run Sandstone, implying presence of stratigraphic traps. Well # 14 shows anomalous high value of sand in western part of study area.

Reservoir Compartmentalization

Interval reservoir heterogeneity can significantly hinder fluid production. Rose Run Sandstone exhibits compartmentalization at three different scales, micro-, meso-, and macro**.**
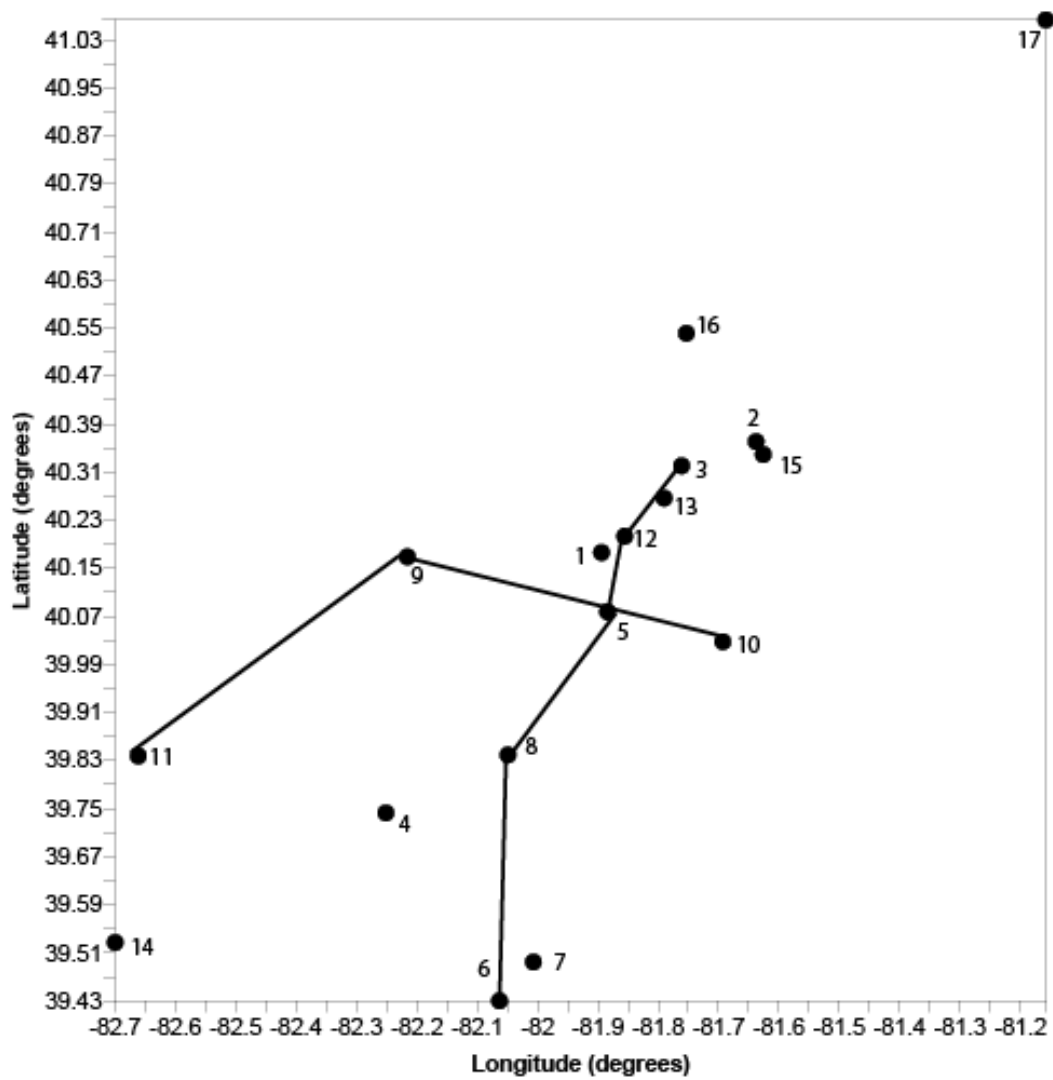
Figure 33. Map showing the location of wells used to construct lithocorrelation profiles.
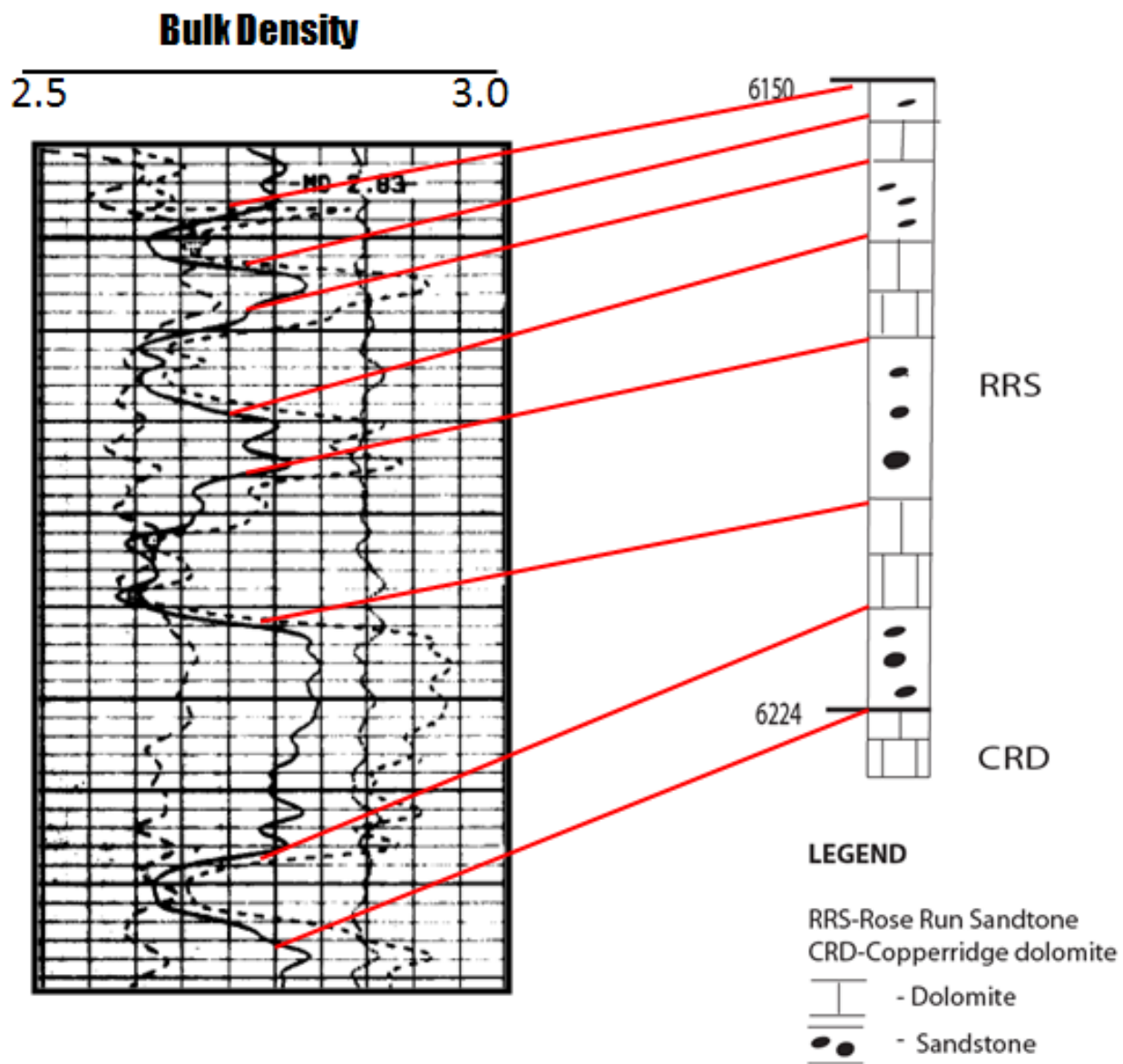
Figure 34. Geophysical log-core correlation of sand bodies for well # 12.
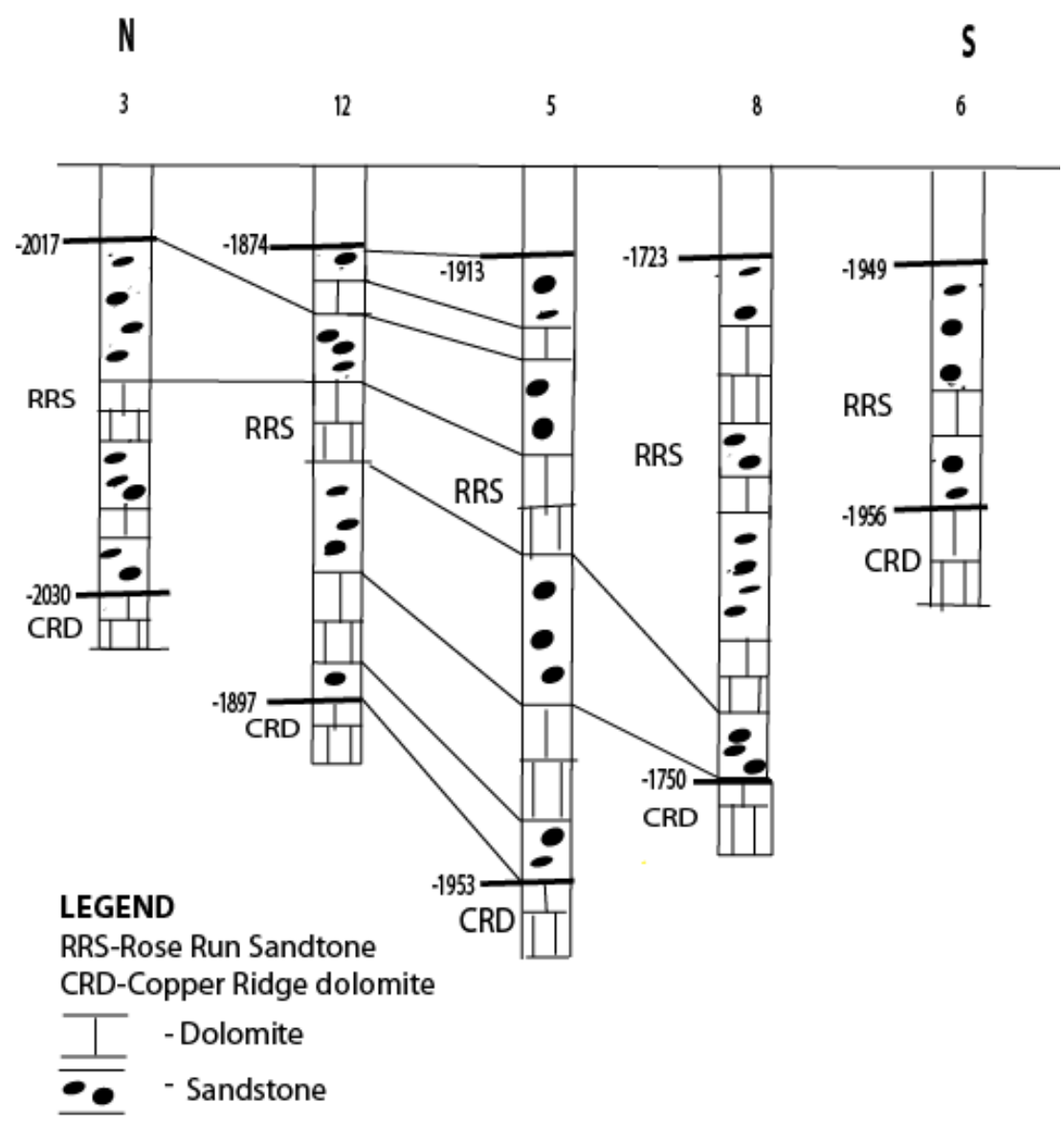
Figure 35. North-south lithocorrelation profile, interpreted to show pinch out of Rose Run Sandstone to the north and south. The lithology is based on density and gamma geophysical logs of 5 wells.
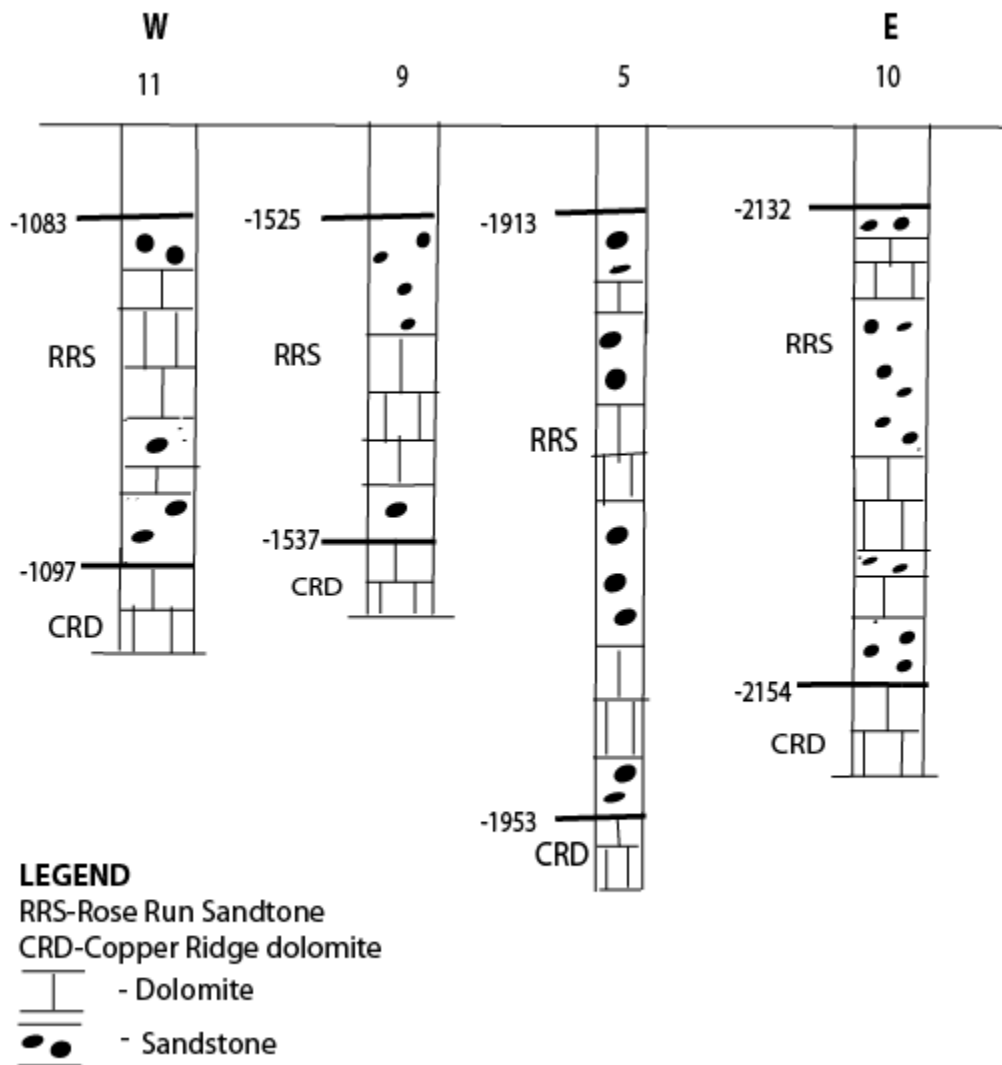
Figure 36. West-East lithocorrelation profiles interpreted to show discontinuous sand bodies. The lithology is based on density and gamma-ray geophysical logs of 4 wells.
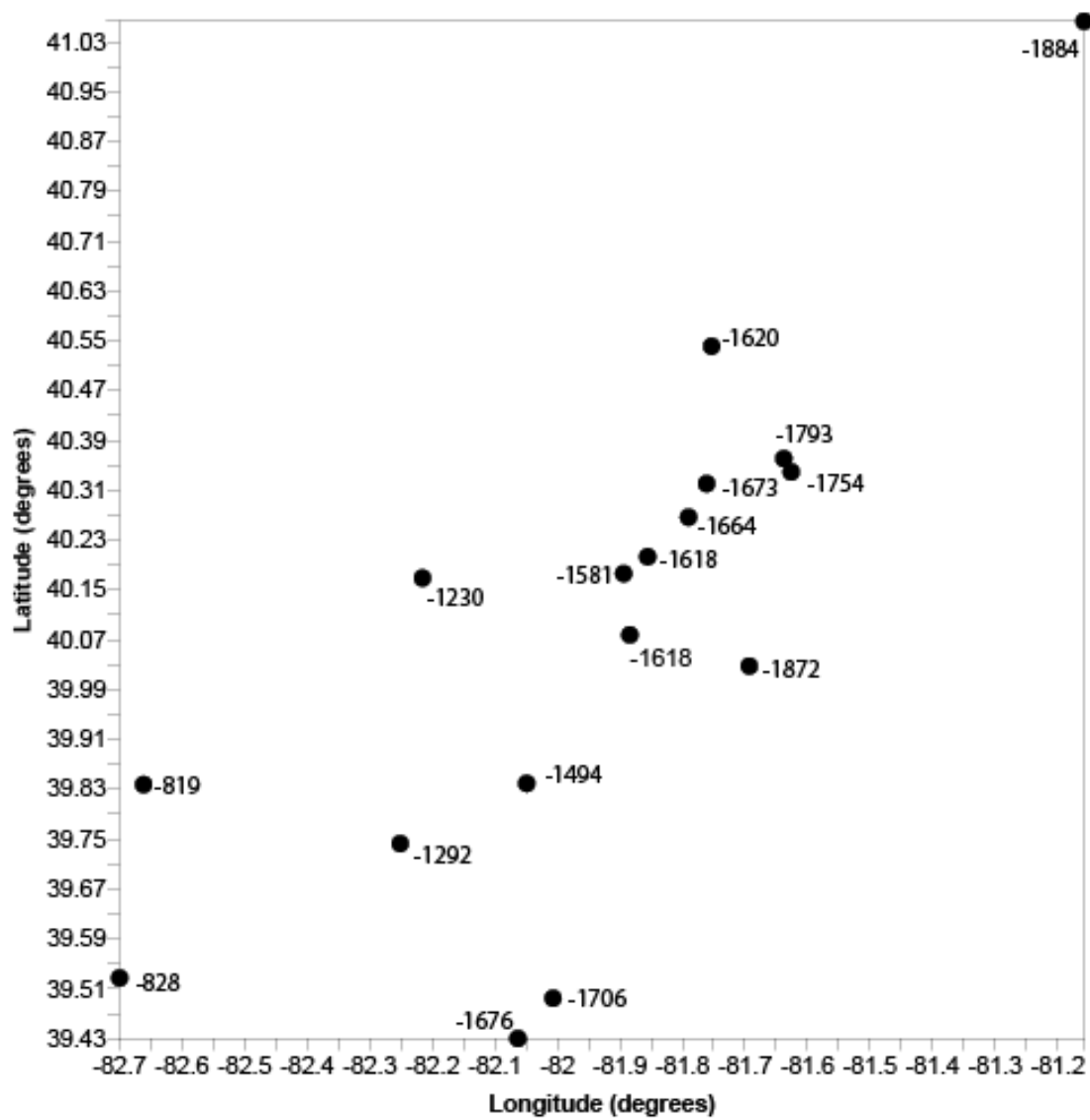
Figure 37. Locations of the wells showing depth to the top of Rose Run Sandstone.
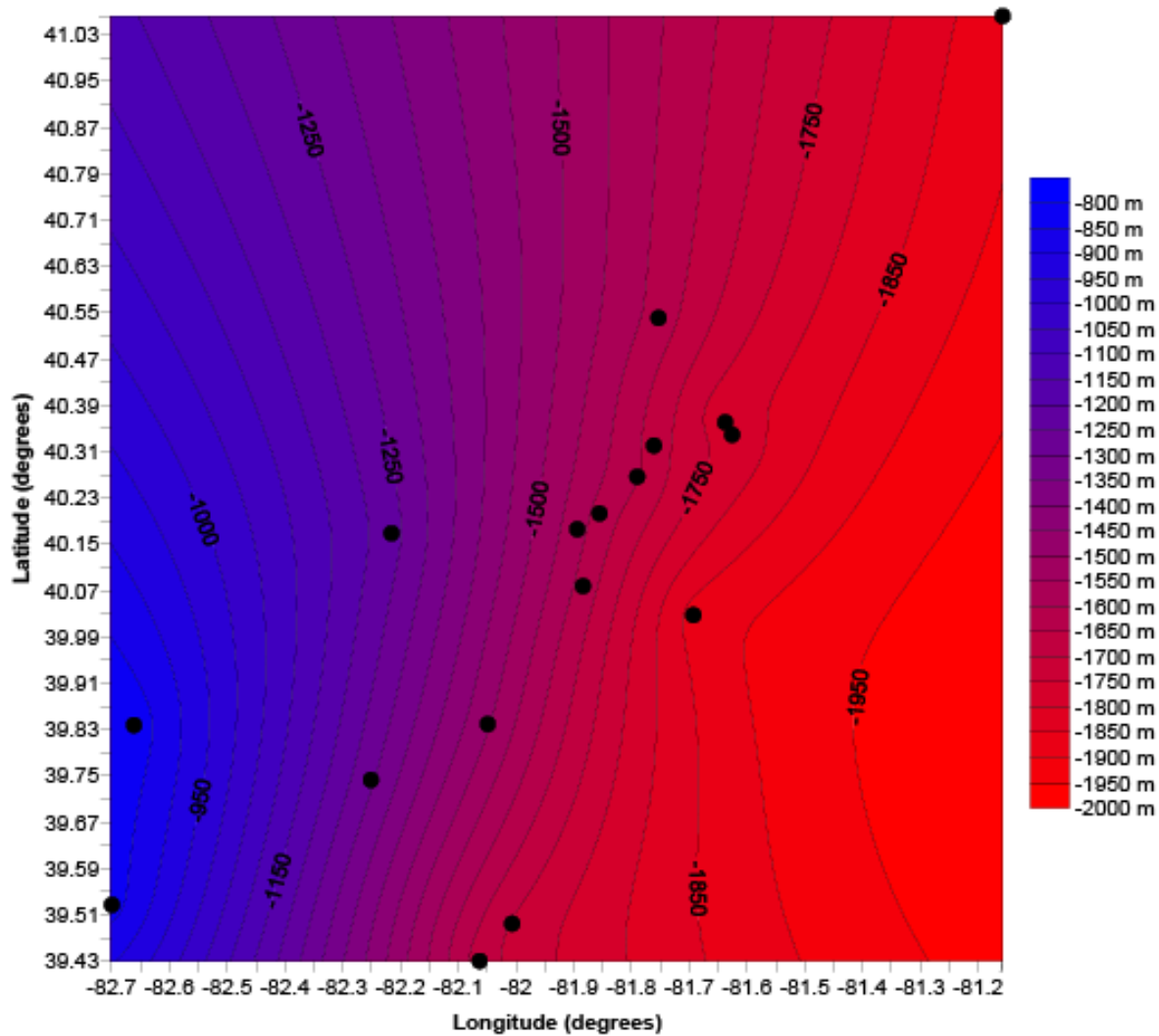
Figure 38. Structure contour map of the top of the Rose Run Sandstone. Contour interval is 50 m.
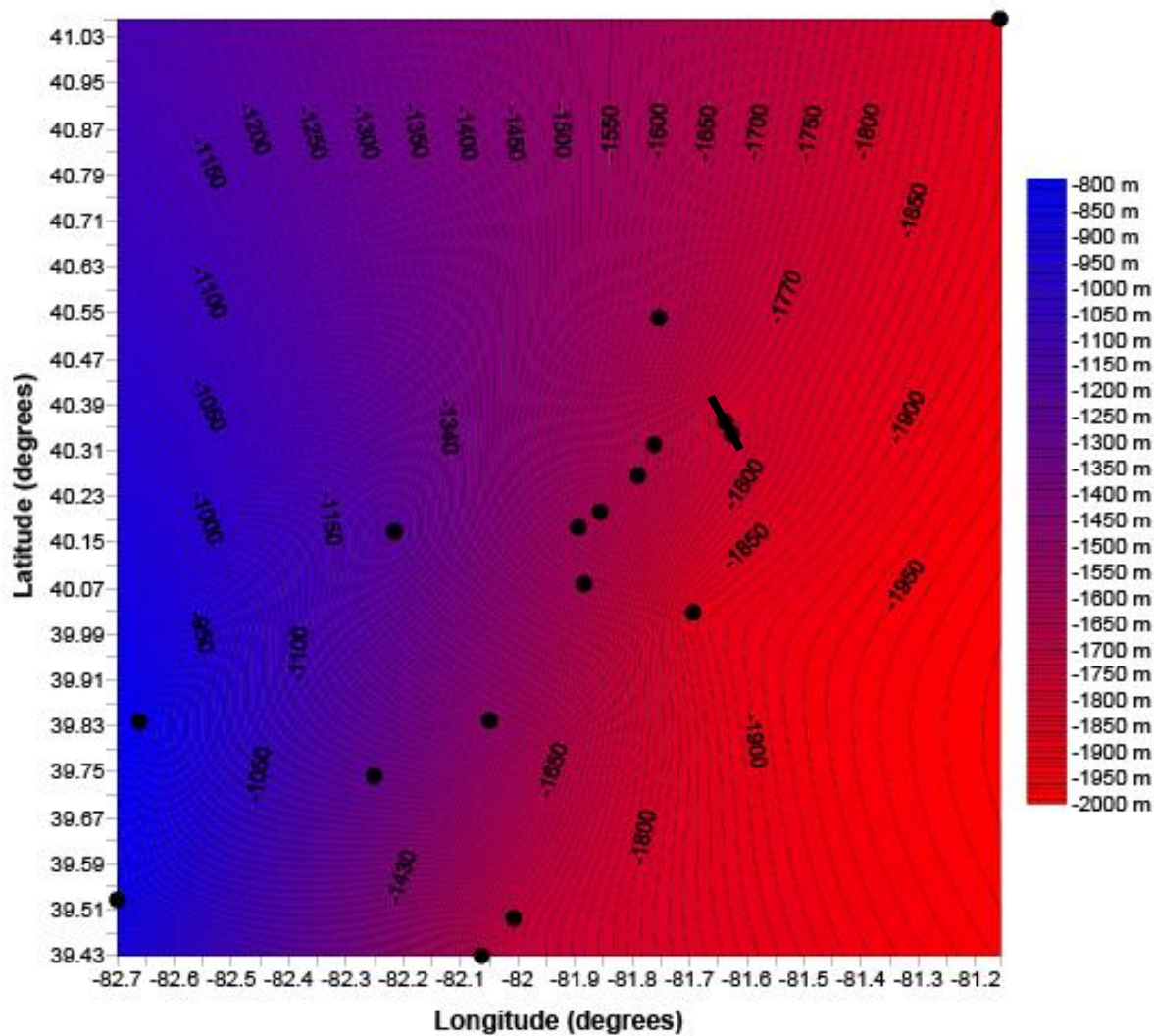
Figure 39. Structure contour map of the top of the Rose Run Sandstone. Contour interval

is 10 m. Map also shows location of profile along an anticlinal structure (Figure 40).
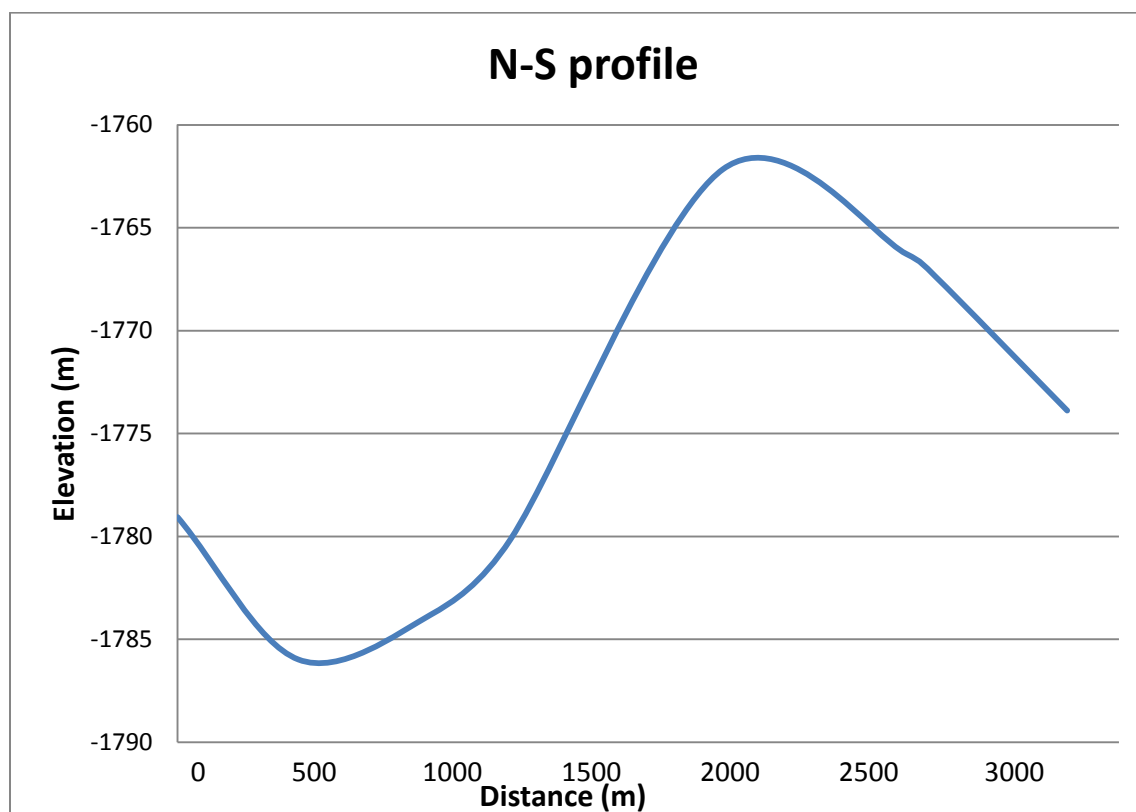
Figure 40. Profile along the pre-depositional structure at the top of Rose Run Sandstone.
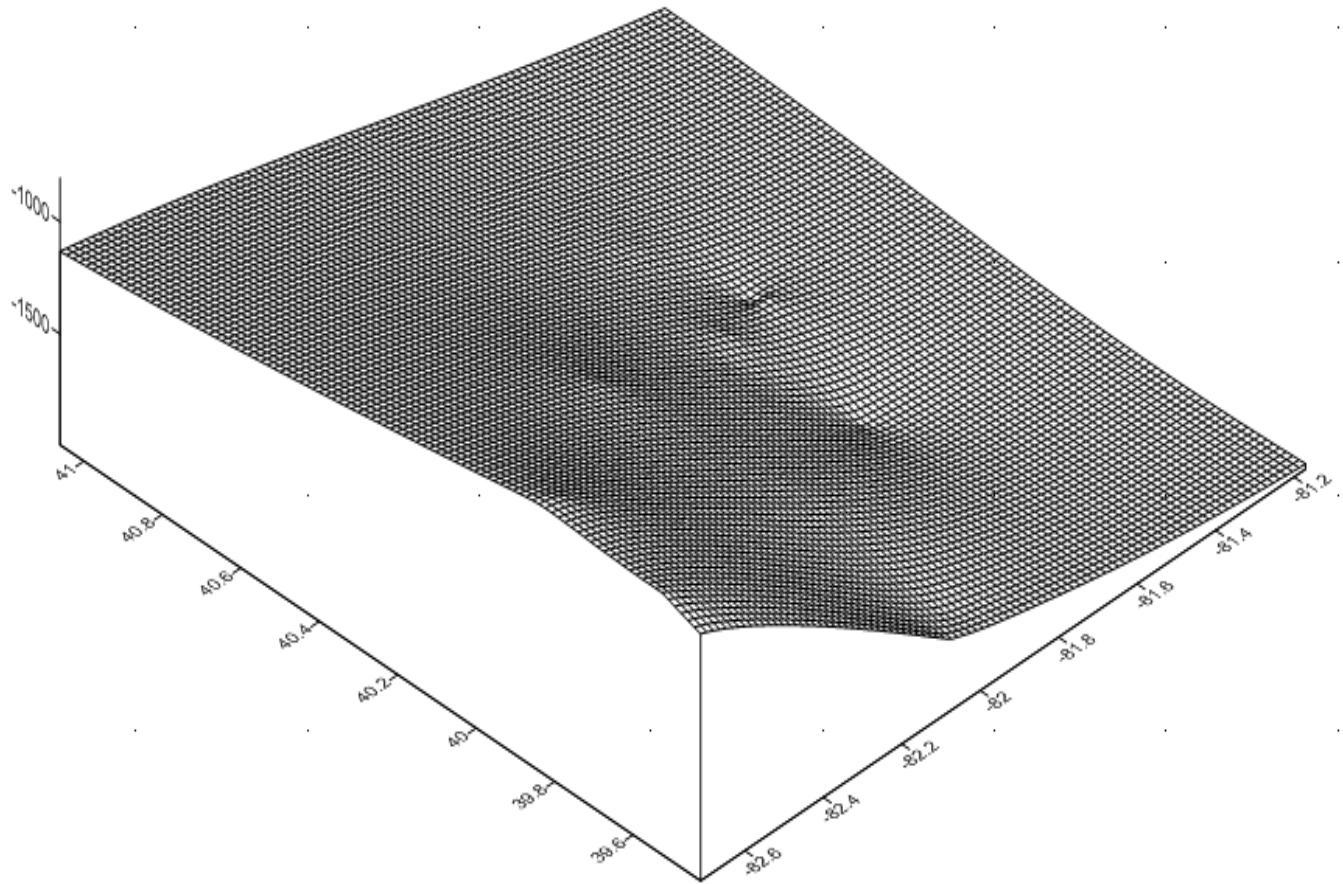
Figure 41. Surface map of the top of the Rose Run Sandstone showing shallowing of the unit towards the western side of study area. Map also shows structural complexity at top of Rose Run Sandstone.
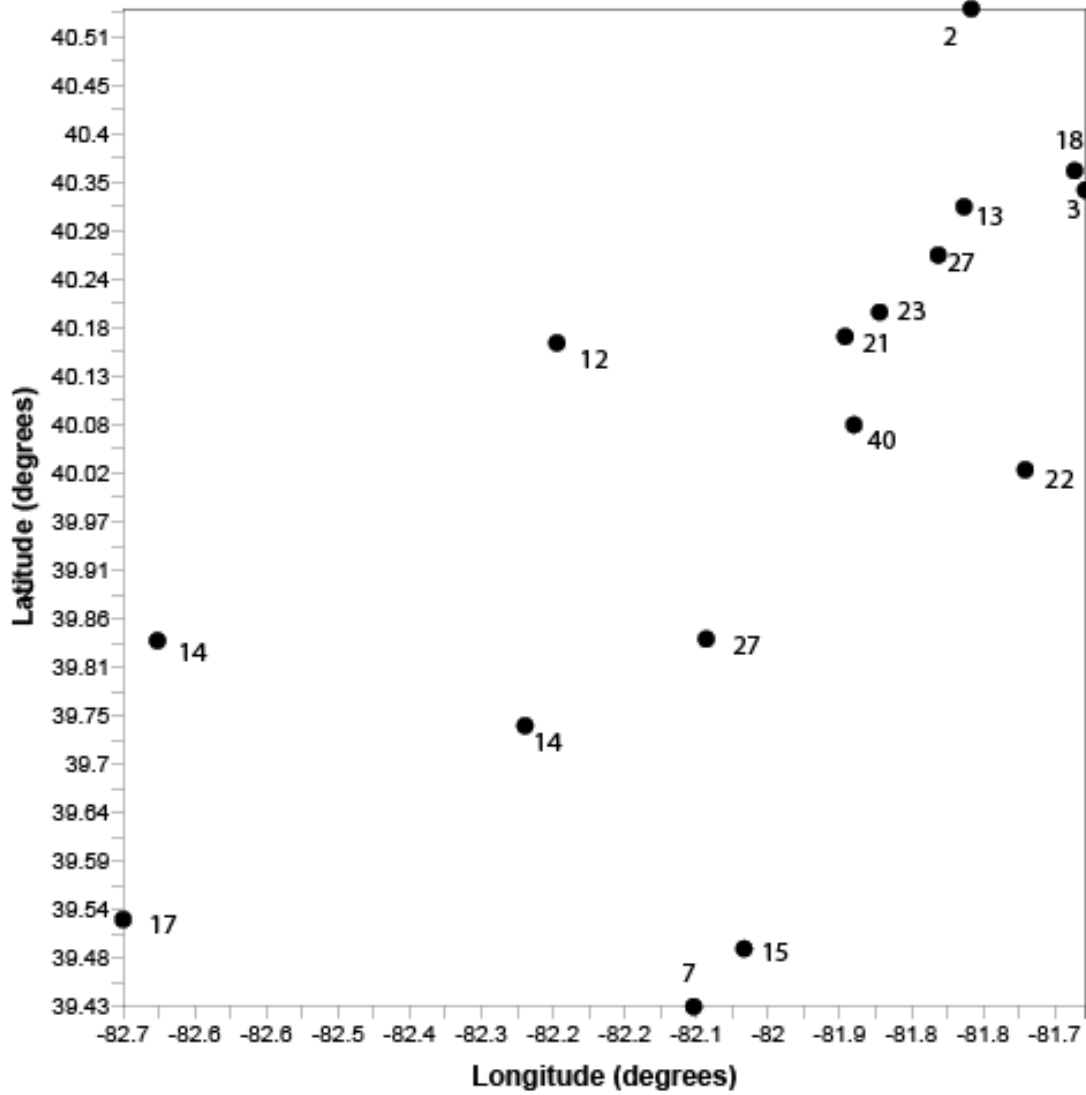
Figure 42. Location of wells with their respective isopach (total thickness) value in m.
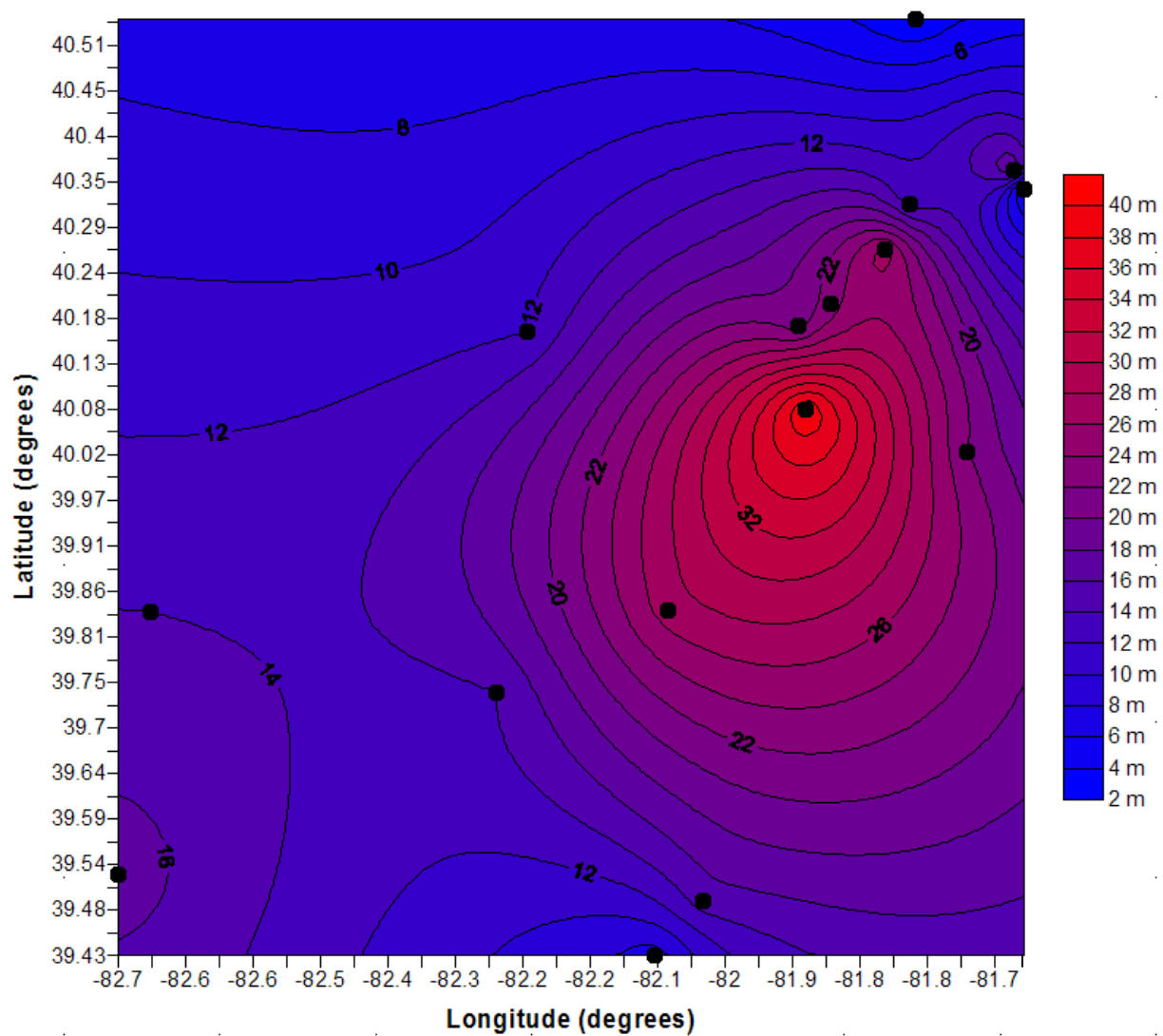
Figure 43. Isopach map of the Rose Run Sandstone in the study area. Contour interval is 2 m.
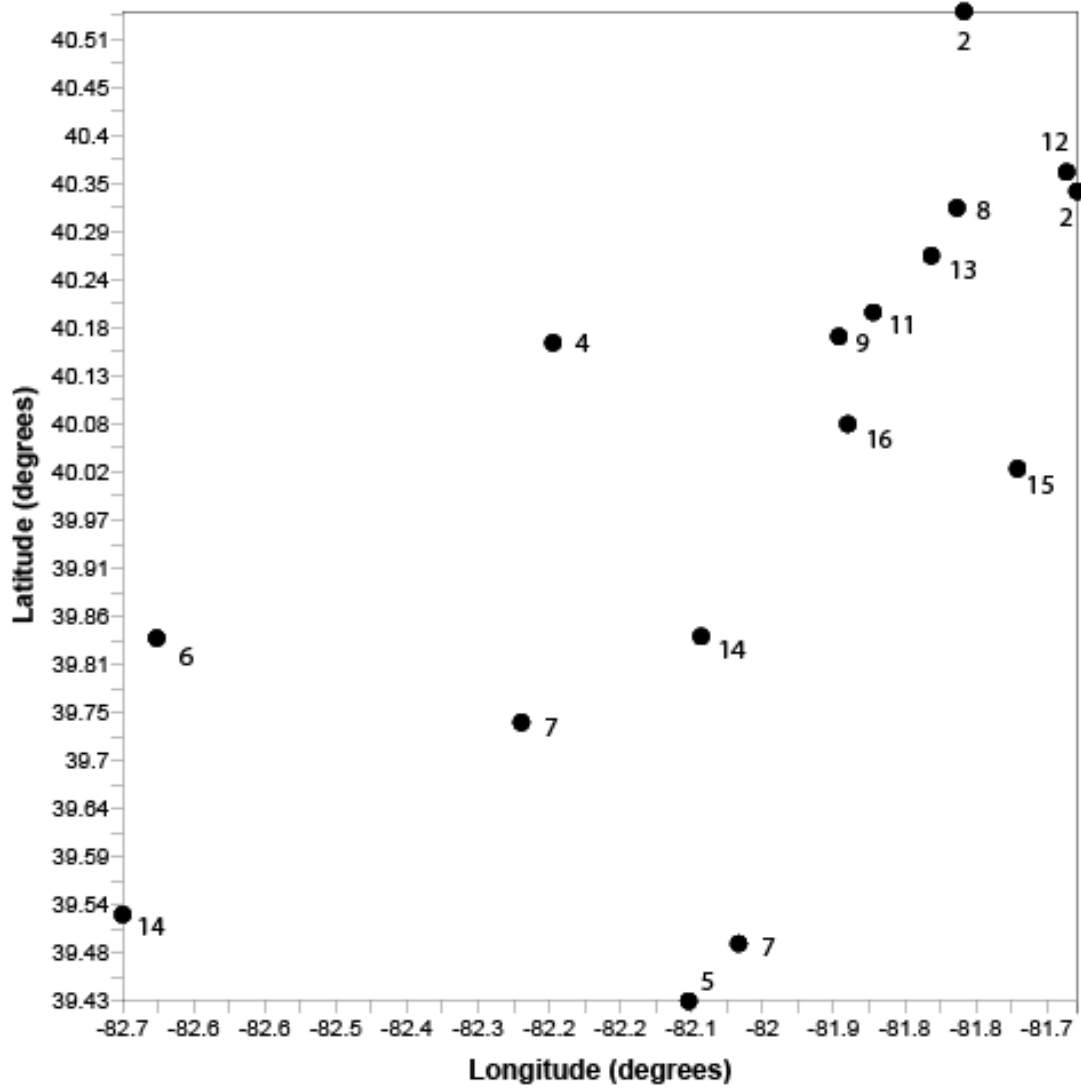
Figure 44. Location of wells with their respective sand isolith values in m.
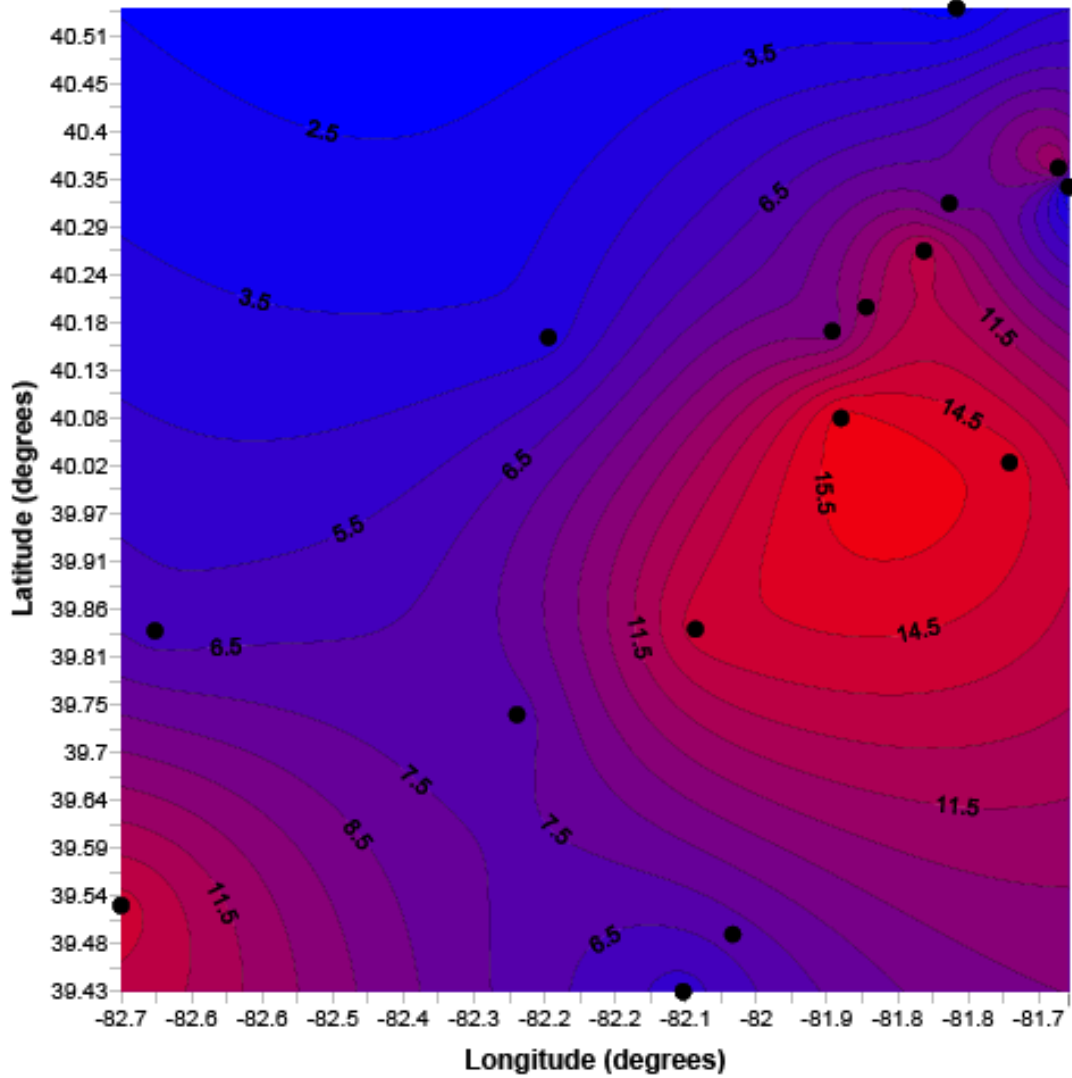
Figure 45. Sand-isolith map of the Rose Run Sandstone (contour interval is 1 m).

Micro-scale

Micro-compartmentalization in the Rose Run Sandstone is mainly controlled by dolomite and quartz overgrowth cements, which influence porosity and possibly permeability. The unit shows about 5 % of porosity which is mainly intergranular in nature. Textural and mineralogical variability caused by different grain size may also influence reservoir quality. Interlaminated clay/mud baffles and stylolites are common and are found throughout the Rose Run Sandstone (Figure 46). Such features act as baffles which can reduce the permeability and could possibly act as effective barrier to fluid flow.

Meso-scale

This study has revealed the heterogeneous stratigraphy of Rose Run Sandstone which is mainly attributed to depositional complexity of the unit. Cyclic global sea level variations in Cambrian resulted into intermixing of different facies and contributing to stratigraphic heterogeneities associated with the unit (Riley et al., 1993). The siliclastic lithofacies shows great deal of heterogeneity with environment of deposition ranging from supratidal to tidal inlet channel and hence reservoir properties are likely to change abruptly. This heterogeneity is compounded by the presence of impervious dolostone and mudstone (Figures 47 and 48), which act as barrier to fluid flow due to low porosity and permeability. In this study, Core # 2923 is the longest cored interval of the Rose Run Sandstone and based on its appearance, upper sandstone units are more porous and continuous whereas the trend downward is toward more cemented sandstone and more interbedded dolostone. Also, it is not very common to see continuous interval of porous sandstone that exceed about 3-4 m. Such thicker porous section is found only in upper section of core # 2923. Based on lithofacies analysis, lithofacies Smg is the most porous unit in the Rose Run Sandstone and its average thickness is about 20 cm. In general, the sandstone is mainly interbedded with dolostone over short intervals of 1.5 to 2 m. However,

there are open fractures in the Rose Run Sandstone which may aid the permeability in the unit. Hence, there is a lot of variation in the quality of the Rose Run Sandstone.

Macro-scale

There is better connectivity of sand bodies in the north-south direction of the study area compared to east-west, with some sand bodies extending regionally over tens of kms or more. Pinching out of sand seems to be more pronounced in east-west direction which would be roughly perpendicular to paleo-shoreline. The pre-Knox shoreline was approximately parallel to sub-parallel to the subcrop of Rose Run Sandstone (Riley et al., 2002). The Rose Run Sandstone shows highest thickness in the east of study area, from where its thickness reduces in all directions. In the northwest portion of the study area, the sandstone almost completely pinches out to shales, deposited above the Knox unconformity. The architecture of the sandstone is laterally wide spread with possible bisection by tidal channels. The average thickness of the unit is about 18 m in the area. On an average, dolostone and mudstone makes up about 40% of the Rose Run Sandstone and their impermiable nature creates vertical and lateral barrier to fluid flow.
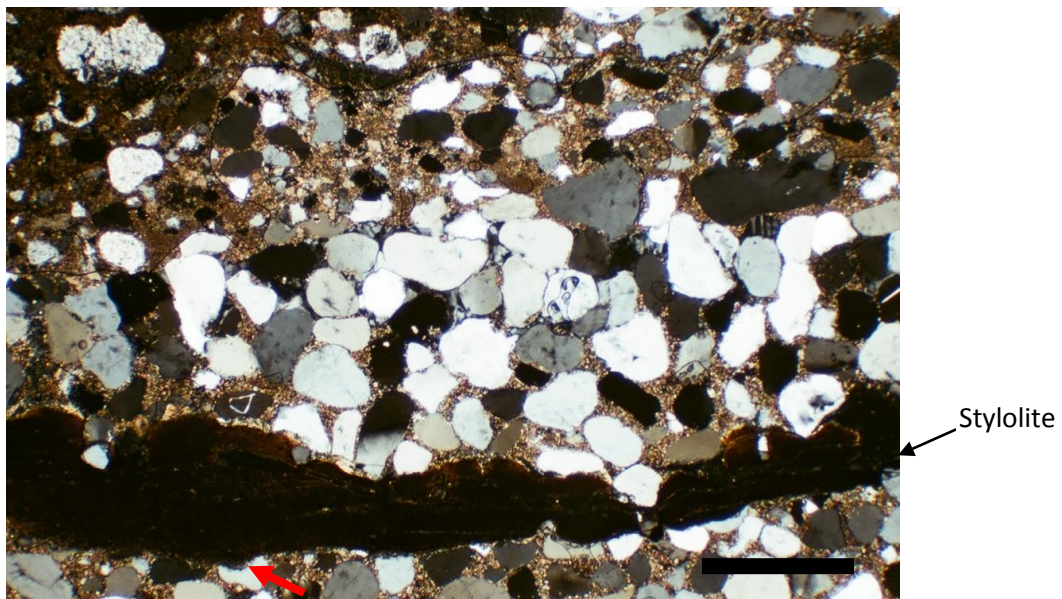
Figure 46. Photomicrograph showing stylolite and truncated quartz grains (due to pressure solution) as indicated by red arrow in sandstone. Scale bar = 1 mm.

Figure 47. Mud baffle in quartz arenite acting as a barrier to fluid flow. Scale bar = 3 cm.
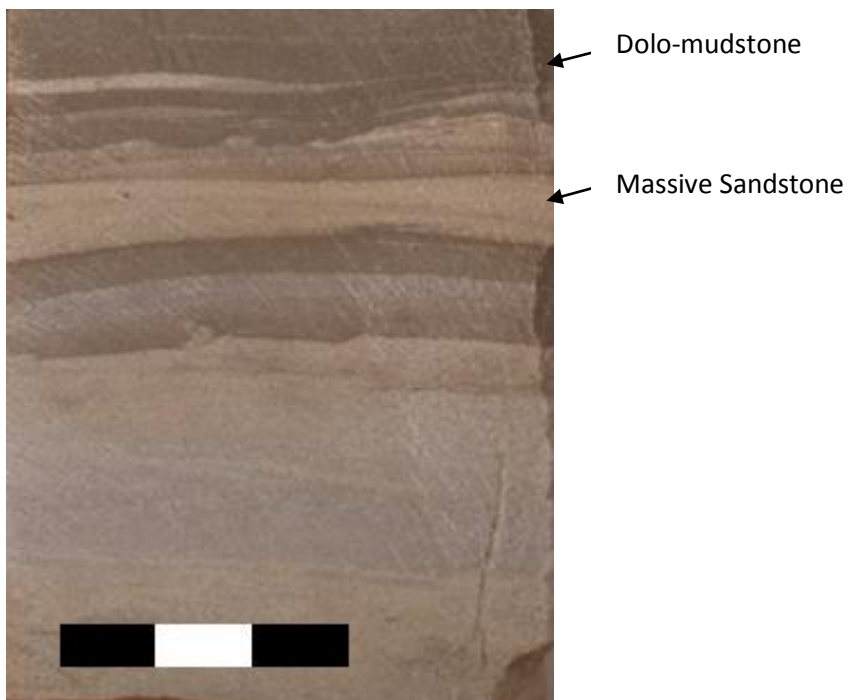
Figure 48. Alternate beds of sandstone and dolo-mudstone. Dolostone acts as a barrier to fluid

flow due to reduced permeability and porosity. Scale bar = 3 cm.

DISCUSSION

Depositional Environment

According to Selley (1973), mixed carbonate-clastic shorelines could be due to three factors: (1) low input of sediment due to low runoff, (2) low sediment availability (if the hinterland is low lying), or (3) if the shoreline itself has a very gentle seaward gradient causing a broad tidal zone and an extremely wide development of the facies belts paralleling the shore. In any such instances, siliciclastic sediment may be deposited near river mouths, on estuarine tidal flats, or on beaches and barrier islands. Finally, there may be instances where current action was insufficient to re-work these deposits and carry sand out to the carbonate barrier zone. In such cases, onshore currents may pile up bars of carbonate sand far to seaward of the river mouth.

Most of previous workers, such as Chuks (2008), Atha (1981), Enterline (1991), and Riley et al. (1993), have interpreted the depositional environment of the Rose Run Sandstone mainly as shallow-marine environment with tidal influence. Atha (1981) interpreted the depositional environment of the Rose Run Sandstone as peritidal. Enterline (1991) interpreted the unit as tidal flat environment with migrating tidal channels. Riley et al (1993) interpreted the depositional environment of the unit as peritidal to shallow marine environment. Chuks (2008) interpreted the depositional environment of the Rose Run Sandstone as tidally influenced, subtidal environment with associated tidal flat deposits and related subtidal channels with migrating sandbars. Based on the lithofacies associations observed in this study, Rose Run Sandstone is interpreted to be associated with following sub environments, 1) clastic tidal flat with associated tidal channels, and 2) peritidal carbonate setting with associated subtidal lagoonal environment.

The geology of tidal depositional systems can be complicated due to the spatial relations of numerous distinct sub-environments such as beach, tidal flats, tidal channel inlet, tidal delta, or lagoon sub-environments. Some of these sub-environments have considerable lateral continuity and some do not. The environmental interpretation is further complicated by variables such as the rate of sea-level change, change in sediment supply and the relative importance of waves versus tides (Davis, 1994). Furthermore, shifting of shoreline landward or seaward depends on interplay between variables such as eustasy, sediment supply, and tectonics. For example, if the sediment supply is greater than the accommodation space created by rise in sea level, the net result would be regression in spite of rise in sea level or vice versa.

Rose Run Sandstone Environments

Clastic tidal flats

The clastic tidal flats can be divided into supratidal zone (above high tide level), intertidal zone (between low tide and high tide level), and subtidal zone (below low tide level). In the Rose Run Sandstone, intertidal deposits are represented by lithofacies SMk, lithofacies SMf, lithofacies SMl, and lithofacies SMw. Mottling due to bioturbation is also very common in intertidal zone and is observed in Rose Run Sandstone. Lithofacies Mm and lithofacies Smm are interpreted to be deposited in intertidal zone. Chakrabarti (2005) interpreted similar sedimentary structures such as lenticular bedding, wavy bedding, flaser bedding, tidal rhythmites, contorted or convolute lamination, or mottling etc. on the east coast of India to have been deposited in intertidal environment. The intertidal zone is also characterized by erosional contacts or abrupt vertical and lateral changes in bedding structures. Abrupt erosional contacts are found in Rose Run Sandstone and are interpreted as active shifting of tidal inlet channels (Figure 26).

The subtidal zone mainly consists of medium- to coarse- sand size sediments. Within this environment, medium- to high- angle cross bedding, parallel lamination, herringbone cross-

stratification, massive sandstone, and intraclasts clasts dominate (Walker, 1992). All these lithofacies are found in Rose Run Sandstone. In addition, lithofacies Smg, lithofacies Sh, and lithofacies Ml are observed in the Rose Run Sandstone and have been interpreted to be deposited in subtidal environment. Enterline (1991) and Chuks (2008) also observed glauconite and ooids in the Rose Run Sandstone and interpreted its presence as indicative of shallow marine subtidal environment.

Tidal inlet deposits in the Rose Run Sandstone are represented by lithofacies Sp, lithofacies Sx, lithofacies Smi, and lithofacies Sm. Lithofacies Sp is indicative of probable migration of dunes/bars within channels. According to Sengupta (2007), cross beds within tidal channels often carries imprints of flood and ebb flows and are naturally bidirectional. Chuks (2008), observed similar lithofacies such as low- to medium- angle planar-tabular cross bedded sandstone and interpreted them as channel deposits.

In general, core data shows a deepening-upward sequence in the Rose Run Sandstone (Figure 49). In core 2989 and core 3385, the siliciclastic sequence starts with lithofacies SMk which then grades into lithofacies SMw, or lithofacies Smm, or lithofacies SMl, transitioning then into lithofacies SMf, and ultimately grades into lithofacies Sm, or lithofacies Sp, or lithofacies Smg. In core 2923, the siliciclastic deposits are mainly of sand flat to subtidal environment and do not show a particular sequence. Tidal inlet channel assemblages are common in core 2923. The main siliclastic lithofacies in core 2923 includes lithofacies Sx, lithofacies Sh, lithofacies Sm, lithofacies Smi, and lithofacies Sl.

Carbonate tidal flats or peritidal facies

 Peritidal environment include areas showing tidal influence during the deposition of carbonate sediments. Lithofacies Cpl is interpreted to be deposited in supratidal zone. Gingras and Pemberton (2012) interpreted biolaminated dolostone in west-central Alberta to be deposited

in supratidal conditions. Also, the dolostone shows vugs filled with chert which could be possibly secondary replacement suggesting arid supratidal conditions (Riley et al, 1993). Lithofacies Cmmc (convoluted bedded dolostone) is interpreted to be deposited in intertidal flats owing to drying (shrinking) and expanding (wetting) of mud during each tidal cycle. Lithofacies Cmm and lithofacies Cm are the most common lithofacies among the carbonates. The mottling in lithofacies Cmm is due to bioturbation caused by organisms, and both the lithofacies are interpreted to be deposited in subtidal-lagoonal setting. Swanson (1981), interpreted mottled dolostone found in Gatesburg formation in Pennsylvania to be deposited in subtidal shelf lagoonal environment whereas Hopkins (2004) interpreted massive dolo-mudstone of the Pekisko formation in Western Canada of subtidal lagoonal origin. Lithofacies Cprm (flat pebble conglomerate) is interpreted to be deposited in subtidal environment under high energy conditions. Sepkoski (1982) has interpreted flat pebble conglomerate in portions of Dresbachian strata in Montana, Wyoming, and South Dakota to be deposited in shallow subtidal environment.

Similar to siliciclastic sequences, the carbonate sequences in Rose Run Sandstone are also indicating deepening-upward conditions. These started with lithofacies Cpl, which then graded into lithofacies Cmmc, transitioned upwards into lithofacies Cm or lithofacies Cmm and finally into lithofacies Cpmr. Vugs filled with chert are often associated with lithofacies Cpl and lithofacies Cmmc.

Environment analysis from Logs

The electrolog correlation profiles of the Rose Run Sandstone show multiple imbricate sand bodies covering large areal distance which is characteristic of tidal sand body (Klein, 1997). Due to insufficient spacing between wells it was difficult to ascertain the geometry of sand bodies. However, the litho-correlation profiles seem to suggest the geometry of the sand body ranges from sheet- like to broadly lenticular. According to Klein (1977) and Pettijohn et al.
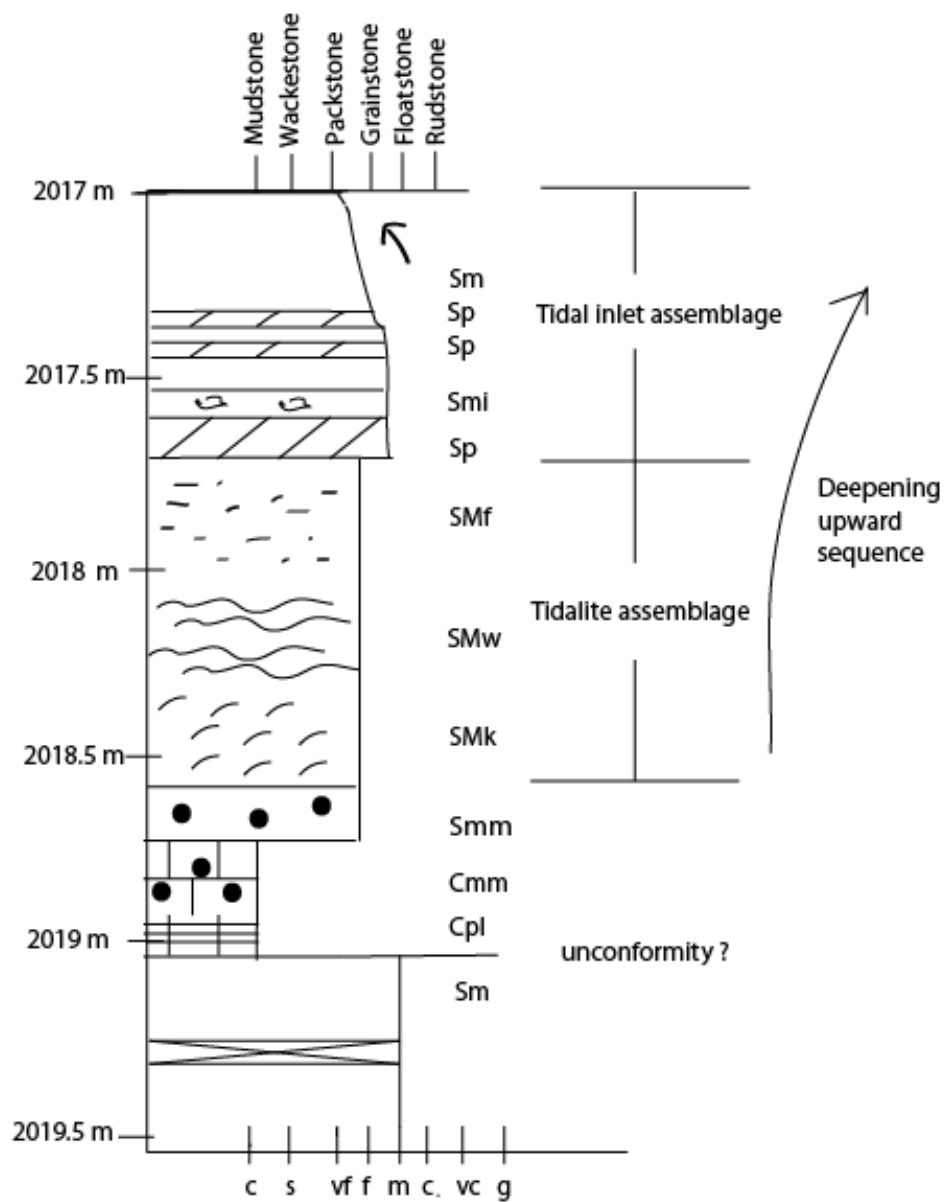
Figure 49. Subtidal to intertidal clastic-carbonate sequence in core 2989

(1973), this basic pattern is characteristic of shallow subtidal, tide dominated sandbodies, which are elongate sheets are oriented parallel to the shoreline and commonly bisected by tidal channels. Such sand bodies also tend to show great variance in dimensions and shape.

Both isopach and sand-isolith maps show a linear feature which is approximately parallel to subparallel the paleo-shoreline. Based on sedimentary structures found in the cores of Rose Run Sandstone, it is possible that the linear feature represents an extensive barrier-island system, as barrier-islands are commonly associated with tidal flats.

Reservoir Compartmentalization

Reservoir compartmentalization is a major factor that controls the recovery of hydrocarbons in a given field. Rose Run Sandstone exhibits heterogeneities at all levels. The implications of these heterogeneities are obvious. On a macro scale, the truncation of Rose Run Sandstone against the Knox unconformity created effective trapping mechanisms for hydrocarbon accumulation. Rise in sea level following the formation of Knox unconformity deposited shales of the Wells Creek Formation which act as an effective seal for entrapment of hydrocarbons. In spite of thicker sandstone in eastern part of study area, most of wells drilled in this area are dry, which could be due to absence of effective trapping mechanism, versus the western part of study area. However, stratigraphic heterogeneity as discussed in previous section could lead to depositional stratigraphic traps in the down-dip directions wherein the sand pinches out in all directions. In the study area, the sand nowhere completely pinches out in all directions but with better well control such spots could be identified. The East Randolph pool in Portage County is the result of a stratigraphic trap which is located down dip of subcrop (Riley et al., 2002). Better well control might also help in bringing out more structural complexity at top of

Rose Run Sandstone which can be potential petroleum targets. Figure 50 shows conceptual model for trapping mechanism in Rose Run Sandstone. In the study area, there is better sand to sand continuity in the north-south direction as compared to east-west. At meso scale, i.e., within a single core there is considerable variation from bed to bed and lithofacies change abruptly. Sandstone itself shows high degree of heterogeneity, which is evident from the number of siliciclastic lithofacies associated with it. This is compounded by interbedded dolostone and mudstone. With such stratigraphic heterogeneity, even small amount of fault throw might juxtapose porous and permeable sandstone to impervious dolostone or mudstone which would further compartmentalize the reservoir. On micro-scale, the thin sections do not show much variance in porosity (5%) and the primary cementing agent is dolomite which is followed by quartz overgrowth. Other minor cements found in Rose Run Sandstone include feldspar overgrowth and clay cement. Presence of matrix and accessory minerals also reduces porosity by filling in the pore spaces. Interlaminated mud baffles and textural differences might influence reservoir properties. According to Riley et al (1993), Rose Run Sandstone has undergone complex burial and diagenetic history wherein dolomitization was associated both during initial burial and later burial (post Knox unconformity) of the unit. He further stated that the formation of Knox unconformity aided secondary porosity by dissolution of dolomite cement by meteoric waters and basinal brines.

Compartmentalization of the Rose Run Sandstone has direct implications on the overall hydrocarbon recovery from the unit and the hydrocarbon exploration in unit has not been uniformly successful due to reasons outlined above and in previous sections.
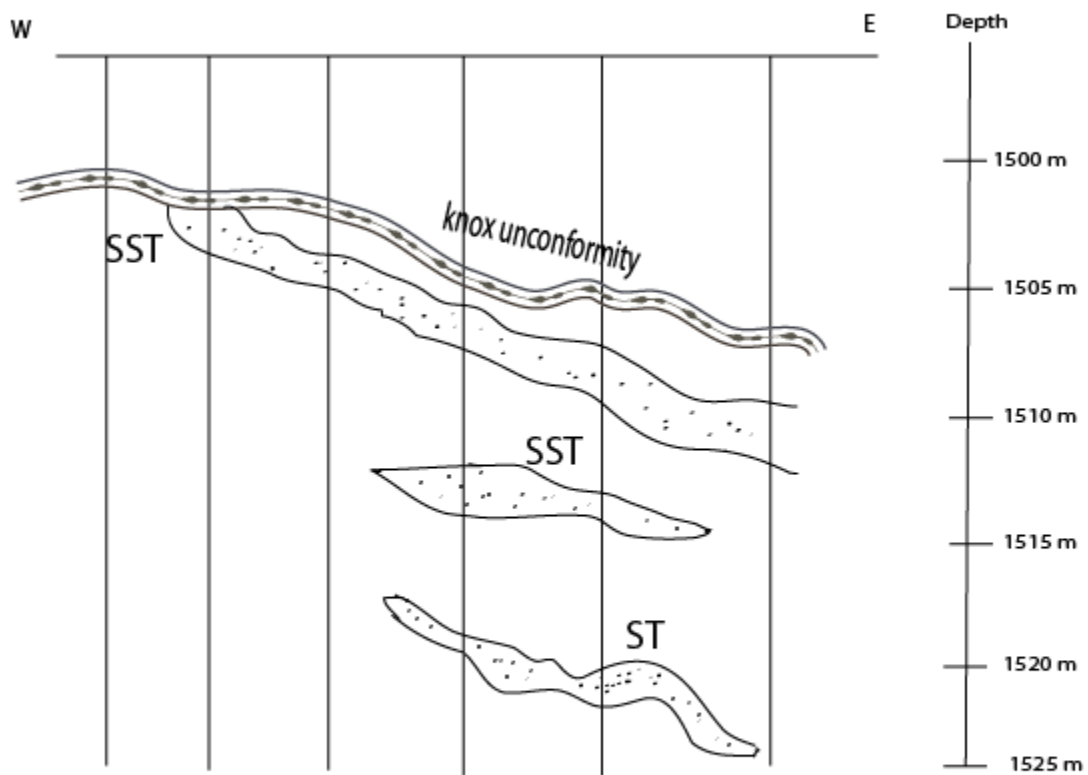
Figure 50. Conceptual model for trapping mechanism in the Rose Run Sandstone. Abbreviations SST and ST stands for stratigraphic trap and structural trap respectively.

SUMMARY AND CONCLUSIONS

This study involved petrofacies analysis from 11 thin sections, lithofacies analysis from 4 cores, and geophysical log analysis from 17 wells logs, to understand the sedimentology, stratigraphy, and architecture of the Rose Run Sandstone. The cores observed in this study show a mixed siliciclastic-carbonate facies in the Rose Run Sandstone. Previous interpretations for the depositional environment are mainly suggested as tidal flats to peritidal environment. This study confirms the results of Chuks (2008), and the depositional environment of the Rose Run Sandstone is interpreted as a shallow marine environment with extensive tidal flats and associated tidal channels and subtidal lagoons, strong tidal influence, and reworking of carbonate materials.

Sedimentary structures found in sandstone includes planar-tabular cross bedding, herringbone cross stratification, flaser bedding, wavy bedding, lenticular bedding, tidal rhythmites, mottling whereas sedimentary structures in dolostone include mottling, intraclasts, massive bedding, cryptalgal lamination. Together, these sedimentary structures suggest strong tidal influence in the deposition of Rose Run Sandstone. Reworking of carbonates is indicated by presence of flat pebble conglomerate.

The Rose Run Sandstone shows compartmentalization at micro-, meso-, and macro-scales. Point count of 4 thin sections shows about 5 % intergranular porosity. Dolomite cement is major cementing agent followed by quartz overgrowths, whereas feldspar overgrowth and clay cement contributes minorly. Within the sandstones, mud baffles are common phenomenon, which may influence permeability. Core analysis reveals nineteen lithofacies in Rose Run Sandstone, underlining the diversity of depositional processes leading to stratigraphic heterogeneity in the unit. The interbedded low permeability dolostones and mudstones may act as barrier to fluid flow between sandstone units. On a macro- scale, truncation of Rose Run

Sandstone against the Knox unconformity creates up dip stratigraphic traps and is a major reason for compartmentalization of the unit. Geophysical log analysis reveals wide areal distribution of Rose Run Sandstone consisting of elongate sheet like to lenticular- sand bodies. There is better sand to sand connectivity in north-south direction. The structure contour map reveals structural complexity at the top of Rose Run Sandstone.

REFERENCES

Ager, D.V., 1974. Storm deposits in the Jurassic of the Moroccan High Atlas. Paleogeography, Paleoclimatology, Paleoecology, 15: 83-93.

Atha,T.M., 1981 . A subsurface study of the Cambro-Ordovician Rose Run Sandstone in eastern Ohio. Unpublished M.S. Thesis, West Virginia University, Morgantown, 66 p.

Banjade, B., 2011. Subsurface facies analysis of the Cambrian Conasauga Formation and Kerbel Formation in East-Central Ohio. Unpublished M.S. Thesis, Bowling Green State University, Bowling Green, Ohio, 156 p.

Babcock, L.E., 1994. Biostratigraphic significance and paleogeographic implication of Cambrian fossils from deep core, Warren County, Ohio. Journal of Paleontology, 68: 24-30.

Bathurst, R.G.C., 1975. Carbonate sediments and Diagenesis (2nd. Ed.). New York: Elsevier, 658 p.

Boggs, S., 2006. Principles of Sedimentology and Stratigraphy, Fourth Edition. Upper Saddle River, N.J.: Prentice Hall, 662 p.

Burst, J. F., 1958. "Glauconite" pellets: their mineral nature and applications to strati-graphic interpretations. American Association of Petroleum Geologist Bul1etin, 42: 310-327 .

Chakrabarti, A., 2005. Sedimentary structures of tidal flats: A journey from coast to inner estuarine region of eastern India. Journal of Earth System Science, 114: 353-368.

Chuks, N.E., 2008. Subsurface Facies Analysis of the Rose Run Formation in South Eastern Ohio. Unpublished M.S thesis, Bowling Green State University, Bowling Green, Ohio, 113 p.

Davis Jr, R.A., 1994. Barrier Island Systems- a geologic overview. In Geology of Holocene Barrier Island Systems, Berlin: Springer, p. 1-46.

Dickinson, W.R. and Suczek, C.A., 1979. Plate tectonics and sandstone compositions: American Association of Petroleum Geologist Bulletin, 63: 2164–2182.

Dunham, R.J., 1962. Classification of carbonate rocks according to depositional texture. In Ham: W.E. (editor), Classification of carbonate rocks. Tulsa, OK: American Association of Petroleum Geologists Memoir 1: 108-121

Einsele, G., 1963, Convolute bedding and ahnliche sedimentsrukturen im rheinischen Oberdevon und anderen Ablagerungen. Neues Jahrbuch fur Geologie and Palaontologie Abh, 116, 162-198.

Enterline, D.S., 1991. Depositional environment of the Cambro-Ordovician Rose Run Formation in N.E. Ohio and equivalent Gatesburg Formation in N.W. Pennsylvania. Unpublished M.S Thesis, University of Akron, Akron, Ohio, 98 p.

Folk, R. L., 1974. Petrology of Sedimentary Rocks. Austin, Texas: Hemphill Publishing Company, 182 p.

Freeman, L.B., 1949. Regional aspects of Cambrian and Ordovician subsurface stratigraphy in Kentucky. American Association of Petroleum Geologists Bulletin, 22: 1655-1681.

Friedman, G.M. and Sanders, J.E., 1978. Principles of Sedimentology. New York: John Wiley and Sons, 792 P.

Gingras, M. K., and Pemberton, S. G., 2012. Reservoir Characterization of Burrow-Mottled Dolomites: Devonian Wabamun Group, West-Central Alberta, Canada. http://www.cspg.org/documents/Conventions/Archives/Annual/2012/core/218_GC2012_Reservoir_Characterization_of_Burrow-Mottled_Dolomites.pdf

Hagadorn, J.W., Dott Jr., R. H., and Damrow, D., 2002. Stranded on a late Cambrian shoreline: Medusa from Central Wisconsin. Geology, 30: 147-150.

Hansen, M.C., 1998, The Geology of Ohio-The Precambrian. Columbus: Ohio Divison of Geological Survey, Geofacts no. 20, 2p.

Harris, L.D., 1978, The eastern interior aulacogen and its relation to Devonian Shale gas production. Preprints, Second Eastern Gas Shales Symposium, METC/SP-78/6, II: 55-72.

Harms, J.C., Southard, J.B., Spearing, D.R., and Walker, R.G., 1975, Depositional environments as interpreted from primary sedimentary structures and stratificationsequences. Tulsa, OK: SEPM Short Course Notes 2, 161 p.

Hayes, M, O., 1979. Barrier island morphology as a function of tidal and wave regime. In: Latherman, S.P. (editor), Barrier Island- From the Gulf of St. Lawrence to the Gulf of Mexico, Academic Press, New York, pp. 1-71.

Hopkins, J. C. (2004). Geometry and origin of dolomudstone reservoirs: Pekisko Formation (Lower Carboniferous), western Canada. In C.J.R. Braithwaite, G. Rizzi, and G. Darke (editors),The geometry and petrogenesis of dolomite hydrocarbon reservoirs: London: Geological Society of London, Special Publication 235: 349-366.

James, N.P., 1984. Introduction to Carbonate Facies Models. In: Walker, R.G. (editor)., Facies Models (2nd ed.). Toronto: Geoscience Canada, Reprint Series 1, p. 213-228.

James, N.P. and Dalrymple, R.W., 2010. Facies Model 4. St. John's, Newfoundland: Geological Association of Canada, 586 p.

Janssens, A., 1973. Stratigraphy of the Cambrian and Lower Ordovician rocks in Ohio. Columbus: Ohio Division of Geological Survey, Bulletin 64, 197 p.

Jolley, S.J., Fisher Q.J., and Ainsworth RB., 2010, Reservoir Compartmentalization: an Introduction. London: Geological Society of London, Special Publication 347 (1), p. 1-8.

Kazmierczak, J. and Goldring, R., 1978, Subtidal flat-pebble conglomerate from the Upper Devonian of Poland: a multiprovenant high-energy product. Geological Magazine, 115: 359–366.

Kerans, C., 1990. Depositional systems and karst geology of the Ellenburger Group (Lower Ordovician), subsurface West Texas. The University of Texas at Austin, Bureau of Economic Geology Report of Investigations No. 193, 63 p.

Klein, G. deV., 1977. Clastic tidal facies. Champaign, Illinois: Continuing Education Publication, 149 p.

Logan, B.W., Hoffman, P., and Gebelein, C.D, 1974. Algal mats, cryptalgal fabrics and structures, Hamelin pool, Western Australia. In: Logan, B.W., Read., Hagan, G. M., Hoffman, P., and Brown, R. G. (editors), Evolution and Diagenesis of Quarternary carbonate sequences, Shark Bay, Western Australia, American Association of Petroleum Geologists memoir, 22: 140-194.

Longhitano, S.G., Mellere, D., Steel, R.J., and Ainsworth, R,B., 2012. Tidal deposistional systems in the rock record: A review and new insights. Sedimentary Geology, 279: 2-22.

Martin A.J., 2000., Flaser and wavy bedding in ephemeral streams: A modern and an ancient example. Sedimentary Geology, 136 (1-2): 1-5.

Martin, C.A.L. and Turner, B.R. 1998. Origins of massive-type sandstones in braided river systems. Earth-Science Review, 44: 15 – 38.

Mazumder, R., and Arima, M., 2004. Tidal rhythmites and their implications. Earth-Science Reviews, 69 (1-2): 79-95.

McGuire, W.H., and Howell, P., 1963. Oil and gas possibilities of the Cambrian and Lower Ordovician in Kentucky. Lexington, Kentucky: Spindletop Research Center, Kentucky Geology Survey, 216 p.

Miall, A.D., 1984. Principles of Sedimentary Basin Analysis. New York: Springer-Verlag, 490 p.

Patchen, D.G., Hickman, J,B., Harris, D.C., Drahovzal, J.A., Lake, P.D., Smith, L. B., Nyahay, R., Schulze, R., Riley, R.A., Baranoski, M. T., Wickstrom, L.H., Laughrey, C.D., Kostlnik, J., Harper, J.A., Avary, K.L., Bocan, J., Hohn, M . E., and McDowell, R., 2006. A geologic playbook for Trenton-Black River Appalachian basin exploration. Report prepared for U.S. Department of Energy, DOE Award No. DE-FC26-03NT41856, 601p.

Patton, J.B., and Dawson, T.O. 1969. Some petroleum prospects of the Cincinnati arch province. Indiana Geological Survey, Special Publication 18, p: 32-39.

Pettijohn, F.J., Potter, P.E., and Siever, R., 1973. Sand and Sandstone. Berlin: Springer-Verlag, 617 p.

Prothero, D.R., and Schwab, F., 1996. Sedimentary Geology. New York: W.H. Freeman and Company, 575 p.

Reineck, H.E. and Wunderlich, F., 1968. Classification and origin of flaser and lenticular bedding. Sedimentology, 11:99-104

Riley, R.A., and Baranoski, M.T., 1991, Regional stratigraphy of the Rose Run sand stone in Ohio (Abstract), In Exploration Strategies in the Appalachian basin, 22nd Annual Appalachian Petroleum Geology Symposium, Morgantown, WV, I.C. White Memorial Fund Pub. 3, 82 p.

Riley, R.A., Harper, J.A., Baranoski, M.T., Laughrey, C.D., and Carlton, R.W., 1993. Measuring and predicting reservoir heterogeneity in complex deposystems: the late Cambrian Rose Run Sandstone of eastern Ohio and western Pennsylvanian. Report prepared for U.S. Department of Energy, Appalachian Oil and Natural Gas Research Consortium, Contract No. DE-AC22-90BC14657, 257 P.

Riley R. A., 1994. Oil and gas exploration in the Rose Run Sandstone. Ohio Geology, Quarterly publication of Ohio division of geological survey, 8 p.

Riley R.A., Wicks, J., and Thomas, J., 2002. Cambrian-Ordovician Knox Production in Ohio: Three Case Studies of Structural-Stratigraphic Traps. American Association of Petroleum Geologists Bulletin, 86: 539-555.

Ryan-Mishkin, K., Walsh, J. P., Corbett, D. R., Dail, M. B., & Nittrouer, J. A. (2009). Modern Sedimentation in a Mixed Siliciclastic-Carbonate Coral Reel Environment, La Parguera, Puerto Rico. Caribbean Journal of Science, *45*(2-3): 151-167.

Ryder, R.T., Repetski, J.E., and Harris A.G., 1997, Stratigraphic framework of Cambrian and Ordovician Rocks in the Central Appalachian Basin from Campbell County, Kentucky, to Tazewell County, Virginia. Washington D.C.: U.S. Geological Survey, Miscellaneous Investigation Series Map I-2530, 53 P.

Saeed, A., 2002. Subsurface facies analysis of the Cambrian Mt. Simon sandstone in Western Ohio. Unpublished M.S. Thesis, Bowling Green State University, Bowling Green, Ohio, 167p.

Selley, R, C., 1973, Ancient Sedimentary Environments, second edition. New York: Cornell University Press, 224 p.

Sengupta, S., 2007, Introduction to Sedimentology, Second Edition. New Delhi: CBS publications, 325 p.

Sepkoski Jr, J. J., 1982. Flat-pebble conglomerates, storm deposits, and the Cambrian bottom fauna. In: Einsele, G. and Seilacher, A., (editors), Cyclic and Event Stratification. Berlin: Springer Heidelberg, p 371-385.

Swanson, R.G., 1981. Sample Examination Manual. Tulsa, OK: American Association of Petroleum Geologists, Methods in Exploration Series,30 p.

Walker, R. G., 1992. Wave and storm dominated shallow marine systems. In: Walker, R.G., and James, N.P., (editors), Facies Modeling Response to Sea Level Change. St. John's, Newfoundland: Geological Association of Canada; p. 219-238.

APPENDIX-I
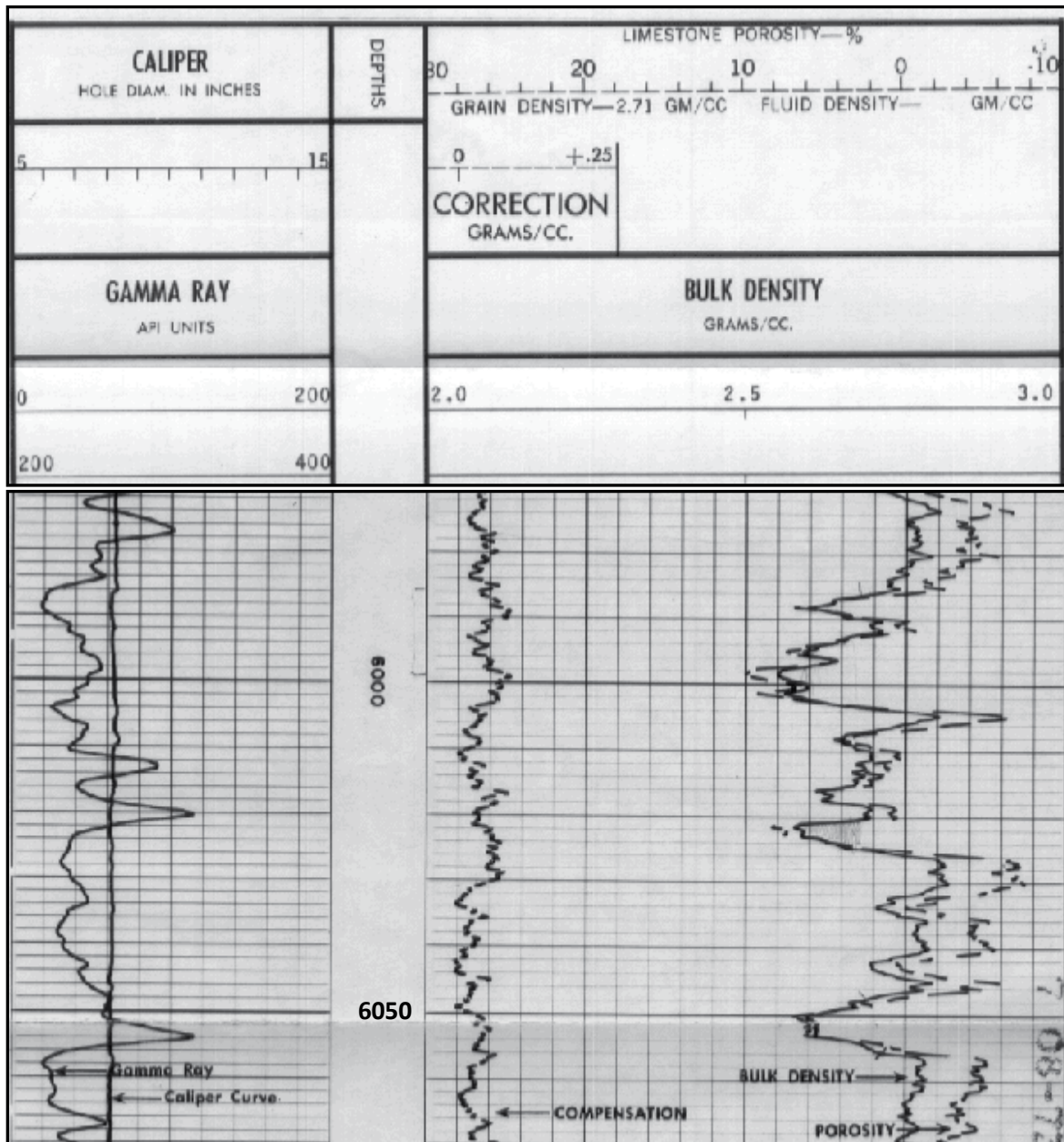
Figure A1. Well log for the well no. 1
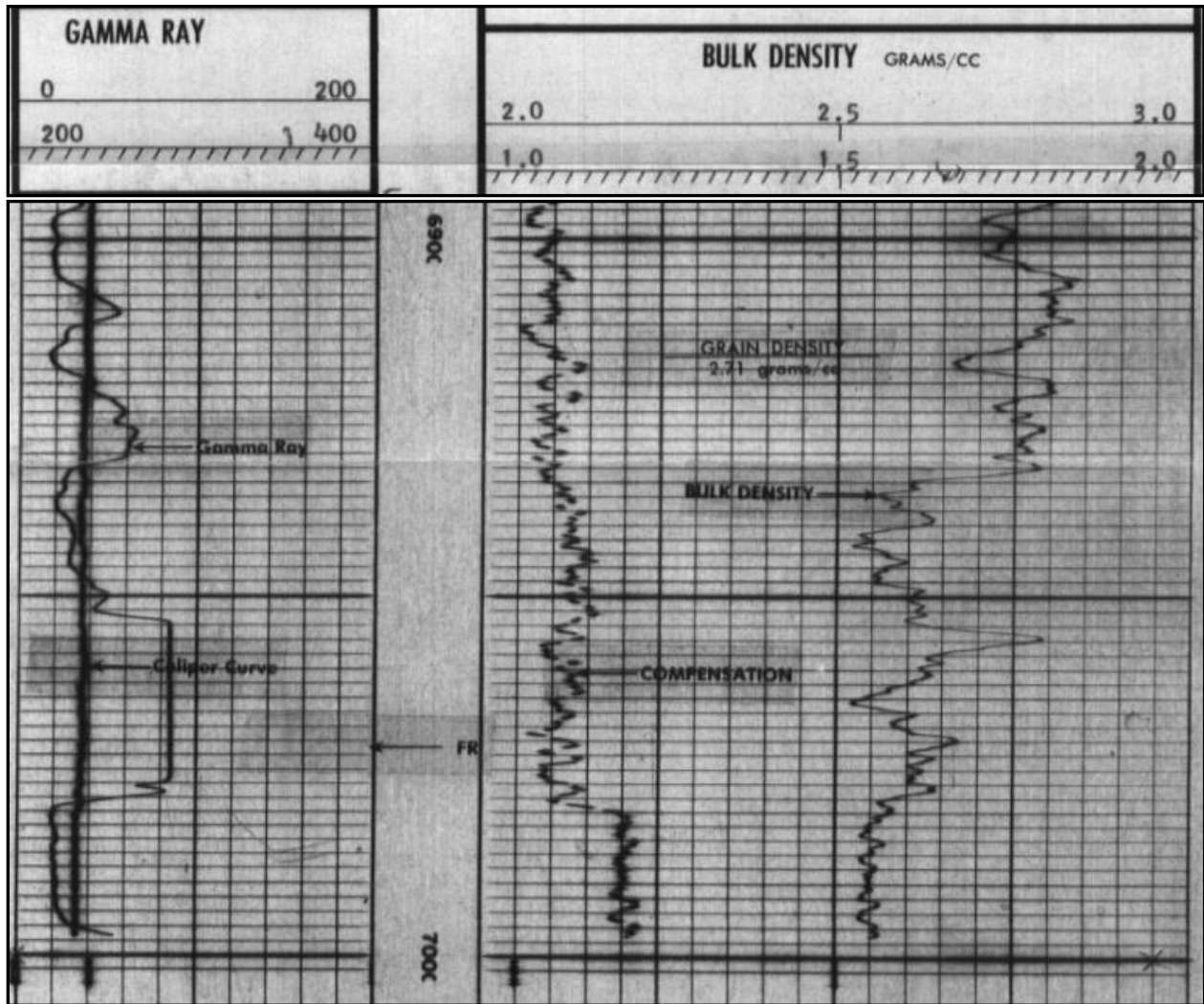
Figure A2. Well log for the well no. 2
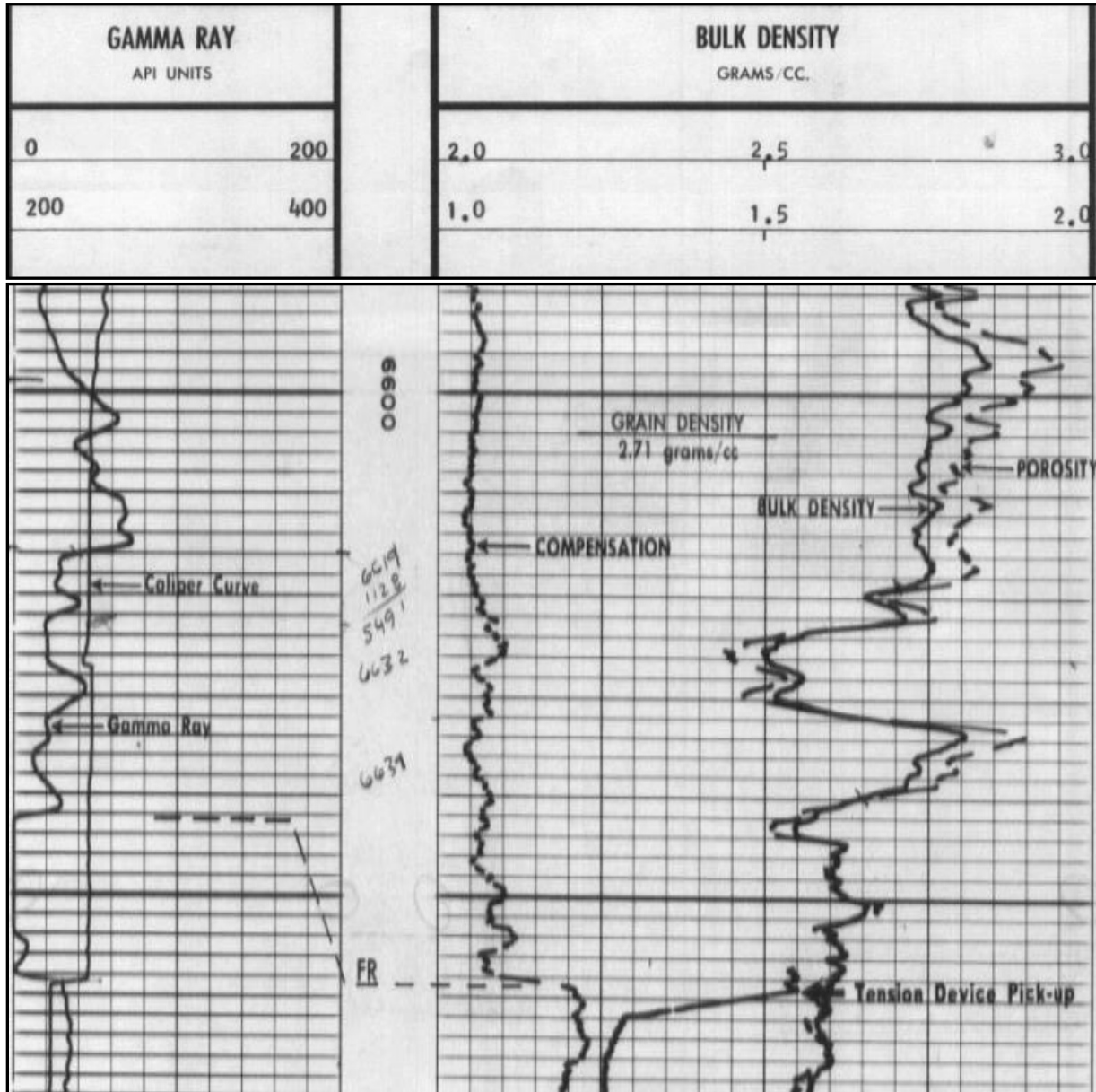
Figure A3. Well Log for the well no. 3
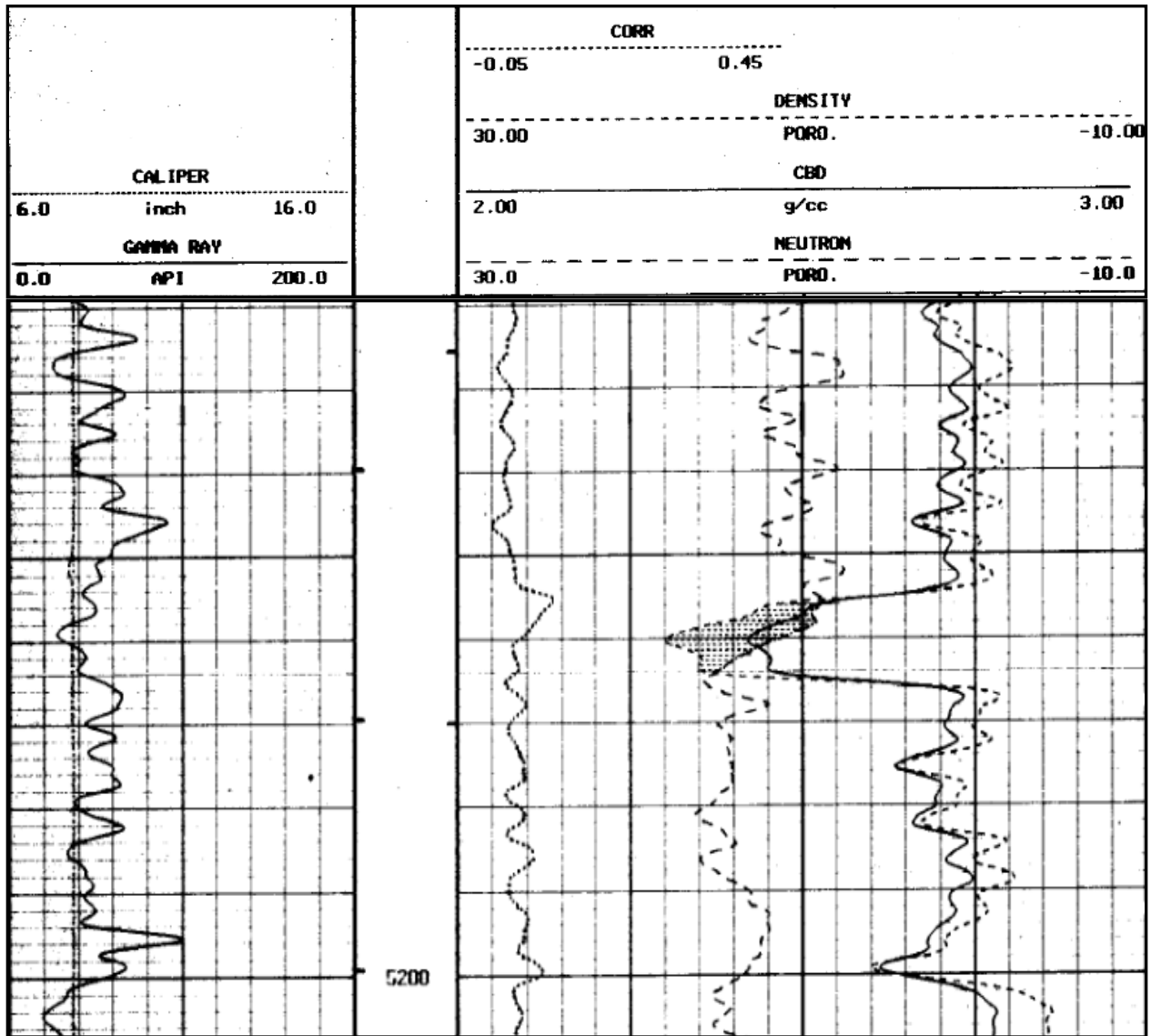
Figure A4. Well Log for the well no. 4
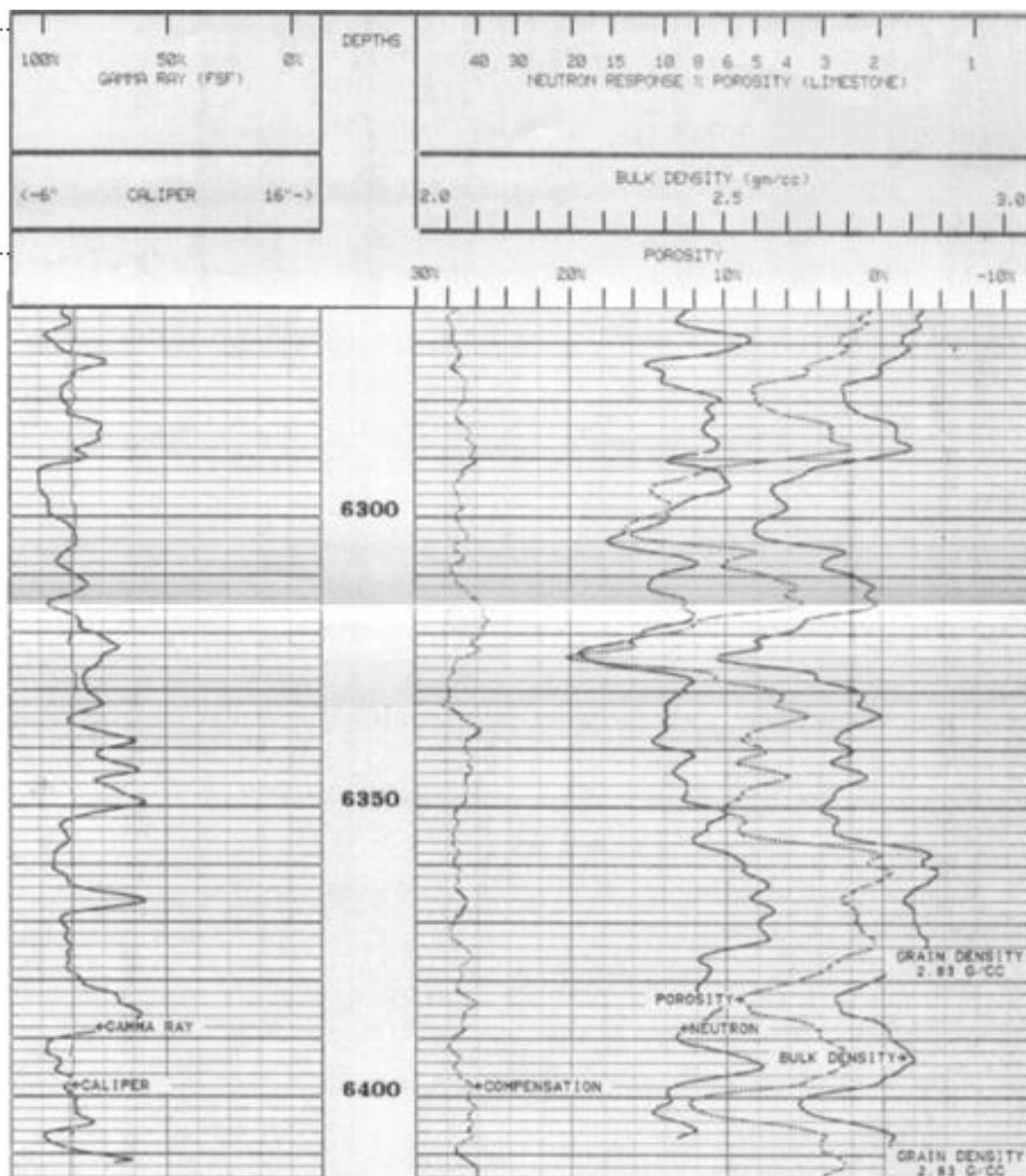
Figure A5. Well Log for the well no. 5
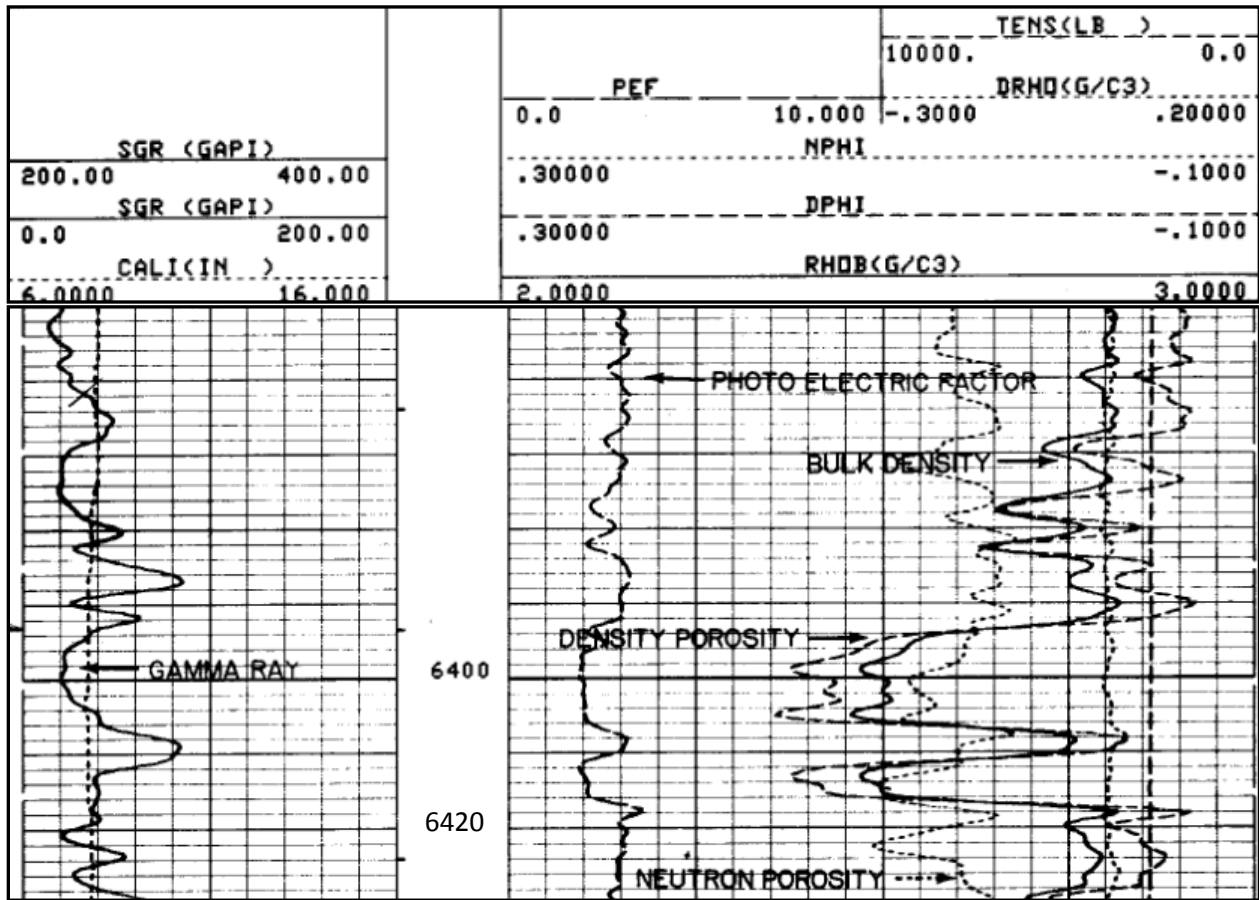
Figure A6. Well Log for the well no. 6
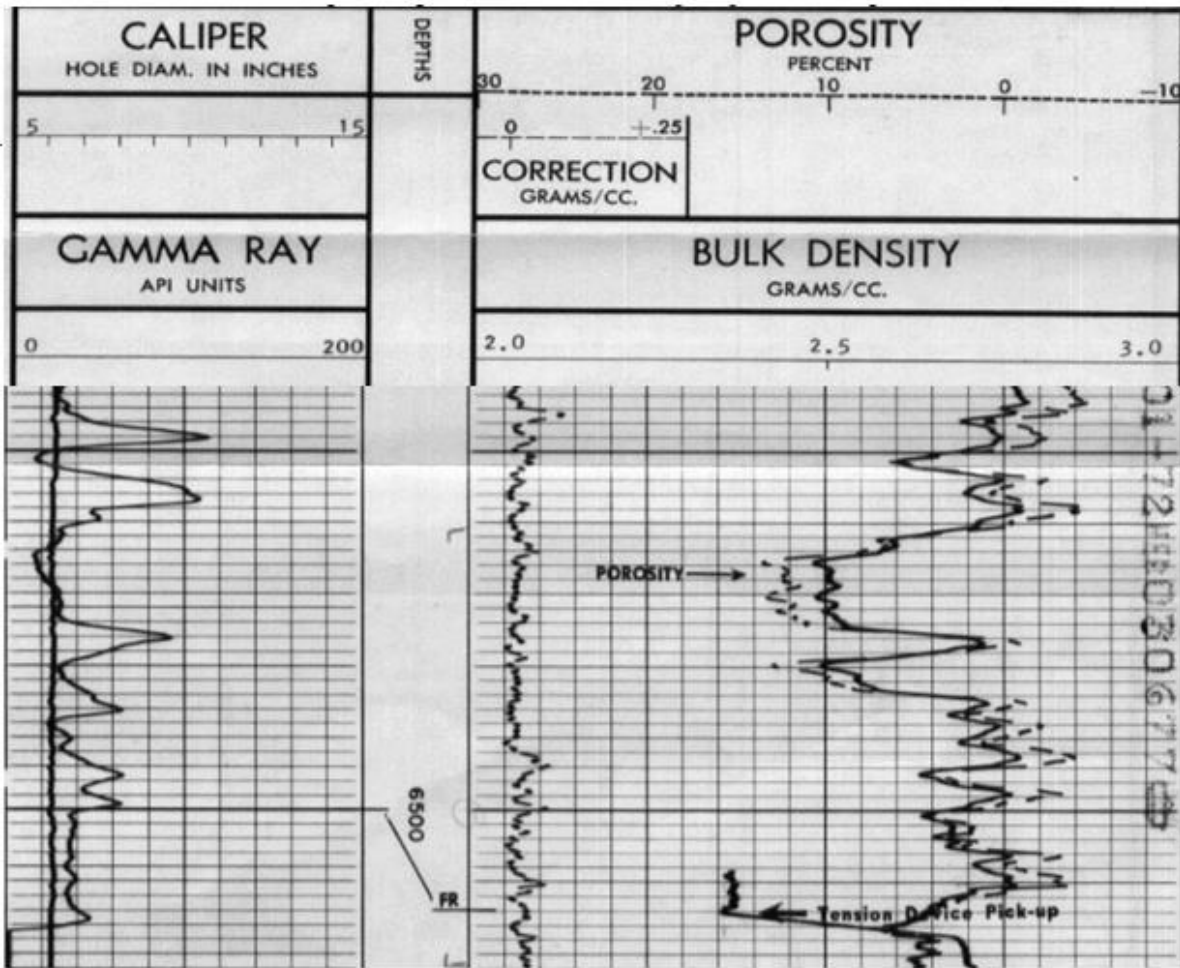
Figure A7. Well log for the well no. 7
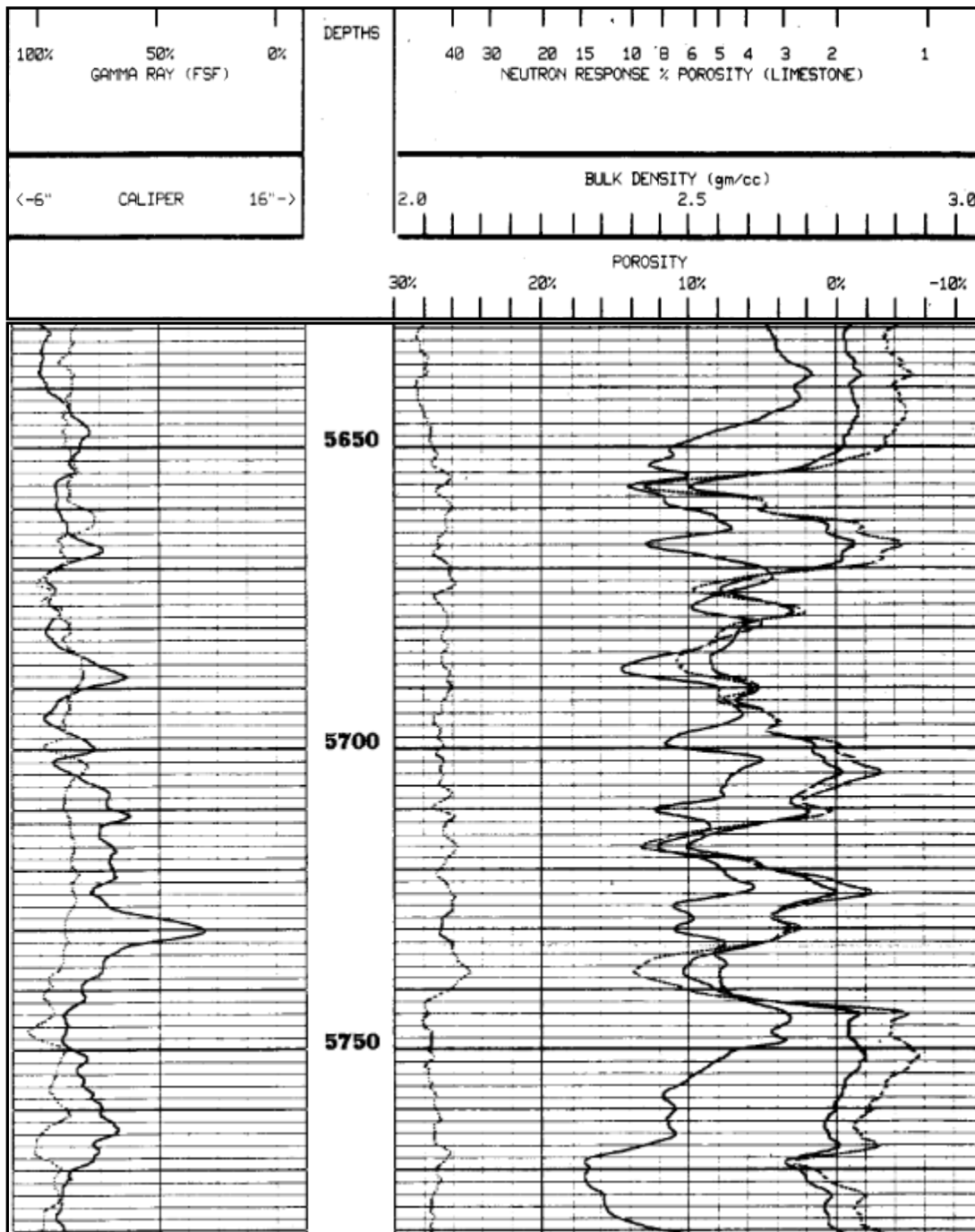
Figure 8. Well Log for the well no. 8
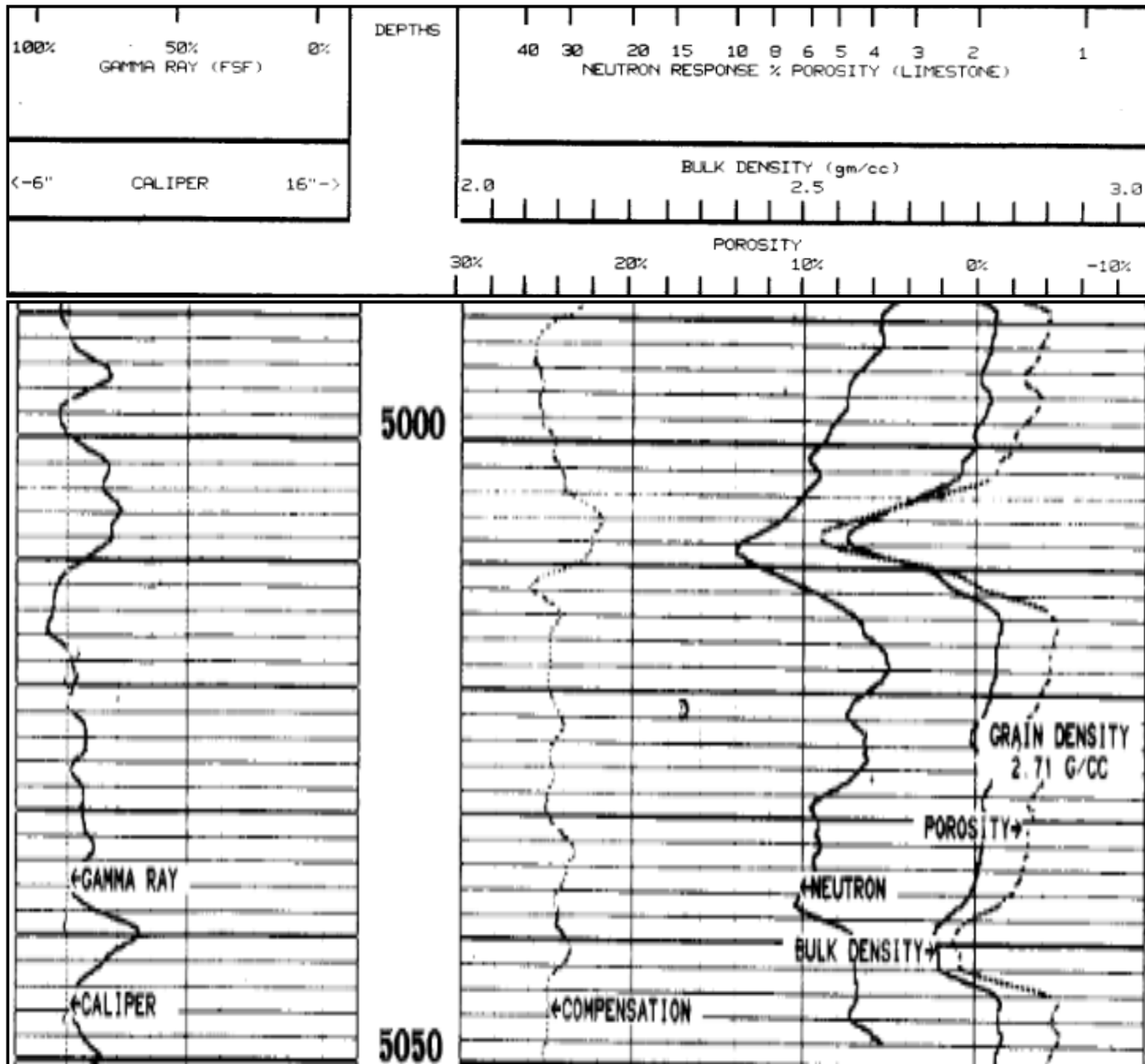
Figure A9. Well Log for the well no. 9
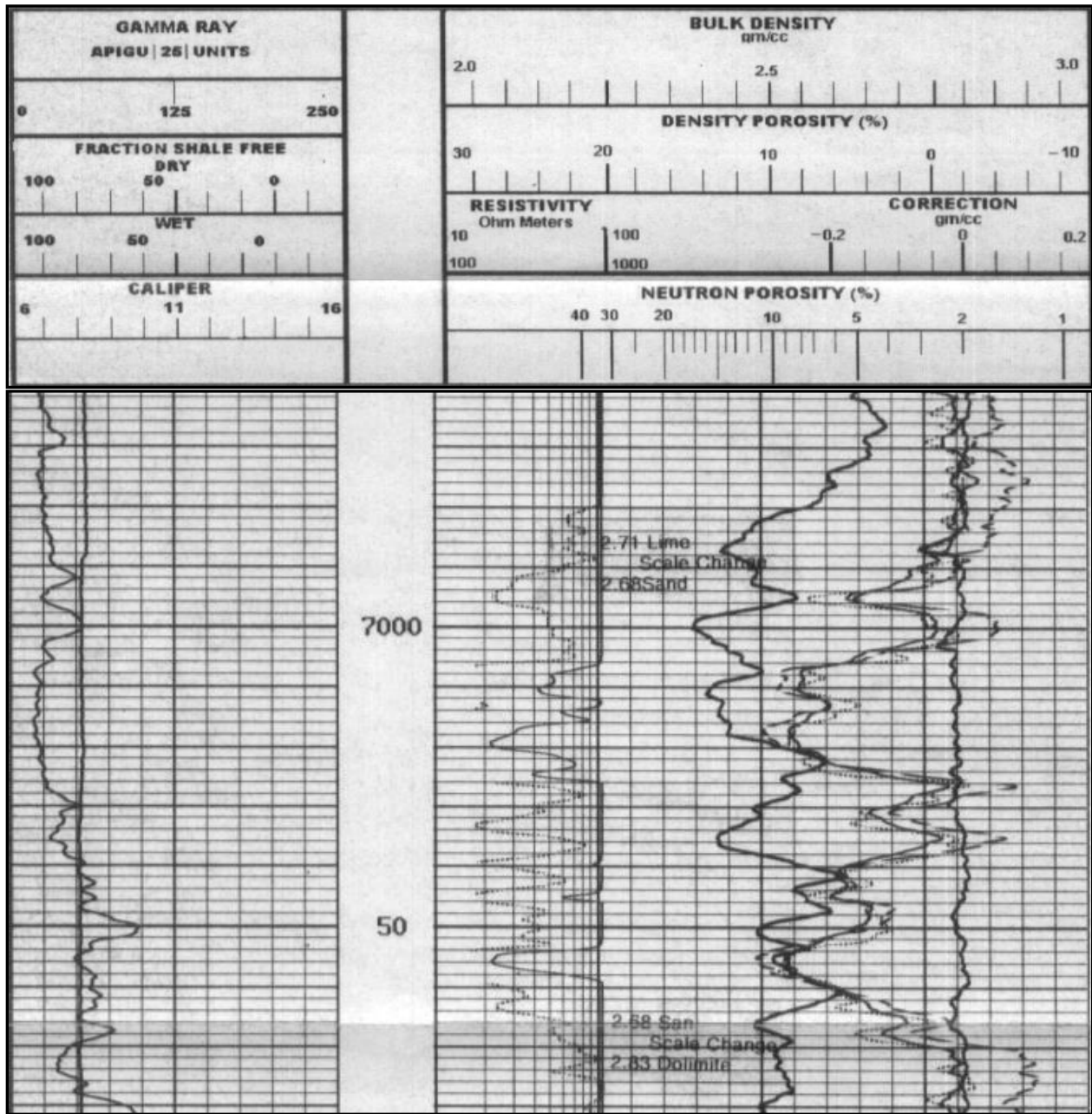
Figure 10. Well Log for the well no. 10
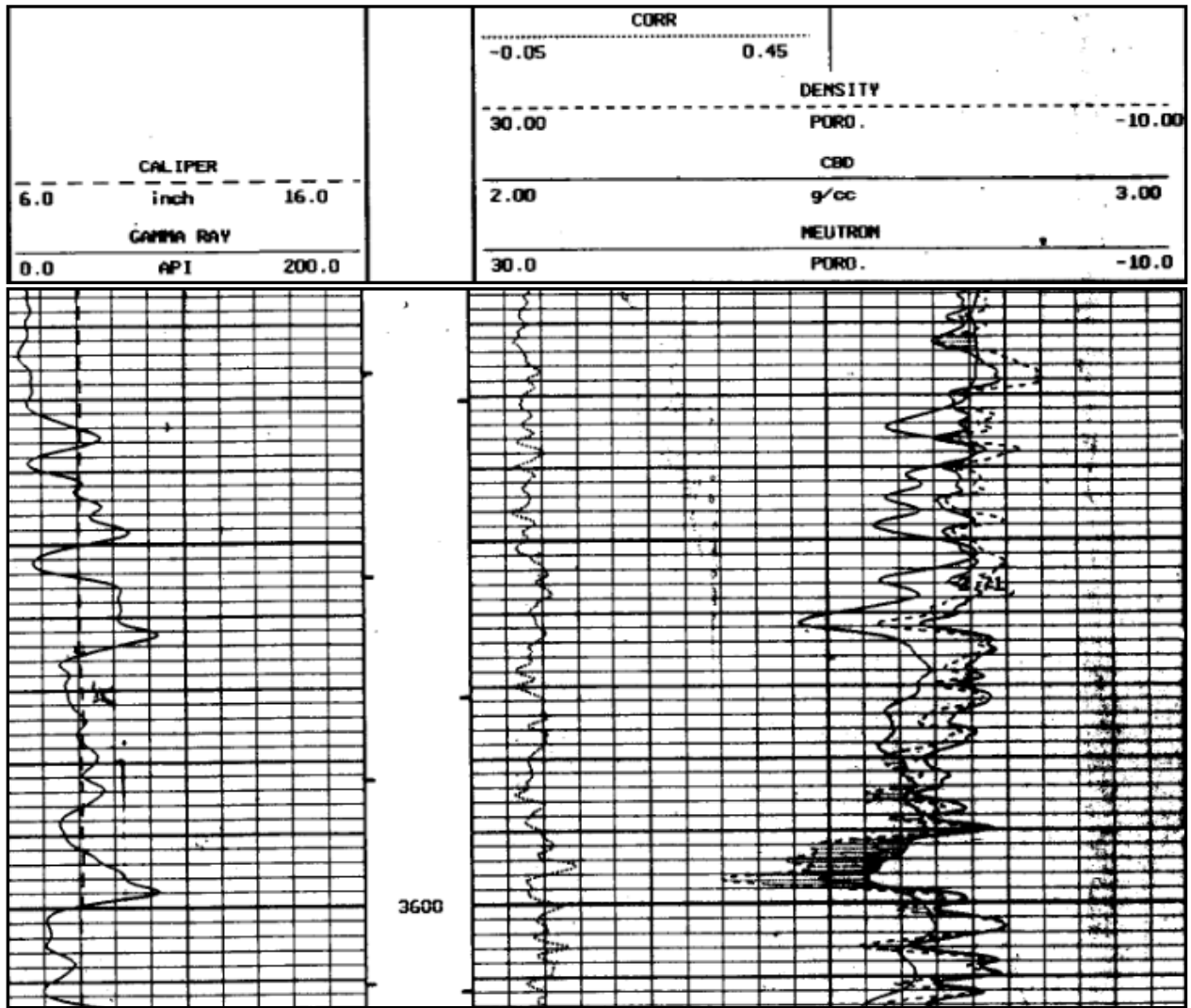
Figure A11. Well Log for the well no. 11
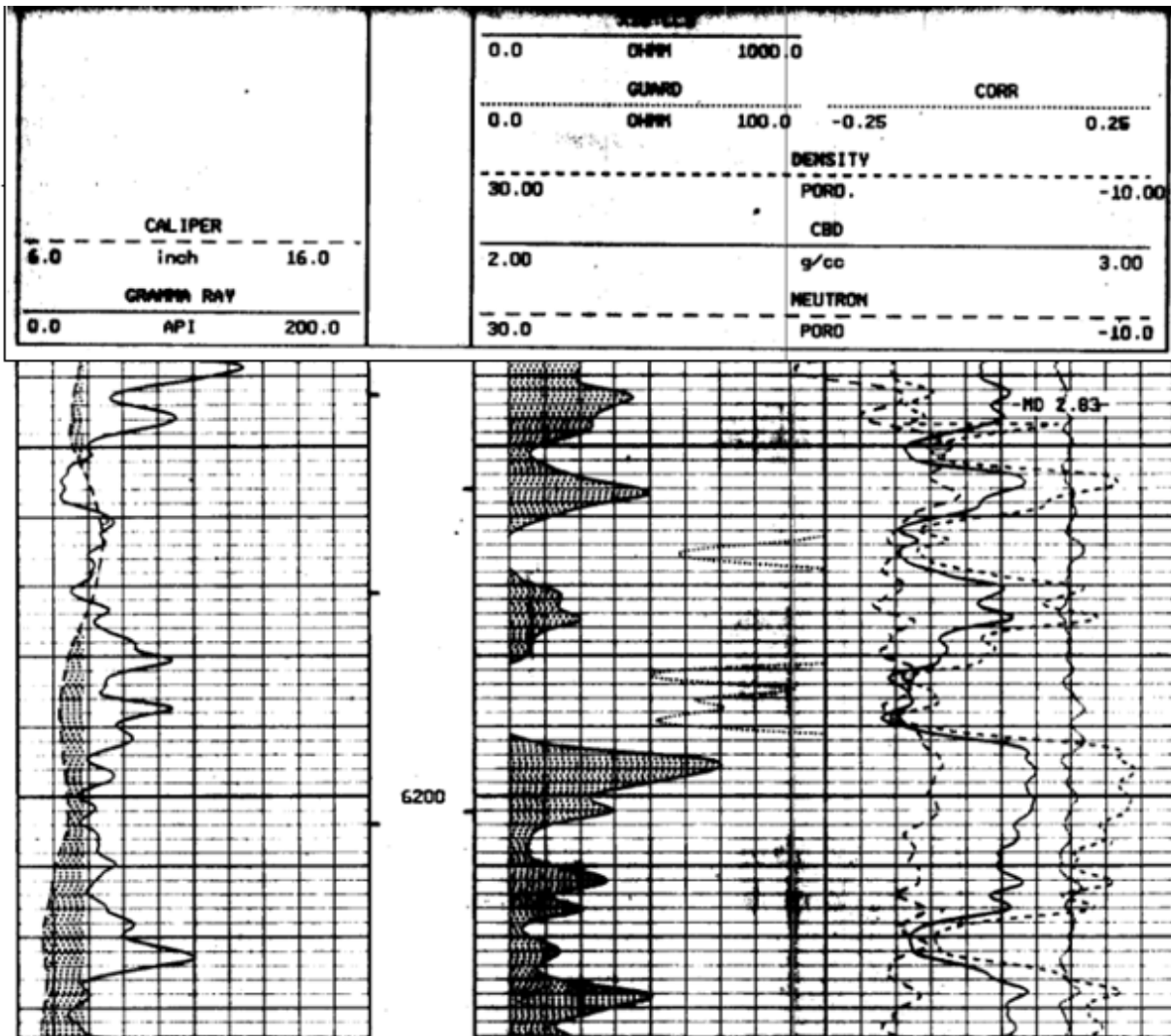
Figure A12. Well Log for the well no. 12
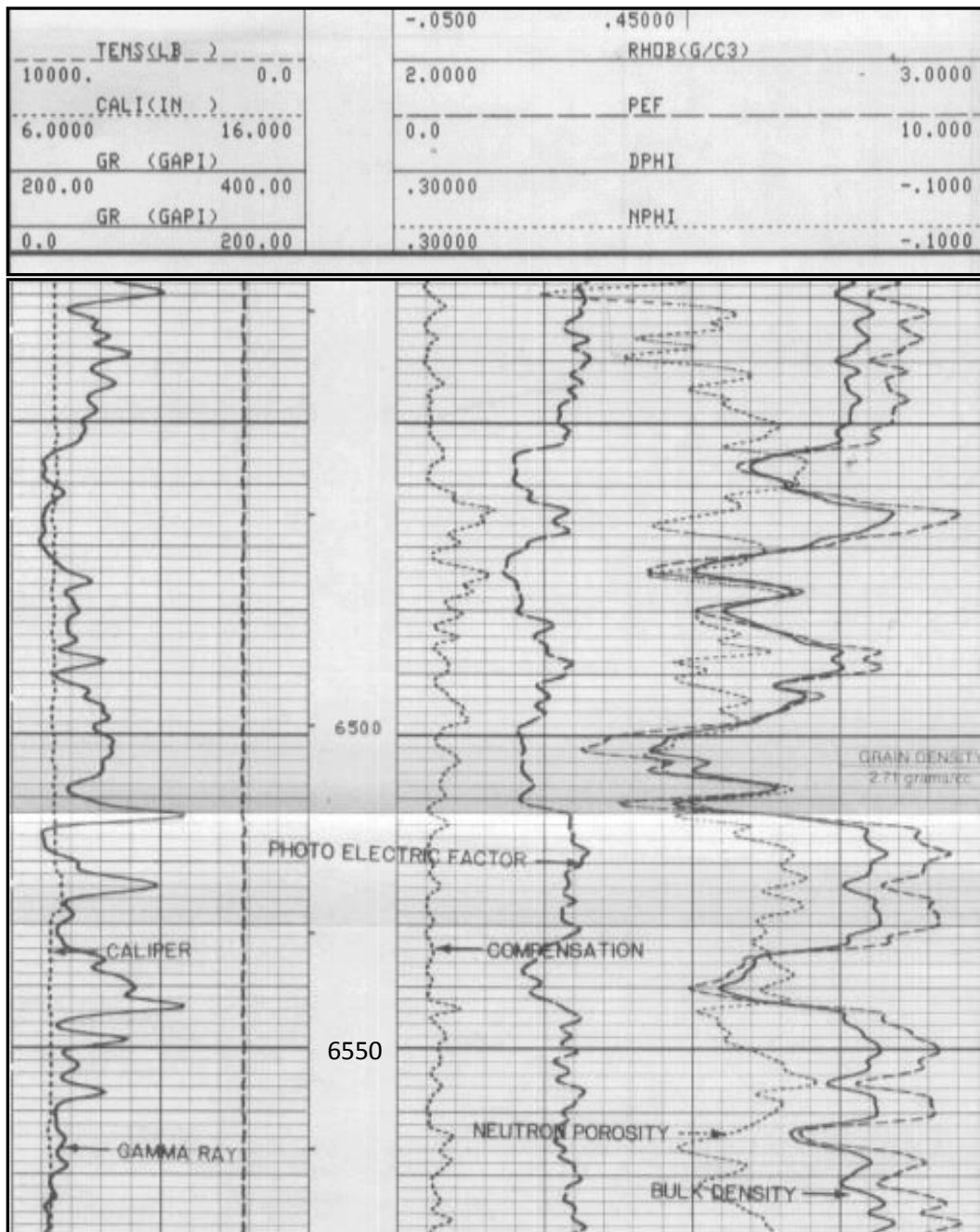
Figure A13. Well Log for the well no. 13
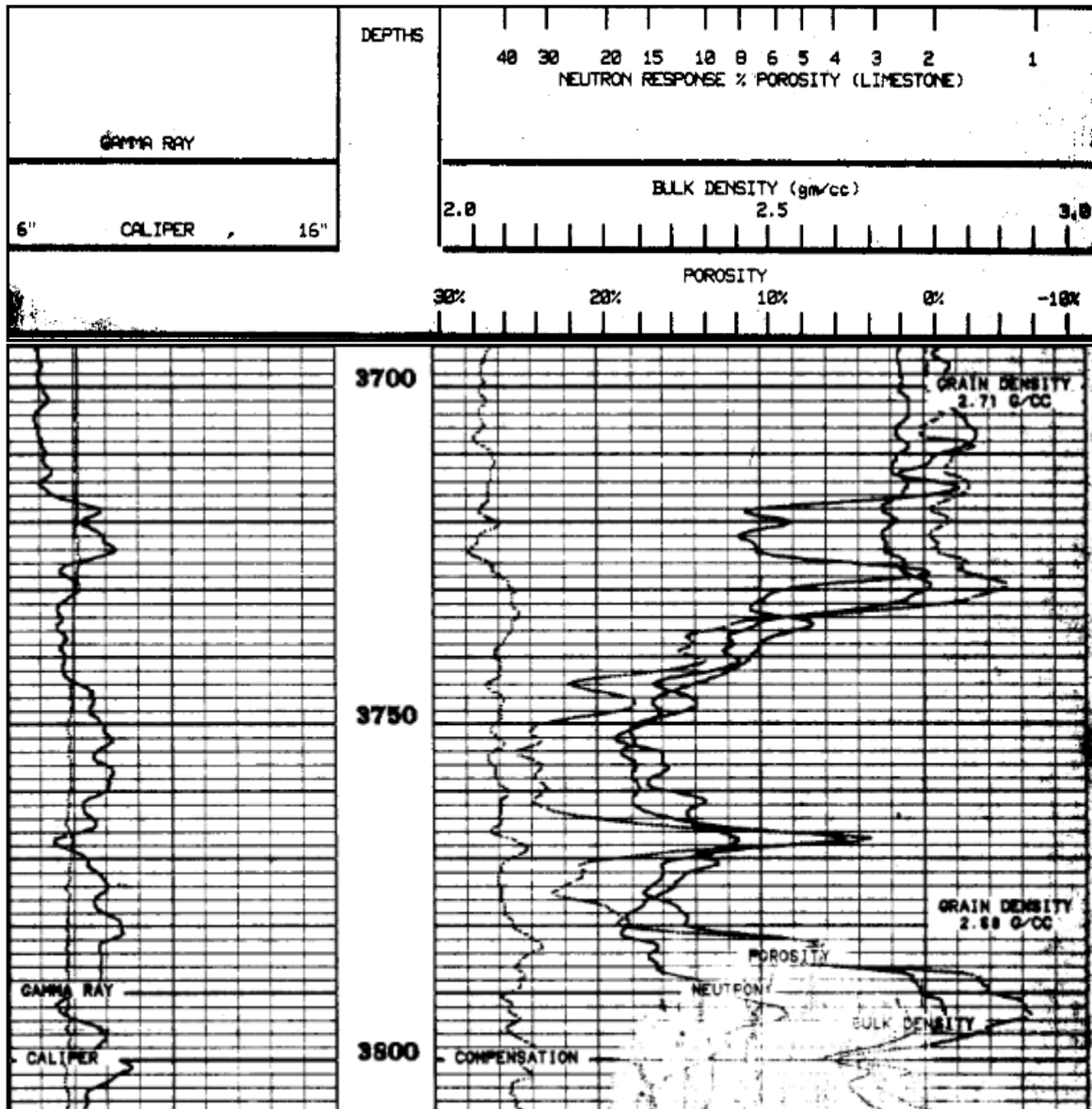
Figure A14. Well Log for the well no. 14
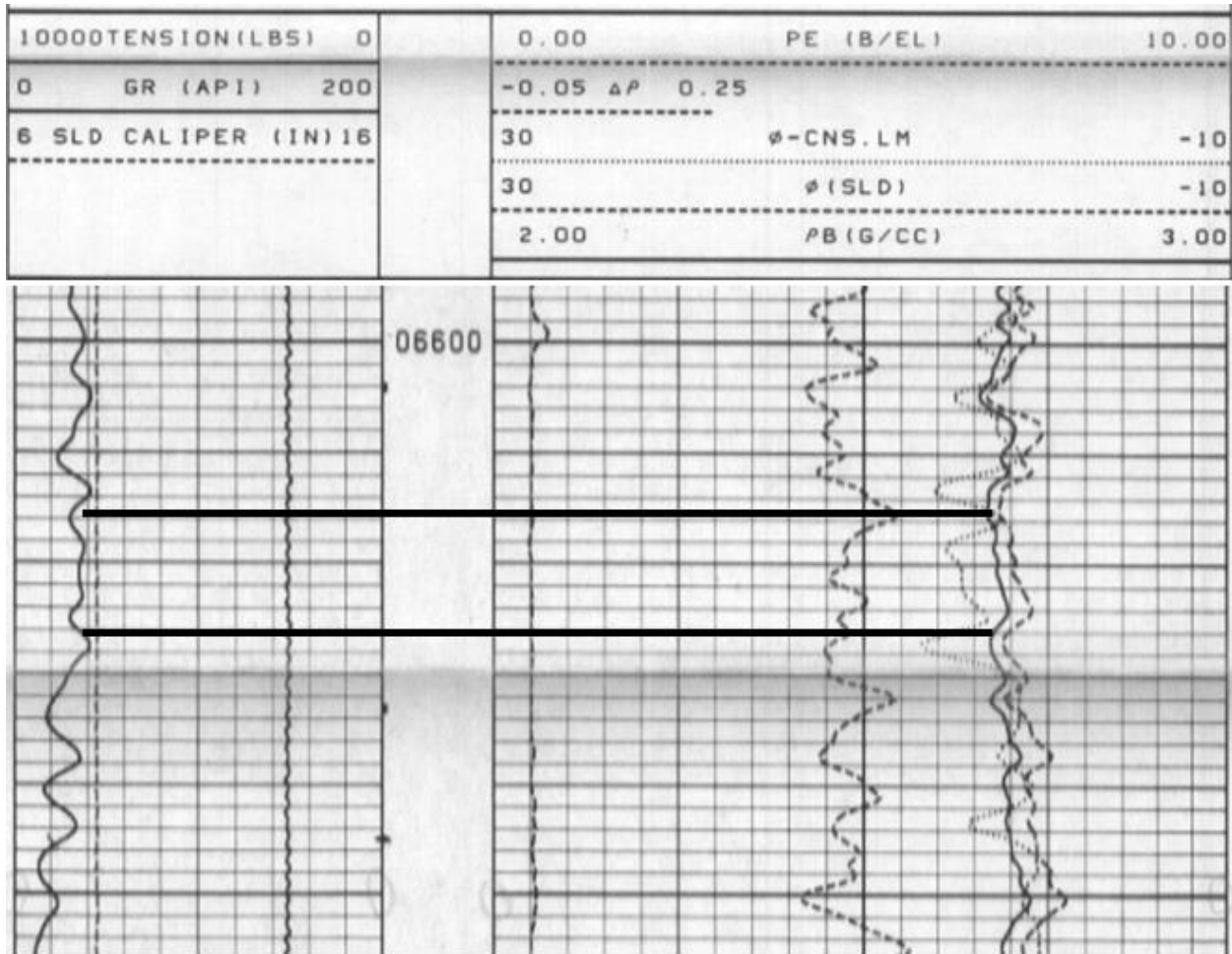
Figure A15. Well log for the well no. 15
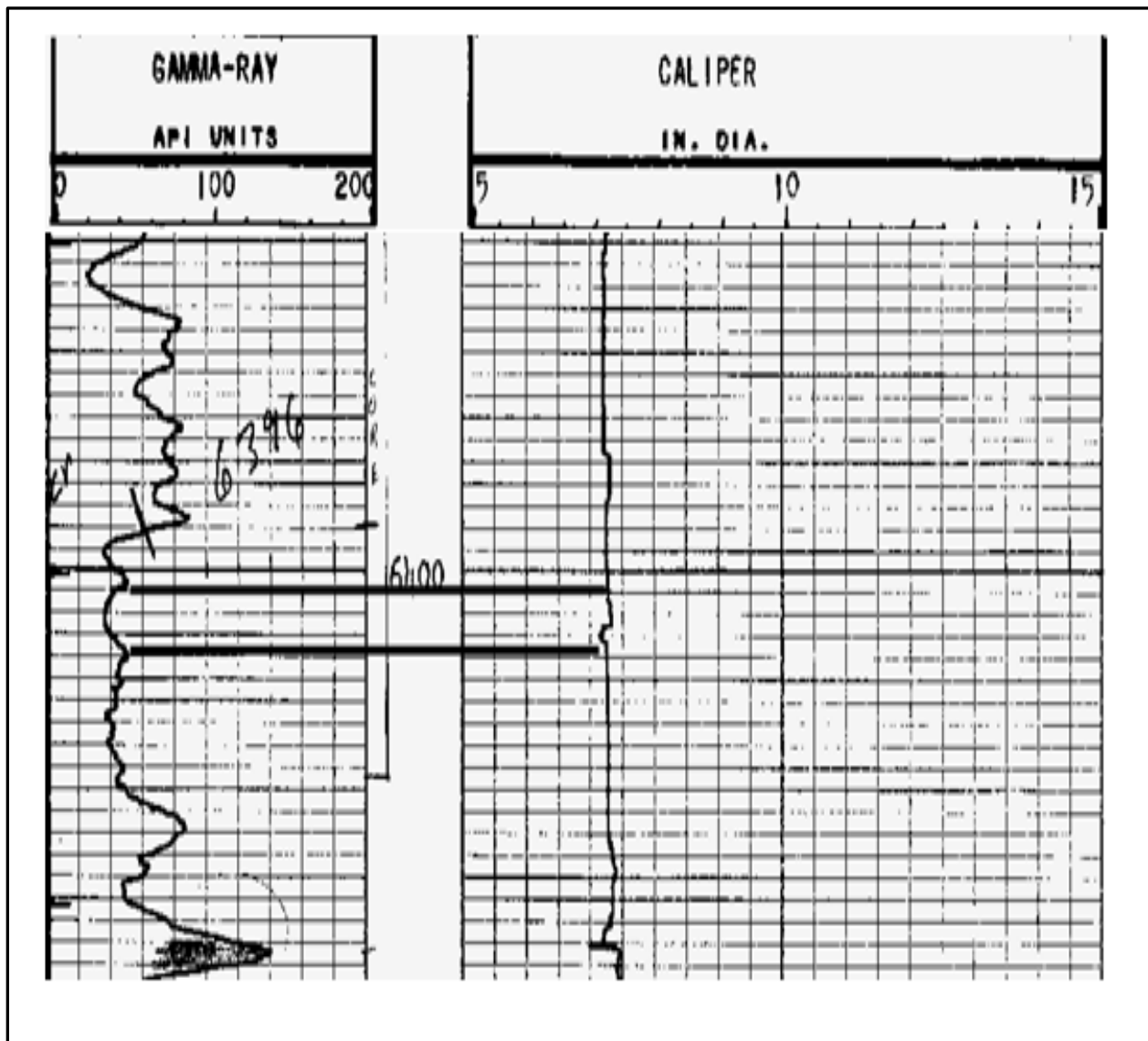
Figure A16. Well Log for the well no. 16
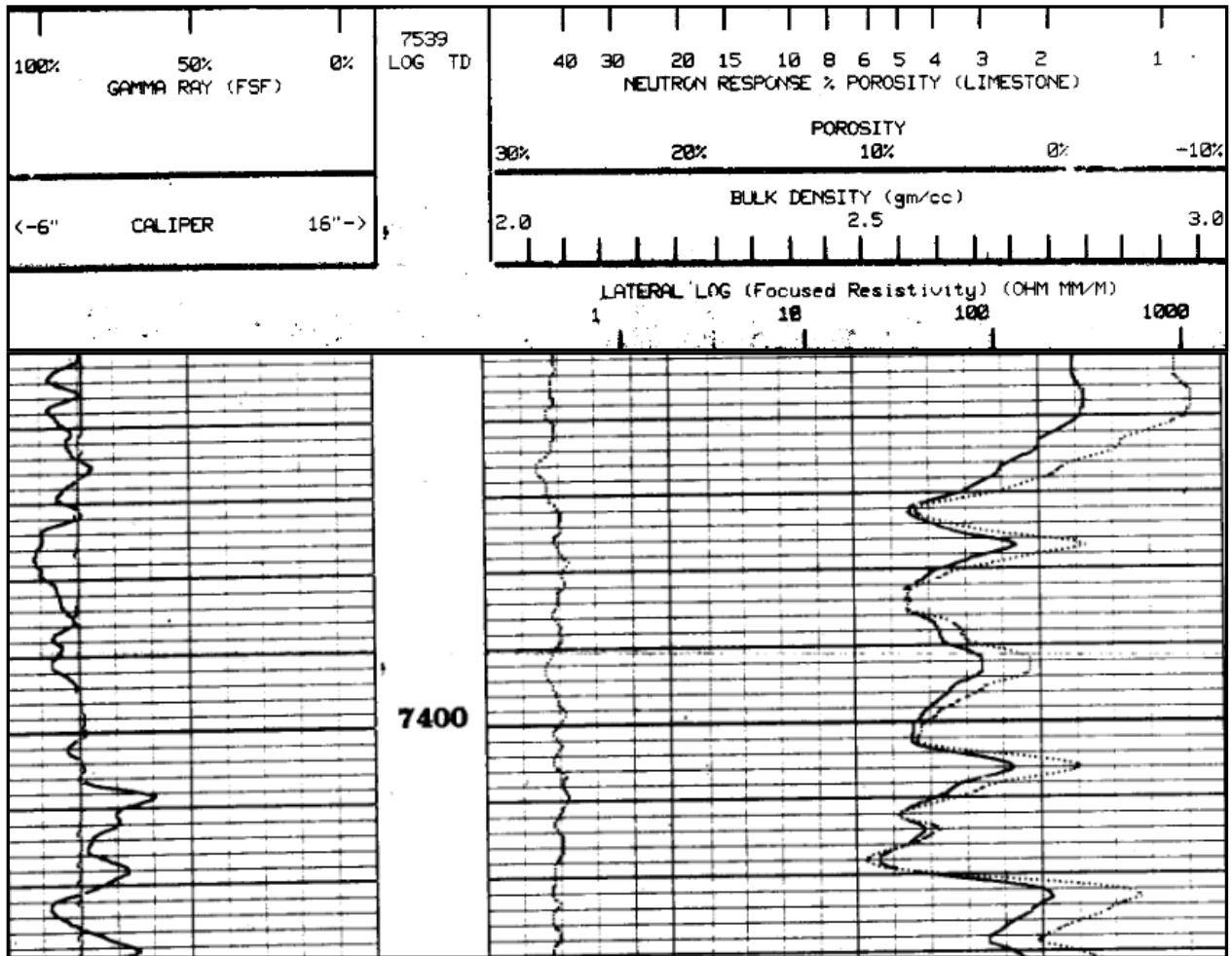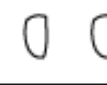
Figure A17. Well Log for the well no. 17

APPENDIX-II

Legend

| Symbol	Description
	Sandstone
	Mudstone
	Dolostone
	Coarsening upward sequence
	Fining upward sequence
	Herringbone cross stratification
	Planar tabular cross bedding
	Shale parting or mud cracks
	Planar lamination
	Mottling
	Intraclasts
	lenticular bedding
	Wavy bedding
	Flaser bedding
	Fracture
	Hummocky stratification
	Erosional contact
	Vug
	Stylolite
	Rip up clast
	Missing interval
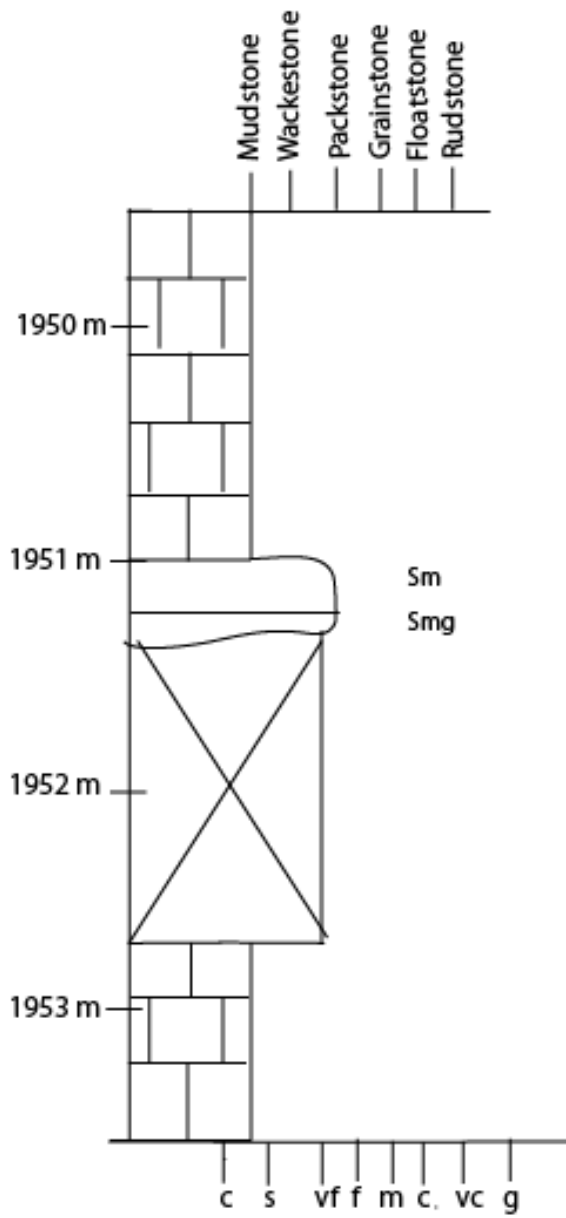
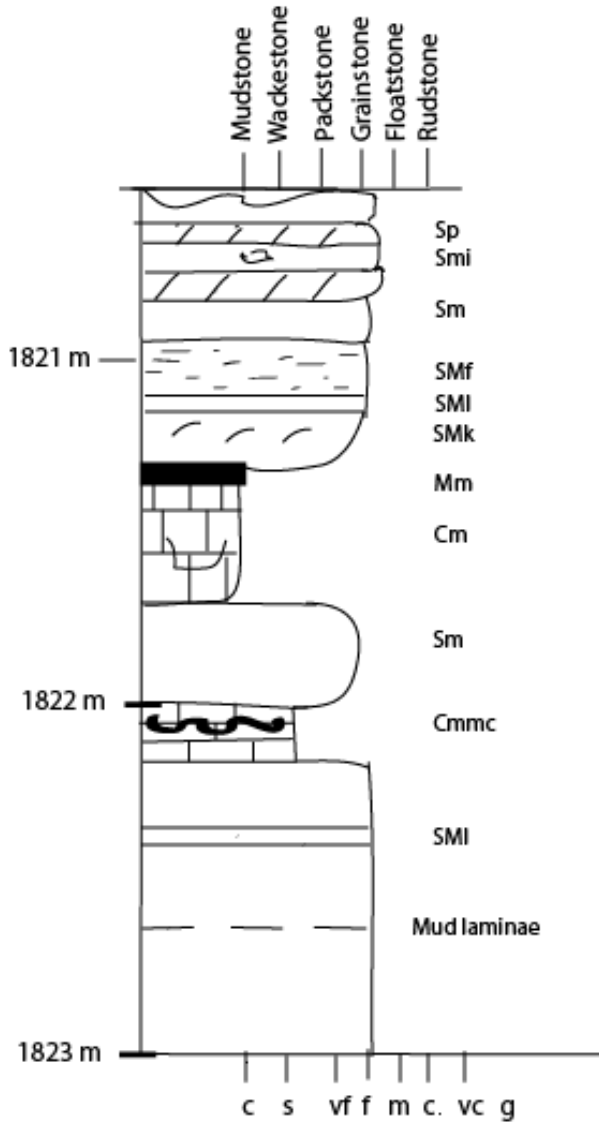Figure AII-1. Core-log of core 2892.

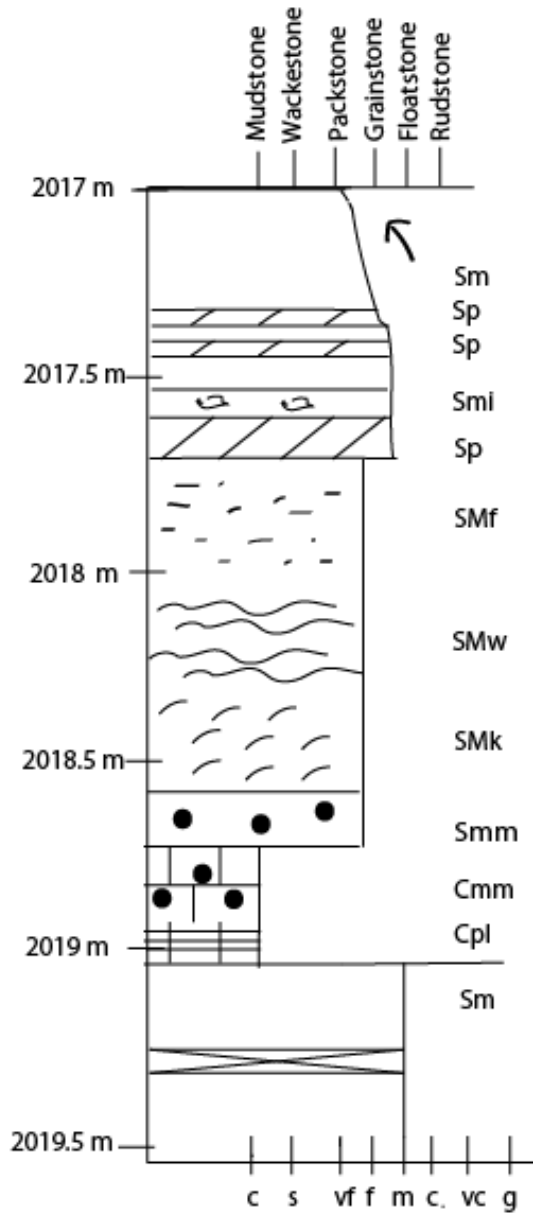Figure AII-2. Core-log of core 3385.
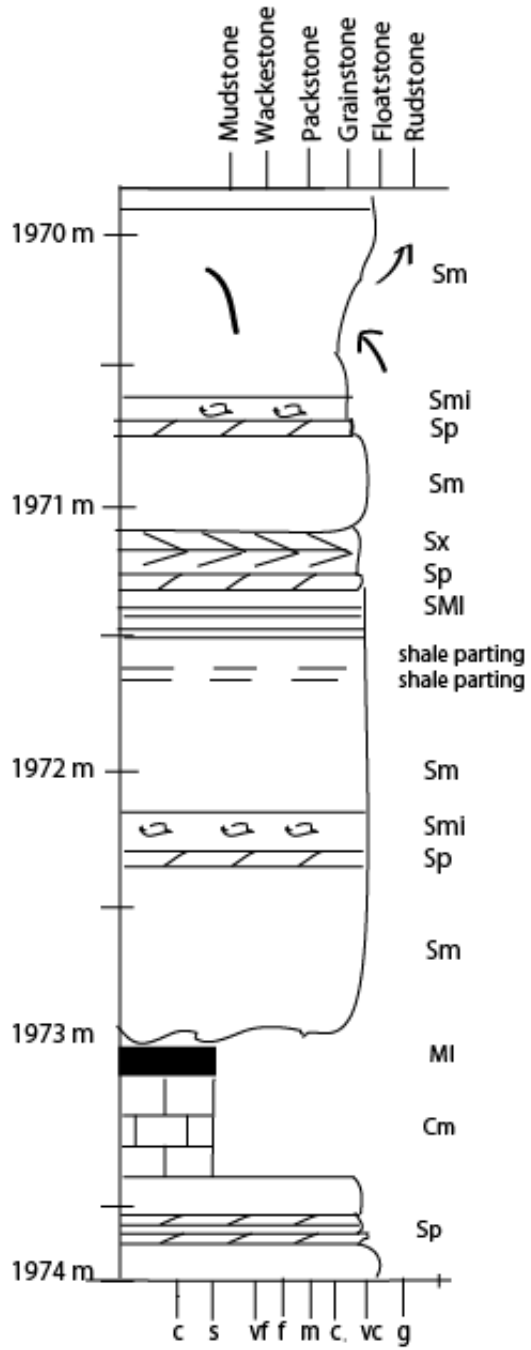
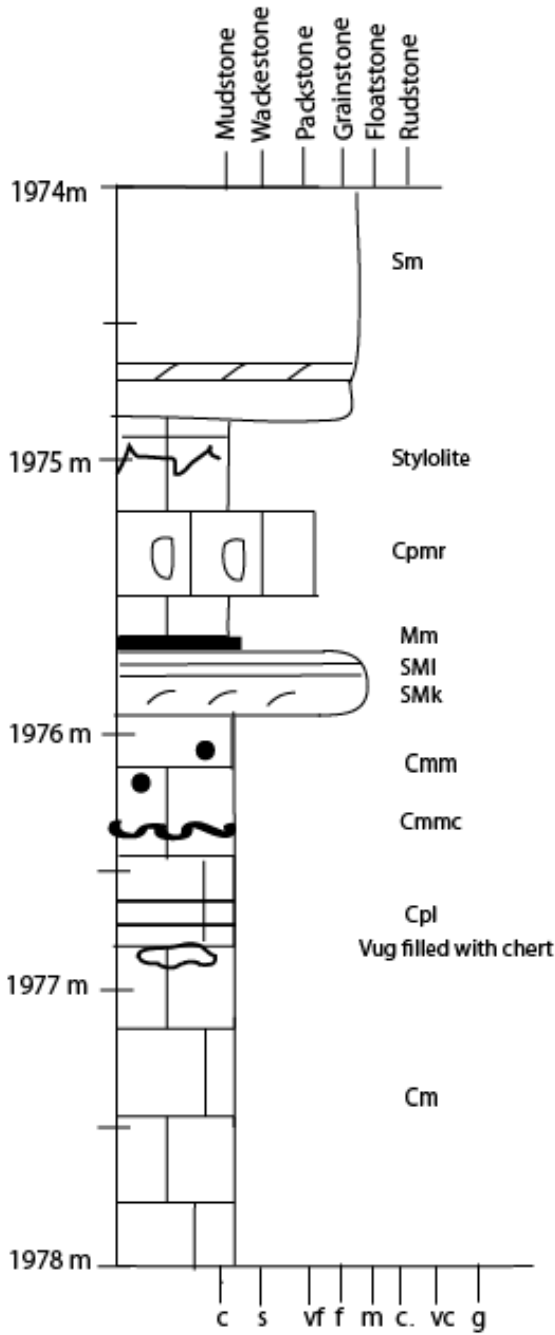Figure AII-3. Core-log of core 2989.

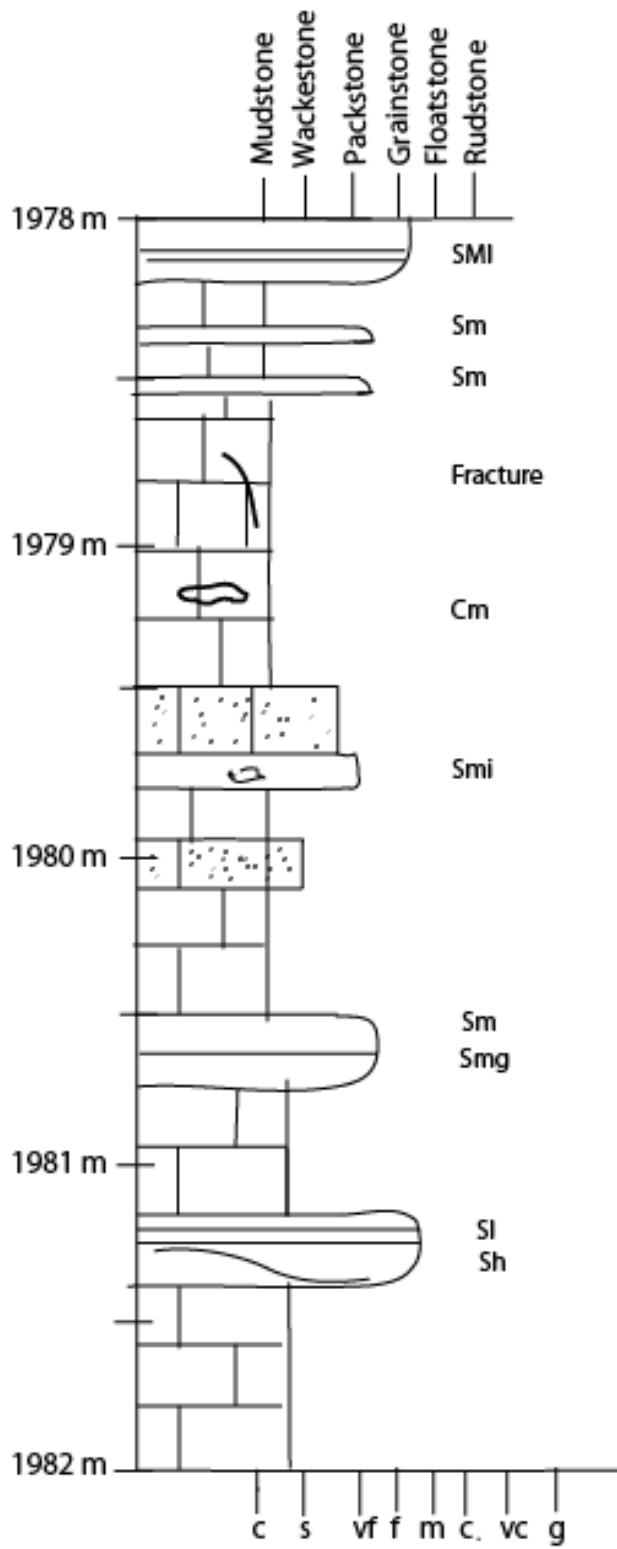Figure AII-4.1. Core-log of core 2923.

Figure AII-4.2. Core log of core 2923.

Figure AII-4.3. Core log of core 2923.

Figure AII-4.4. Core log of core 2923.
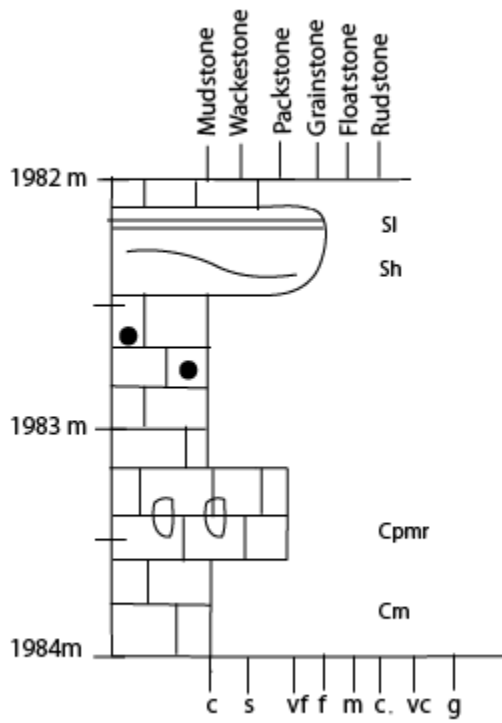
APPENDIX-III

		MS01		MS02		MS06		MS07		Mean %	Std. D
		Point count	%	Point count	%	Point count	%	Point count	%		
Quartz	Monocrystalline	84	27	60	20	59	20	78	26	23	4
	Polycrystalline	73	24	75	25	63	21	54	18	22	3
	Cryptocrystalline	10	3	25	8	16	5	19	6	6	2
Feldspar	Plagioclase	16	5	20	7	34	11	30	10	8	3
	Potassium	2	1	10	3	16	5	4	1	3	2
Lithic	Sedimentary	5	2	0	0	0	0	0	0	0	1
	Volcanic	0	0	0	0	2	1	2	1	0	0
	Metamorphic	0	0	0	0	1	0	0	0	0	0
	Accessories	18	6	16	5	22	7	21	7	6	1
	Voids	15	5	12	4	15	5	16	5	5	1
	Dolomite Cement	48	16	45	15	33	11	41	14	14	2
	Quartz cement	15	5	19	6	7	2	16	5	5	2
	Feldspar cement	0	0	0	0	2	1	4	1	0	1
	Clay cement	0	0	0	0	9	3	6	2	1	1
	Matrix	22	7	19	6	23	8	9	3	6	2
	Total	308	100	301	100	302	100	300	100		